

**ISM BAND INDOOR WIRELESS
CHANNEL AMPLITUDE
CHARACTERISTICS: PATH LOSS vs.
DISTANCE AND AMPLITUDE vs.
FREQUENCY**

A thesis presented to
the faculty of
the Russ College of Engineering and Technology of
Ohio University

In partial fulfillment
of the requirements for the degree
Master of Science

Jyotika Vig

June 2004

This thesis entitled

ISM BAND INDOOR WIRELESS CHANNEL AMPLITUDE
CHARACTERISTICS: PATH LOSS AND GAIN vs. DISTANCE AND
FREQUENCY

BY

JYOTIKA VIG

has been approved for

the School of Electrical Engineering and Computer Science
and the Russ College of Engineering and Technology by

David W. Matolak

Assistant Professor, School of Electrical Engineering and Computer Science

R. Dennis Irwin

Dean, Russ College of Engineering and Technology

VIG, JYOTIKA. M.S. June 2004. Electrical Engineering

ISM Band Indoor Wireless Channel Amplitude Characteristics: Path Loss and Gain vs. Distance and Frequency (150 pp.)

Director of Thesis: David W. Matolak

Abstract

This thesis deals with the characterization of indoor wireless channels in the ISM bands (902-928 MHz and 2.4-2.5 GHz). This characterization encompasses estimation of propagation path loss vs. distance, magnitude of the channel transfer functions and amplitude correlation functions using propagation measurements. The thesis explains the various propagation models, their importance and the parameters used in these models to characterize indoor channels. The experiments supporting this thesis were conducted in Stocker Center, the engineering school of the university. In the first part, path loss vs. distance on various floors was measured. The results were used to determine the path loss exponent and standard deviation. The second part of the thesis addresses dispersive channel parameters and measurements of the amplitude-squared transfer functions and amplitude correlation functions. These measurements and models are a useful first-order description of the channel.

Approved:

David W. Matolak

Assistant Professor,

School of Electrical Engineering and Computer Science

Acknowledgements

I would like to thank my advisor Dr. David W. Matolak for his help, guidance and abundant knowledge throughout the course of this thesis. I would also like to thank the faculty and staff of the department of Electrical Engineering and Computer Science particularly my committee members Dr. Jeffrey C. Dill and Dr. Joseph E. Essman, for all that I have learnt from them, and my graduate secretary Tammy Jordan.

I would also like to thank all my friends I made here at Athens over the last two years. And finally I would like to thank my parents and my brother for their constant support and words of wisdom and belief that kept me driven and focused throughout my goal of achieving my Masters.

Table of Contents

Abstract.....	3
Acknowledgements.....	4
Table of Contents.....	5
List of Figures.....	8
List of Tables	10
Chapter 1	11
Introduction.....	11
1.1 Wireless Channel	12
1.2 Indoor Propagation.....	15
1.3 Thesis Scope	15
Chapter 2	17
Review of Propagation Model.....	17
2.1 Physics of Propagation.....	17
2.1.1 Free Space Propagation.....	17
2.1.2 Log-Normal Shadowing.....	18
2.2 Outdoor Propagation Models.....	20
2.2.1 Longley-Rice Model	20
2.2.2 Okumura-Hata Model	21
2.3 Indoor Propagation Models.....	23
2.3.1 Log-Distance Path Loss Model.....	24
2.3.2 Attenuation Factor Model	24
2.4 Parameters Used in Propagation Models	25

2.4.1 Limitations of Indoor Propagation Models.....	28
2.5 Dispersive Channel Parameters	29
2.5.1 Channel Multipath Delay Spread.....	30
2.5.2 Frequency Correlation Functions.....	31
2.5.3 Coherence Bandwidth.....	32
Chapter 3	34
Propagation Measurements and Analysis	34
3.1 Measurement Description	34
3.1.1 Equipment Used.....	34
3.1.2 Procedure	35
3.2 Stocker Floor Plans	38
3.3 Example Measurement Results.....	40
3.4 Data Analysis.....	46
3.4.1 Computation of Path Loss Exponent and Standard Deviation	47
3.5 Discussion.....	48
Chapter 4	50
Dispersive Channel Measurements	50
4.1 Measurement Description	50
4.1.1 Equipment Used.....	50
4.2 Example $ \mathbf{H}(\mathbf{f}) ^2$ Results	53
4.3 Data Analysis.....	63
4.3.1 Approximation of Frequency Correlation Functions.....	63
4.4 Summary.....	64

Chapter 5	65
Conclusions and Future Work.....	65
5.1 Summary of Research	65
5.2 Future Work	66
References.....	68
Appendix A: Stocker Floor Plans	70
Appendix B: Experimental Data	75
Appendix C: Path Loss vs. Distance Plots.....	87
Appendix D: Experimental Data.....	99
Appendix E: Amplitude Transfer Function Plots	107
Appendix F: Matlab Programs.....	111

List of Figures

Figure 1.1. Block diagram of a digital communication system	11
Figure 3.1. Block Diagram of the Measurement Setup.....	35
Figure 3.2. Data collection for a given distance d_0	37
Figure 3.3. Layout of floor plan of second floor with transmitter and receiver locations	39
Figure 3.4. 900 MHz LOS Path Loss in Ground Floor of Stocker	41
Figure 3.5. 900 MHz LOS Path Loss in all floors of Stocker.....	42
Figure 3.6. 900 MHz NLOS Path Loss in all floors of Stocker.....	44
Figure 3.7. 900 MHz Path Loss in all floors of Stocker	44
Figure 3.8. 2.4 GHz LOS Path Loss in all floors of Stocker	45
Figure 3.9. 2.4 GHz Path Loss in all floors of Stocker	45
Figure 4.1. Transmitted signal for a single sweep	51
Figure 4.2. Data collection for a given distance d_0	53
Figure 4.3. Example Plot showing $(\Delta H^2)_{max}$	54
Figure 4.4. Variation of power with frequency for Measurement #1 on Ground Floor of Stocker center at various distances from the transmitter for 902-928 MHz	56
Figure 4.5. Variation of power with frequency for Measurement #1 on First Floor of Stocker center at various distances from the transmitter for 902-928 MHz	56
Figure 4.6. Variation of power with frequency for Measurement #1 on Second Floor of Stocker center at various distances from the transmitter for 902-928 MHz	57

Figure 4.7. Variation of power with frequency for Measurement #1 on Third Floor of Stocker center at various distances from the transmitter for 902-928 MHz ..	57
Figure 4.8. Variation of power with frequency for Measurement #1 on Fourth Floor of Stocker center at various distances from the transmitter for 902-928 MHz ..	58
Figure 4.9. Variation of power with frequency for Measurement #1 on Third Floor of Stocker center at various distances from the transmitter for 2.4-2.5 GHz	58
Figure 4.10. Variation of power with frequency for Measurement #1 on Second Floor of Stocker center at various distances from the transmitter for 2.4-2.5 GHz	59
Figure 4.11. Spaced frequency amplitude autocorrelation (902-928 MHz) for Ground Floor	60
Figure 4.12. Spaced frequency amplitude autocorrelation (902-928 MHz) for First Floor	60
Figure 4.13. Spaced frequency amplitude autocorrelation (902-928 MHz) for Second Floor	61
Figure 4.14. Spaced frequency amplitude autocorrelation (902-928 MHz) for Third Floor	61
Figure 4.15. Spaced frequency amplitude autocorrelation (902-928 MHz) for Fourth Floor.....	62
Figure 4.16. Spaced frequency amplitude autocorrelation (2.4-2.5 GHz) for Second Floor	62
Figure 4.17. Spaced frequency amplitude autocorrelation (2.4-2.5 GHz) for Third Floor	63

List of Tables

Table 2.1. Path Loss Exponents for Different Environments	26
Table 2.2. Path loss exponent and standard deviation measured in different buildings.....	27
Table 2.3. Average Floor Attenuation Factor in dB for One, Two, Three and Four Floors in an Office Building.....	27
Table 3.1. Amplitude Accuracy of E4432B ESG-D Signal Generator	36
Table 3.2. Path loss exponent (n) and standard deviation (σ) calculated for different floors.....	43
Table 4.1. Range of received power levels (in dB) [$(\Delta H^2)_{\max}$]	55

Chapter 1

Introduction

Digital communications is playing an increasingly dominant role in the telecommunication industry. It offers faster data processing and more flexibility than analog transmission. Unlike analog communications, extremely low error rates can be achieved using digital signals, leading to better signal quality and reliability. The signal flow and processing involved in a typical digital communication system are as shown in Figure 1.1 [1].

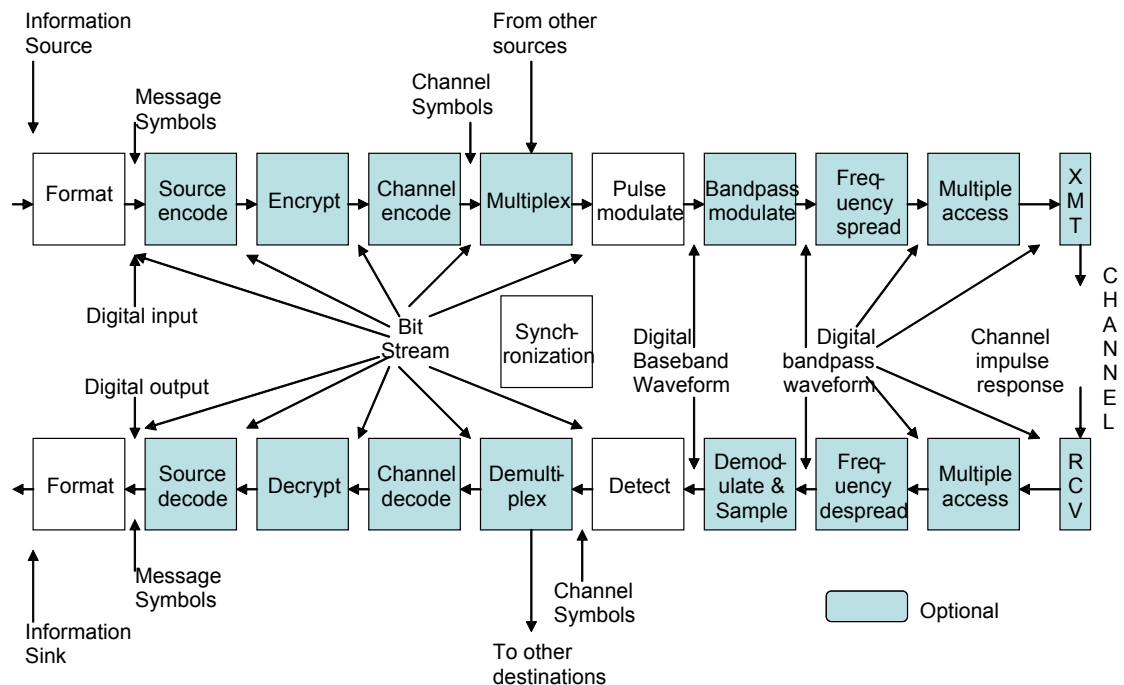


Figure 1.1. Block diagram of a digital communication system [1].

The diagram consists of an upper and lower set of blocks. The upper set depicts the flow of data from the information source to the transmitter output (left to right). The lower set depicts the flow of data from the receiver input to the information sink (right to left). The transformations performed in each block are done to enable the transmission of source signals across a communication channel. The communication channel is a physical medium used to transmit data to the receiver(s), e.g., a coaxial cable for wired systems, air for wireless systems. During the transmission process the input source information is often converted to binary digits (bits), which are then grouped to form message symbols. Error correction techniques may be applied, and then modulation is done to convert symbols to waveforms that are compatible for transmission over the channel. In the reverse direction, the receiver employs demodulation techniques to restore the waveform to an optimally shaped base band pulse for detection. Detection is the selection of one symbol, from the finite set of possible transmitted signals, as the estimate of what was transmitted. This differs from analog transmission, where a potentially infinite number of waveforms can be transmitted.

1.1 The Wireless Channel

Transmitting a signal over the air presents some difficult challenges that must be overcome using a thorough understanding of the propagation environment. A propagating electromagnetic wave incurs various effects such as reflection, diffraction and scattering. Reflection occurs when the electromagnetic wave is incident on an object which has large dimensions compared to the wavelength. Diffraction is a phenomenon that takes place

when the path between the transmitter and receiver is obstructed by an irregular sharp surface. This results in the bending of waves around the obstacle even in the absence of a line of sight (LOS) path between the transmitter and the receiver. Scattering takes place when the wave travels through a medium and encounters obstacles of dimensions smaller than the wavelength of the incident wave. The phenomenon known as multipath fading can be described by the physics of these three propagation mechanisms. Multipath propagation is when the signal travels multiple paths from the transmitter to the receiver.

A wired channel is a relatively static channel and is spatially confined. There is efficient use of transmitted energy and these channels cause minimal interference to users on other wires when properly designed. A wireless channel on the other hand is dynamic and transmitted signals can spread out over space. There is often significant multipath energy and it can cause considerable interference to nearby users. This is one of the major challenges faced by wireless networks.

In most practical situations there is not just a single line of sight path between a transmitter and receiver. The various objects present in the environment that are capable of reflecting the wireless signal provide alternate paths for the signal from the transmitter to the receiver. In many cases the line of sight component may be absent. A common example of this is cellular transmission when the mobile user is indoors. As noted, when the transmitted signal reaches the receiver via multiple paths, this is termed multipath propagation. As a result, this signal sent by the transmitter arrives at the receiver from different directions and different delays. The superposition of all these versions of the original signal has a deterministic amplitude and phase, which depends on the positions, orientations, and the electrical properties of the reflectors. Yet in most situations, the

propagation environment is sufficiently complex so that modeling each wave deterministically is difficult, and computationally intensive. Hence, much research has been done to model the propagation environment statistically—that is, certain propagation effects can be well modeled as random phenomena. If the reflectors and/or transmitter and/or receiver are in motion, then the received signal amplitude will vary with time. At some instants of time, the amplitude of the signal at the receiver may become too low to be detected. This variation in signal strength with time is known as fading. This time variation is also well-modeled using random processes. Also, generally, the strengths of the received waves decrease as the distance between the transmitter and receiver increases.

Propagation models are designed to measure the average received signal power at a given distance from the transmitter and also the variation of the signal strength in close proximity to a particular site. These models are often used to predict the Signal- to - Noise Ratio (SNR—the measure of signal strength relative to background noise) for a mobile communication system using what are called path loss models. There are two types of propagation models:

1. Large Scale propagation models-These models predict the local average signal power for any arbitrary distance between the transmitter and receiver. They are useful to depict the radio coverage area of the transmitter.
2. Small-scale or fading models-These models predict the fluctuations of the received signal over very small distances or durations (typically on the order of a carrier frequency wavelength). In such cases the received power may vary by many orders of magnitude when the receiver is displaced only by a fraction of a wavelength.

1.2 Indoor Propagation

Indoor radio propagation has been used for a long time, but only recently has it become widely used. It can be more complicated and “harsh” than outdoor propagation because there may be more and more varied obstacles in the environment. In addition, radiated power levels in indoor environments must often be kept at significantly lower levels than in outdoor environments, reducing communication link range. Researchers have shown that there are many factors that contribute to the propagation characteristics, including the building layout, the presence of hard partitions (a partition that extends to ceiling) or soft partitions (a partition that does not extend to the ceiling), the composition of the wall material, the presence of open space, whether a door is open or closed, and for between floors, the floor attenuation factor [2]. The position of antennas also plays an important role.

1.3 Thesis Scope

This thesis entails the measurement and characterization of propagation path loss vs. distance on single and multiple floors in an indoor environment: Stocker Center at Ohio University, Athens, OH. We collected propagation measurement data in two popular frequency bands: the Industrial, Scientific, and Medical (ISM) bands at 900 MHz and 2.4 GHz. From this data we obtain statistical parameters useful in the broad characterization of this indoor channel. We estimate the propagation path loss exponent, standard deviation of path loss, and attenuation factors between floors. These measurements are for narrowband channel characterization.

We also obtained estimates of the magnitude of the channel transfer function, its spatial variation, and approximate frequency correlation functions, from additional propagation measurements on all the floors of Stocker Center. The frequencies were the same ISM bands as for the path loss measurements.

Chapter 2 is a review of propagation models-the various outdoor and indoor propagation models and the key parameters used in these models. We also describe various dispersive channel parameters used in characterizing wireless channels, such as correlation functions, coherence bandwidth, and multipath delay spread. In Chapter 3 we discuss the measurements and results of our path loss vs. distance measurements in the two ISM bands. Chapter 4 describes the dispersive channel (transfer function amplitude) measurements and results. Finally in Chapter 5 we conclude the thesis by summarizing the results and by suggesting some future work.

Chapter 2

Review of Propagation Models

2.1. Physics of Propagation

In this Chapter, we briefly describe various indoor and outdoor propagation models. We also discuss various propagation loss parameters and dispersive channel parameters. This information is used to calculate and understand the various parameters calculated later in the thesis.

2.1.1. Free Space Propagation

The most basic model of radio wave propagation is the so called free space propagation model. It is useful in predicting signal strength when there is a direct line-of-sight (LOS) path between the transmitter and the receiver without any obstructions. In this model, radio waves emanate from a point source of radio energy, traveling in all directions in a straight line, filling the entire spherical volume of space with radio energy that varies in strength with a $(1/\text{range})^2$ rule (or 20 dB decrease per decade increase in range).

The actual power received by the receiving antenna at a distance d from the transmitting antenna is given by the Friis free space equation [2]:

$$P_r(d) = P_t G_t G_r \lambda / [(4\pi d)^2] L \quad (2.1)$$

where P_t is the transmitted power, $P_r(d)$ is the received power at distance d , G_r is the receiver antenna gain, G_t the transmitter antenna gain, L is the system loss factor not related to propagation ($L \geq 1$), and λ is the wavelength in meters.

The gain of an antenna is given by

$$G = 4\pi A_e / \lambda^2, \quad (2.2)$$

where A_e is the effective aperture of the antenna, which is defined as the ratio of the available power at the terminals of the antenna to the radiation intensity of the plane wave incident on the antenna in a given direction. The wavelength λ is equal to c/f , with c equal to the speed of light in meters per second, and f the carrier frequency in Hz.

2.1.2. Log-Normal Shadowing

Real world radio propagation rarely follows this simple free space model. In addition to possible free-space propagation, three additional “basic” mechanisms of radio propagation may be present as mentioned in Chapter 1: reflection, diffraction and scattering. All three of these phenomena can cause additional signal propagation losses. So in general, the average received power at a distance d from the transmitter is proportional to d^{-n} , where n is known as the *propagation path loss exponent*. The value of n is 2 for free space, 1.6-1.8 for indoor LOS [2], 4-6 for obstructed indoor [2], and often equal to 3-5 for outdoor terrestrial environments. In many cases, particularly for mobile communication, we do not attempt to predict signal strength precisely, but instead are interested in averages. In a given environment, we often seek a “local mean” value of received power. This local mean value of received signal power experiences variation

due to an effect called shadowing when there is no LOS. Shadowing occurs when the propagation path is obstructed by a very large obstacle (many wavelengths), analogous to the notion of optical shadowing. The additional shadowing loss can be modeled as a log-normal random variable [2]. We then can model the large scale propagation as follows:

$$P(d)(dBm) = P(d_0)(dBm) - 10n \log(d / d_0) + X_\sigma \quad (2.3)$$

where

$P(d)(dBm)$ = received power in dBm

$P(d_0)(dBm)$ = received power in dBm at a “close-in” reference distance d_0

n = path loss exponent parameter

d = distance between transmitter and receiver

d_0 = “close in” reference distance

X_σ = Gaussian random variable with zero mean and variance σ^2

The choice of close-in reference distance is important for design considerations and capacity analysis. It is a point from which a best fit mean-path loss exponent extends. The reference distance should always be in the far field of the antenna so that the near-field effects do not alter the reference path loss [3]. For microcellular and PCN systems, reference distances on the order of 1m to 100m are appropriate whereas in large coverage cellular systems, a 1km reference distance is commonly used [3].

2.2. Outdoor Propagation Models

Radio transmission often occurs over irregular terrains. The terrain profile effects the path loss and varies from region to region. Outdoor propagation models aim to predict signal strength at a particular point or a specific area. We discuss some of the common outdoor models for comparison with indoor propagation models and also for completeness.

2.2.1. Longley-Rice Model

The Longley/Rice propagation model is also known as the Irregular Terrain Model (ITM) [2]. It is intended for use with frequencies from 20 MHz to 20,000 MHz, and distances less than 2,000 km, for propagation near the earth's surface (typically ground-based transmitters and receivers). The model, which is based on electromagnetic theory and on statistical analysis of both terrain features and radio measurements, predicts the median attenuation of a radio signal as a function of distance and the variability of the signal in time and in space. It can also be executed as a computer program. The program takes various parameters into account as inputs, such as transmission frequency, path length, polarization (vertical or horizontal), antenna height (0.5-3000 meters), surface refractivity, effective radius of the earth, ground conductivity, ground dielectric constant, and climate. It can be executed in two different forms:

1. Point-to-Point Mode prediction-This is useful when a detailed terrain path profile is available and path specific parameters such as horizon distance of the antennas, horizon elevation angle, angular trans-horizon distance and terrain irregularity can be calculated easily.

2. Area Mode prediction-This mode is useful when a detailed terrain path is not available and the Longley-Rice model provides methods to calculate the above mentioned path specific parameters.

A large number of changes have been made in the original model since its publication [2]. One of the major drawbacks of the model is that there is no way to correct errors arising due to the effects of buildings and foliage around the receiver. Multipath fading is also not taken into account.

2.2.2. Okumura-Hata Model

One of the most commonly used outdoor signal prediction models is the Okumura model [2]. It is totally based on measurements and does not involve any analytical explanation. It is a highly simple and practical model and is widely used in modern land mobile radio systems in Japan and elsewhere.

The model operates in the frequency range 150 MHz to 1920 MHz and for distances of 1 km to 100 km. It is employed for base station antenna heights in the range of 30 m to 1000 m. Okumura, et. al. [2] developed a set of curves that show the median attenuation (A_{mu}), relative to free space as a function of frequency and distance, over a quasi-smooth terrain. Using Okumura's model, path loss can be determined by calculating the free space path loss and then adding the value of $A_{mu}(f, d)$, along with correction factors to account for the type of terrain. The model can be expressed as follows:

$$L_{50}(dB) = L_F + A_{mu}(f, d) - G(h_{te}) - G(h_{re}) - G_{area} \quad (2.4)$$

where L_{50} is the 50th percentile (median) path loss, L_F is the free space path loss, $G(h_{te})$ is the transmitter gain factor, $G(h_{re})$ is the receiver antenna gain factor, and G_{area} is the gain due to the type of environment. All these gain factors can be obtained using a set of equations given by Okumura.

One of the major shortcomings of the model is that it responds very slowly to the changes in terrain. Therefore it is suitable for urban and suburban areas but not quite accurate for rural areas.

The curves plotted by Okumura were reduced to a set of empirical formulae by Hata [4]. Hata considered the urban area propagation loss as a standard, and formulated modified equations to apply to other environments and situations. The basic formula for the median propagation loss given by Hata is,

$$L_{50}(urban)(dB) = 69.55 + 26.16\log(f_c) - 13.82\log(h_{te}) - a(h_{re}) + (44.9 - 0.55\log(h_{te}))\log(d) \quad (2.5)$$

where h_{te} and h_{re} are the base station and mobile station antenna heights in meters, respectively, d is the link distance (or cell radius) in kilometers, f_c is the centre frequency in megahertz, and the term $a(h_{re})$ is a vehicular station antenna height-gain correction factor that depends upon the environment.

The mobile antenna correction factor is given by the following:

For a small or medium sized city:

$$a(h_{re}) = (1.1 \log(f_c) - 0.7)h_{re} - (1.56 \log(f_c) - 0.8)dB \quad (2.6)$$

For a large city:

$$a(h_{re}) = 8.29(\log(1.54h_{re}))^2 - 1.1dB \quad \text{for } f_c \leq 300MHz \quad (2.7)$$

$$a(h_{re}) = 3.2(\log(11.75h_{re}))^2 - 4.97dB \quad \text{for } f_c \geq 300MHz \quad (2.8)$$

The results of the Hata model agree closely with the original Okumura model as long as d exceeds 1 km. This model is suitable for large cell mobile systems but not for personal communication systems as they often have cells on the order of 1km radius.

2.3. Indoor Propagation Models

With the increased use of wireless Local area networks (LANS) and personal communication systems, indoor propagation models have become very important. Indoor propagation is highly influenced by the wide assortment of construction materials used indoors, and there exists a great variation in possible transmitter (Tx) and receiver (Rx) placements relative to obstructions. In addition, depending upon carrier frequency, other effects caused by, for example, movement of people, may be present. The propagation in the interiors of buildings depends on factors such as the layout of the building, the construction material and the building type. We also have the following two types of losses [2]:

- 1) Same-Floor Partition Losses: Different buildings have different partitions and obstacles that form the internal and external structure. For instance there can be hard

partitions (that are part of the building structure) and soft partitions (movable and not attached to the ceiling). Due to the variations in their physical and electrical characteristics, it is difficult to apply one general model to account for such variations, but researchers have extensive data bases of losses for a number of partitions.

2) Between-floors Partition Losses: These losses are determined using the characteristics of the material employed for their construction, and the dimensions of the building.

2.3.1. Log-distance Path Loss Model

Theoretical and empirical models indicate that the average received signal power decreases logarithmically with distance for indoor wireless channels [2]. Indoor models mostly follow the distance power law equation-

$$PL(d)(dB) = PL(d_0)(dB) + 10n \log(d / d_0) + X_\sigma \quad (2.9)$$

where the path loss exponent n depends on the surroundings and building type, and varies in the range of 2 to 10, and X_σ is a normal (Gaussian) random variable in dB, having zero mean and standard deviation of σ dB. The equation for this model is functionally the same as that used in the discussion of log-normal shadowing.

2.3.2. Attenuation Factor Model

Seidel, et. al., [2] gave a model that includes the effects of building type as well as the variations caused by obstacles. It is flexible and was shown to reduce the standard deviation from 13 dB to 4 dB when the log distance model was employed for a selected set of two buildings. It is given by

$$PL(d)(dB) = PL(d_0)(dB) + 10n_{sf} \log(d / d_0) + FAF(dB) \quad (2.10)$$

where n_{sf} is the exponent value for the ‘same floor’ measurement, and FAF is a floor attenuation factor. This floor attenuation factor can be replaced by the exponent which considers the effects of multiple floor separation.

$$PL(d)(dB) = PL(d_0) + 10n_{mf} \log(d / d_0) \quad (2.11)$$

where n_{mf} is the path loss exponent based on measurements through multiple floors, i.e.,

$$n_{mf} = n_{sf} + FAF / [10 \log(d / d_0)] \quad (2.12)$$

2.4. Parameters Used in Propagation Models

In both indoor and outdoor radio channels, the average signal power received at the receiver decreases with distance. For any chosen Tx-Rx distance, the average path loss can be expressed as a function of distance by using a path loss exponent, n [2]:

$$PL(d) \propto (d / d_0)^n, \quad (2.13)$$

The path loss exponent depicts the rate at which path loss increases with distance. The value of n depends on the type of propagation environment. Researchers have calculated various values for different environments. Table 2.1 below shows some representative values [2].

Table 2.1. Path Loss Exponents for Different Environments [2].

Environment	Path Loss Exponent, n
Free Space	2
Urban area cellular radio	2.7 to 3.5
Shadowed urban cellular radio	3 to 5
In building line-of-sight	1.6 to 1.8
Obstructed in building	4 to 6
Obstructed in factories	2 to 3

The path loss for any random location having a particular Tx-Rx distance is typically statistically estimated using the close in reference distance (d_0), path loss exponent (n), and the standard deviation (σ). In practice, the values of n and σ are computed from measured data, using linear regression such that the difference between the measured and estimated path losses is minimized in a mean square error sense over a wide range of measurement locations and T-R separations [2].

Table 2.2 shows some example path loss exponents and standard deviation measured in different buildings [2]. Table 2.3 shows some example floor attenuation factors for two buildings [2].

Table 2.2. Path loss exponent and standard deviation measured in different buildings [2].

Building	Frequency (MHz)	n	σ (dB)
Retail Store	914	2.2	8.7
Office, hard Partition	1500	3.0	7.0
Office, soft Partition	900	2.4	9.6
Factory LOS	1900	2.6	14.1
Textile/Chemical	1300	2.0	3.0
Metal Working	1300	1.6	5.8
Indoor Street	900	3.0	7.0

Table 2.3. Average Floor Attenuation Factor in dB for One, Two, Three and Four Floors in an Office Building [2].

Building	FAF(dB)	σ(dB)	Number Of Locations
Office Building 1:			
Through One Floor	12.9	7.0	52
Through Two Floors	18.7	2.8	9
Through Three Floors	24.4	1.7	9
Through Four Floors	27.0	1.5	9

It can be observed that the attenuation between two of the floors in the building is greater than the incremental attenuation caused by each additional floor [2]. For instance the value of FAF through the first floor of the building is 12.9 dB, but with the addition of another floor the FAF only increases to 18.7 dB, which is an increment of only 5.7 dB—much smaller than the floor attenuation of 12.9 dB just on a single floor. Also, there

is an increase in floor attenuation of only 2.6 dB with four floors from a floor attenuation factor of 24.4 dB through three floors. It can be observed that even in a single building the FAFs vary considerably.

2.4.1. Limitations of Indoor Propagation Models

Improved propagation models are required to achieve reliable and accurate propagation predictions and help enable system designs that can overcome many indoor propagation impairments. The various challenges facing the development of indoor propagation models are as follows:

- 1) Propagation measurements primarily depend on often unavailable building construction parameters such as wall thickness, materials, and indoor building structures.
- 2) A large number of prediction methods require computation of the effects of multiple reflections and transmissions and hence become time consuming and computationally inefficient.
- 3) Most of the techniques are applicable to high frequencies and thus the dimensions of some indoor structures may not necessarily satisfy the large dimensions compared to the wavelength criterion required by these methods.
- 4) Nearly all data can be considered site specific.
- 5) The presence and motion of people inside the buildings also leads to inaccurate, or at least variable results.

With the increase in demand for indoor network planning tools, new propagation models and techniques are being developed. There has been ongoing work to study and

optimize models for short range communications, and many researchers are conducting measurements to validate the accuracy and improve the efficiency of conventional and new models [14].

2.5. Dispersive Channel Parameters

The mobile channel can be modeled as a linear, time varying filter with impulse response $c(t, \tau)$, which represents the response at time t to an impulse response at time $t-\tau$ [5].

In a mobile channel, a signal might be received via multiple propagation paths. Associated with each path are a propagation delay and an attenuation factor. Both these factors are generally time variant. Time variation results from spatial displacement (i.e., movement) of the Tx, the Rx or the scatterers, or a combination, or from time-varying effects in the medium. The latter effects are mostly negligible in the lower atmosphere at current day frequencies of operation. The received band pass signal over such a channel may be expressed as follows [5]:

$$x(t) = \sum_n \alpha_n(t) s(t - \tau_n(t)) \quad (2.14)$$

where

$\alpha_n(t)$ = attenuation factor for the signal received on the n^{th} path;

$\tau_n(t)$ = propagation delay for the n^{th} path.

$s(t)$ = transmitted signal

The time-variant impulse response is expressed as follows [5]

$$c(\tau; t) = \sum_n \alpha_n(t) e^{-j2\pi f_c \tau_n} \delta(\tau - \tau_n(t)) \quad (2.15)$$

where

$c(\tau; t)$ = response of the channel at time t due to an impulse input at time $t - \tau$;

f_c = carrier frequency.

The frequency domain representation of the impulse response is the transfer function, obtained by applying the Fourier transform to $c(\tau; t)$ [5]:

$$C(f; t) = \int_{-\infty}^{\infty} c(\tau; t) e^{-j2\pi f \tau} d\tau. \quad (2.16)$$

2.5.1. Channel Multipath Delay Spread

A number of useful correlation functions and power spectral density functions help to define the characteristics of a fading multipath channel. We use the equivalent low-pass impulse response $c(t; \tau)$, which is characterized as a complex-valued random process in the t variable. The impulse response $c(t; \tau)$ is assumed to be wide-sense stationary (in time). Then the autocorrelation function of $c(t; \tau)$ is defined as [5]

$$\phi_c(\tau_1, \tau_2; \Delta t) = \frac{1}{2} E[c^*(\tau_1; t) c(\tau_2; t + \Delta t)]. \quad (2.17)$$

where the asterisk denotes complex conjugation.

Generally, the attenuation and phase shift of the channel associated with path delay τ_1 is uncorrelated with that of path delay τ_2 . This is called uncorrelated scattering. It has the following effect upon the correlation function:

$$0.5E[c^*(\tau_1; t)c(\tau_2; t + \Delta t)] = \phi_c(\tau_1; \Delta t)\delta(\tau_1 - \tau_2) \quad (2.18)$$

If $\Delta t = 0$, the resulting autocorrelation function $\phi_c(\tau; 0) \equiv \phi_c(\tau)$ is simply the average power output as a function of the time delay τ . The range of values of τ over which $\phi_c(\tau)$ is essentially nonzero is called the multipath delay spread of the channel and is denoted by T_m . This function $\phi_c(\tau)$ is called the multipath delay profile, or power delay profile.

2.5.2. Frequency Correlation Functions

For randomly time varying channels, statistical moments of the channel's variations are often estimated to aid in the use of analytical methods for performance prediction. A key function on any fading channel is its spaced frequency correlation function (FCF). This function portrays information on the correlation of fading among different spectral regions over the proposed transmission bandwidth. If this correlation function's width relative to the signal bandwidth is small, signal distortion and intersymbol interference will occur during transmission.

When the transfer function of the channel is assumed to be a wide-sense stationary process (in frequency), its autocorrelation function is defined as [5]

$$\phi_C(\Delta f; \Delta t) \cong E[C^*(f; t)C(f + \Delta f; t + \Delta t)] \quad (2.19)$$

The autocorrelation function of $C(f; t)$ in frequency is a function of the frequency difference $\Delta f = f_2 - f_1$. Thus $\phi_C(\Delta f; \Delta t)$ is called the spaced-frequency, spaced-time correlation function of the channel. In practice, it can be measured by transmitting a pair of sinusoids separated by Δf and cross-correlating the two separately received signals with a relative delay Δt [5].

In general for a given value of Δt and Δf , we have an approximation to (2.18) as

$$\phi_C(\Delta f; \Delta t) \cong \frac{1}{N} \sum_{n=1+\Delta t}^N r_{f_1}(n) r_{f_1+\Delta f}^*(n - \Delta t) \quad (2.20)$$

where r_{f_1} is the received signal at frequency f_1

For $\Delta t = 0$ we have,

$$\phi_C(\Delta f) = \frac{1}{N} \sum_{n=1}^N r_{f_1}(n) r_{f_1+\Delta f}^*(n) \quad (2.21)$$

which represents the spaced frequency correlation function of the channel at time difference $\Delta t = 0$.

2.5.3. Coherence Bandwidth

As $\phi_C(\Delta f)$ is an autocorrelation function in the frequency variable it provides us with a measure of the frequency coherence of the channel. Due to the Fourier transform

relationship between $\phi_c(\Delta f)$ and $\phi_c(\tau)$, the reciprocal of the multipath spread is a measure of the coherence bandwidth of the channel. It is given by the expression

$$(\Delta f)_c \approx \frac{1}{T_m} \quad (2.22)$$

where, $(\Delta f)_c$ is the coherence bandwidth.

The coherence bandwidth indicates the range of frequencies over which the channel can be considered to have a nearly flat amplitude response; it thus predicts the frequency selectivity during transmission. If the coherence bandwidth is small compared to the bandwidth of the transmitted signal, the channel is known as frequency-selective and the signal can be severely distorted by the channel. On the other hand, if the coherence bandwidth is large in comparison to the bandwidth of the transmitted signal, the channel is said to be frequency-nonselective.

Chapter 3

Propagation Measurements and Analysis

The aims of these experiments were to measure the propagation path loss vs. distance on single and multiple floors, measure path loss due to walls, and characterize path loss in Stocker Center statistically. The values of path loss exponent (n) and standard deviation (σ) were calculated for each floor under the assumption that the path loss model is a log distance path loss model (equation (2.9)). As noted the frequencies used were the Industrial, Scientific, and Medical (ISM) bands at 900 - 928 MHz and 2.4 - 2.5 GHz.

3.1. Measurement Description

3.1.1. Equipment Used

The following equipment was used for the measurements:

- Spectrum Analyzer: Agilent E4404B ESA-E series spectrum analyzer (Serial No. US40240903). Frequency range: 9 kHz -6.7 GHz
- Signal Generator: Agilent E4432B ESG-D Signal Generator (Serial No. US40053897). Frequency range: 250 kHz- 3.0 GHz
- RF antennas, cables, measuring tapes, connectors and equipment cart.

3.1.2. Procedure

The experiments were conducted on all the five floors of Stocker Center. Line of Sight (LOS) and Non Line of Sight (NLOS) measurements were taken for each floor. A simplified block diagram of the measurement setup is shown in Figure 3.1

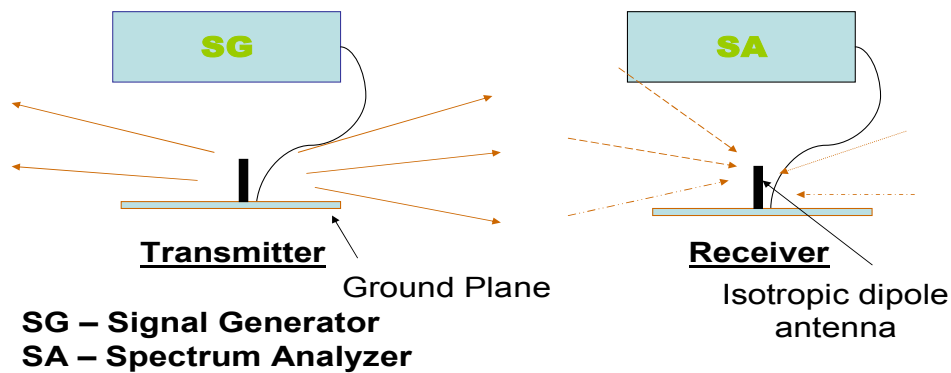


Figure 3.1 Block Diagram of the Measurement Setup

The signal generator is used as the transmitter and the spectrum analyzer as the receiver. The signal was transmitted either in the 900 MHz or 2.4 GHz band, with a transmit power value of -10dBm using the signal generator. The resolution bandwidth used was 50 kHz. A single sinusoidal tone was transmitted. The signal generator has a frequency accuracy of 0.005% typically. Table 3.1 gives the amplitude accuracy [6].

Table 3.1: Amplitude Accuracy of E4432B ESG-D Signal Generator

Level accuracy (dB) ¹	Output power		
	+7 to -120 dBm		
	(+10 to -120 dBm, -120 to -127 dBm, <-127 dBm)		
Freq range	Option UNB)	-127 dBm	<-127 dBm
250 kHz to 2 GHz	±0.5	±0.5	±1.5
2 to 3 GHz	±0.9	±0.9	±2.5
3 to 4 GHz	±0.9	±0.9 (±1.5, Option UNB)	±2.5

Retractable antennas were used as the transmitter and receiver antennas for convenience, and they were 1λ long, where λ is the radio frequency wavelength, approximately. The frequencies used were 900 MHz and 2.4 GHz. The wavelength λ is 0.33 meters at 900 MHz and 0.125 meters at 2.4 GHz. The antenna cable (cable connecting antenna to receiver (Rx)/transmitter (Tx)) had a cable loss of approximately 1.38 dB at 900 MHz and 2.98 dB at 2.4 GHz. The minimal value of SNR for these measurements was 11 dB. The sequence of steps followed for the experiments, for instance on third floor, was as follows:

- 1) The transmitter was placed at the east end of the central corridor outside room no. 323 (refer section 3.2).
- 2) The signal power at the receiver was first measured at a close in reference distance of 1 meter.
- 3) The first testing point was at a distance of 5 meters from the transmitter and each successive measurement was taken at a distance with an increment of 5 meters.

- 4) For every test distance, the received signal power level was measured five times and observations were recorded in the same plane at a distance of approximately $\lambda/4$ from the initial position. Averaging of the received power was done over these five measurements. Figure 3.2 illustrates how we collect data for a given distance.
- 5) The signal level was recorded at an interval of distance mentioned above until the receiver reached the west end of the main corridor.
- 6) A similar procedure was employed for measuring NLOS signals propagation. The distances for NLOS measurements were calculated using the shortest distance formula (Pythagorean Theorem).

This procedure was repeated for all the floors in Stocker Center. The table of measured data for path loss for all the floors is attached as Appendix B.

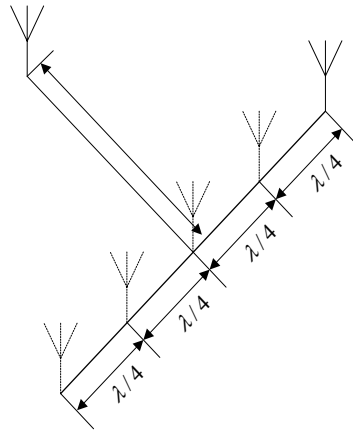


Figure 3.2. Data collection for a given distance d_0

3.2 Stocker Floor Plans

As stated earlier the measurements were conducted in the Stocker Engineering building. Figure 3.3 is an example floor plan of the second floor in Stocker, which illustrates the physical conditions for the measurement setup. The various labels are for the different transmitter and receiver positions. The symbols TX is the transmitter position for the Line of Sight and Non Line of Sight case. The Tx locations were chosen at the end of corridors to enable coverage of maximum distance. The symbols I to $I5$ are the receiver locations for the LOS condition and $N1$ to $N8$ are the receiver locations for NLOS. The plans for rest of the floors are placed in Appendix A.

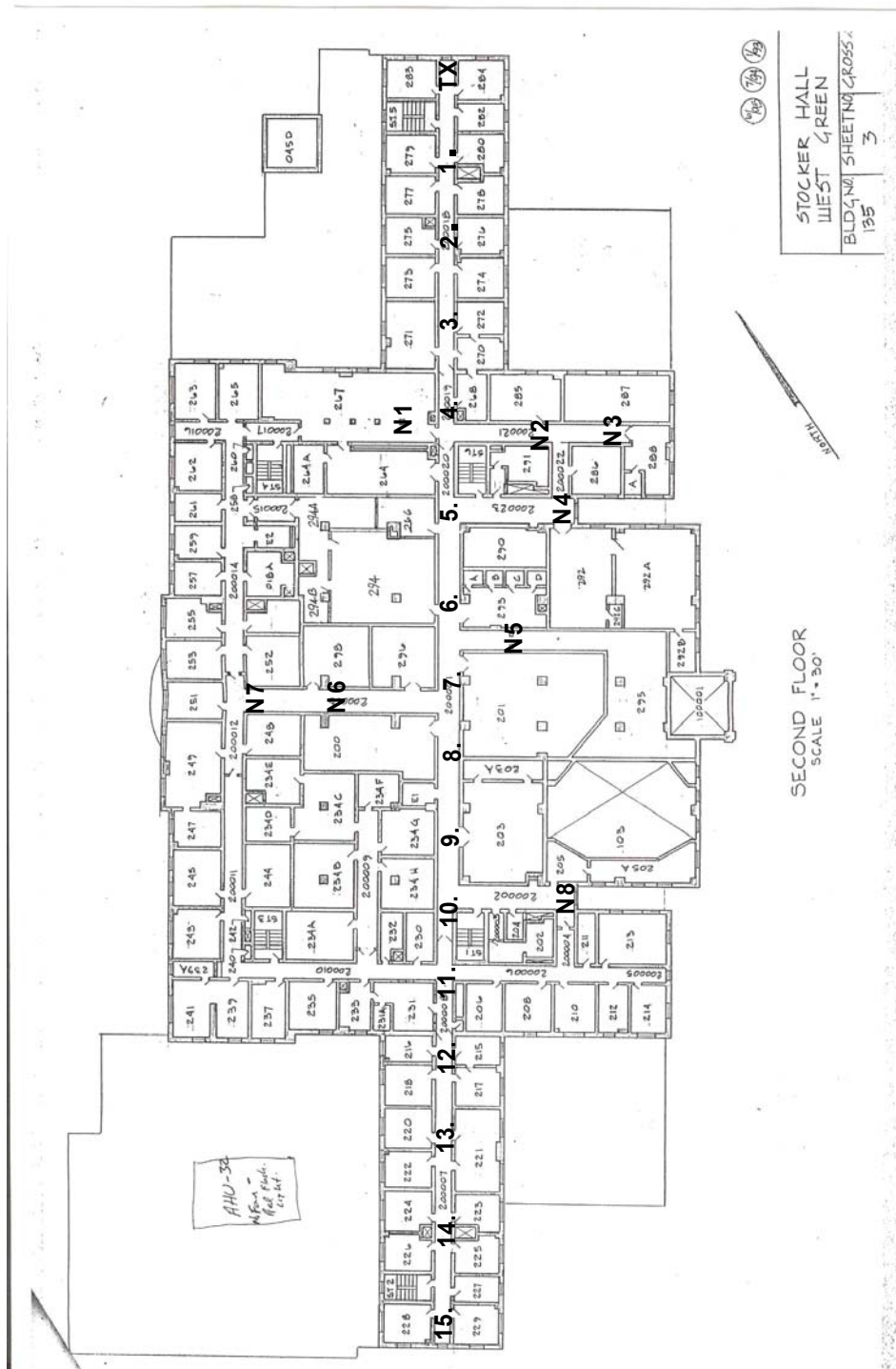


Figure 3.3. Layout of floor plan of second floor with transmitter and receiver locations

3.3. Example Measurement Results

The path loss data for characterizing the indoor wireless channel was measured at several points on each of the floors of the Stocker Center. In each plot the abscissa represents the distance in meters and the ordinate represents the path loss in dB. Within these plots (for each frequency), the plots are arranged in increasing order of floors (ground floor – fourth floor). For brevity only a few example plots are shown here, and the rest of the plots are attached as Appendix C. The equations needed to calculate the values of n and σ and the curve fit method are described in Section 3.4 below.

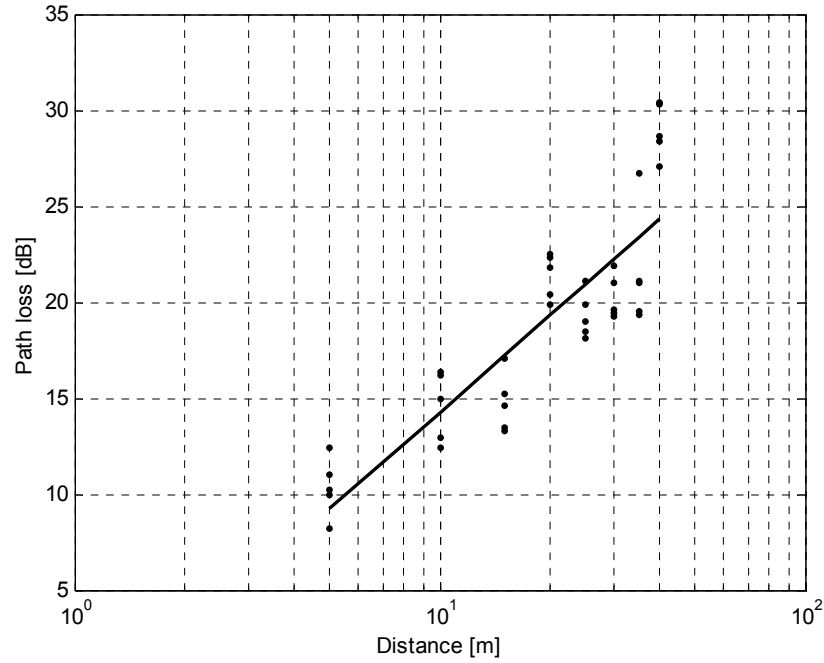


Figure 3.4. 900 MHz LOS Path Loss in Ground Floor of Stocker.

Figure 3.4 shows the path loss vs. distance on the ground floor of Stocker. It can be observed that as the distance increases, the path loss increases. The value of n was calculated as 1.67 and the standard deviation σ was equal to 2.7782 (refer table 3.2). The plot demonstrates the random variations about the mean path loss due to shadowing at different TX/RX locations. For this case, we obtained five values of path loss for each value of distance. These five different values were at different physical locations (refer Figure 3.2). The value of n depicts the rate at which the path loss increases with distance. It is in accordance with the values calculated by other researchers in similar environments [2].

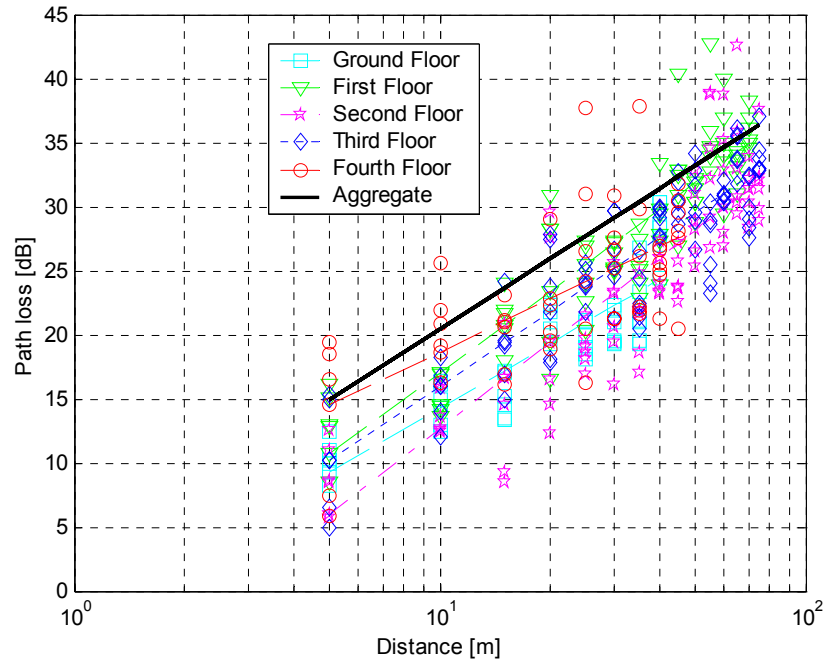


Figure 3.5. 900 MHz LOS Path Loss in all floors of Stocker.

Figure 3.5 shows the data and linear fits for all the floors in Stocker and also an aggregate fit for the data of all the floors. The different values of n and σ for different floors are presented in Table 3.2. For the best fit path loss exponent, σ was minimized over the entire scatter plot [3]. It can be observed from the different values that the Ground Floor has the best fit path loss exponent as the value of σ equals 2.7782 which is the lowest among all the floors.

Figures 3.6 to 3.9 shows plots of path loss vs. distance for different floors for the NLOS, LOS + NLOS cases in the 900MHz band and similar cases in the 2.4 GHz band. The fitted parameter values for different cases can be compared with reference to Table 3.2. The values of path loss exponent (n), standard deviation (σ), maximum and minimum spread of measurements on different floors are shown in the Table 3.2.

Table 3.2. Path loss exponent (n) and standard deviation (σ) calculated for different floors

Frequency-Mode-Floor	n	σ [dB]	Max-Spread[dB]	Min-Spread[dB]
900MHz-LOS-Ground	1.67	2.7782	7.4	2.58
900MHz-LOS-1 st	2.1184	3.4349	14.4	2.4
900MHz-LOS-2 nd	2.2133	4.4223	17.22	2.76
900MHz-LOS-3 rd	1.9335	3.2344	10.4	1.6
900MHz-LOS-4 th	1.3746	4.8635	21.37	5.41
900MHz-LOS-All floors	1.8275	6.4194	21.37	1.6
900MHz-NLOS- Ground	0.49901	3.9439	8.88	0.42
900MHz-NLOS-2 nd	0.53838	1.6381	7.13	0.08
900MHz-NLOS-3 rd	1.227	1.8528	7.6	0.5
900MHz-NLOS-All floors	1.602	4.1039	8.88	0.08
900MHz- Ground	1.1603	3.8901	21.37	0.08
900MHz- 2 nd	2.7777	7.6065	8.88	0.42
900MHz- 3 rd	2.2964	3.5796	17.22	0.08
900MHz-All floors	2.2099	6.8314	10.4	0.5
2.4GHz-LOS- Ground	1.8638	3.5454	5.07	1.77
2.4GHz-LOS-1 st	0.79895	3.9701	10	4.6
2.4GHz-LOS-2 nd	1.6993	2.9507	14.54	0.03
2.4GHz-LOS-3 rd	1.2331	5.006	8.2	1.8
2.4GHz-LOS-4 th	1.0074	3.2242	12.11	0.9
2.4GHz-LOS-All floors	1.1051	6.6067	14.54	0.03
2.4GHz-NLOS- Ground	-3.3315	3.3411	10	0.88
2.4GHz-NLOS-2 nd	-0.069686	0.28436	0.9	0.08
2.4GHz-NLOS-3 rd	1.2155	3.1905	1.7	0.48
2.4GHz-NLOS-All floors	0.73094	4.4362	10	0.08
2.4GHz- Ground	1.0476	5.5924	10	0.88
2.4GHz- 2 nd	1.6269	2.7393	14.54	0.03
2.4GHz- 3 rd	1.95	5.8594	8.2	0.48
2.4GHz-All floors	1.3084	6.6424	14.54	0.03

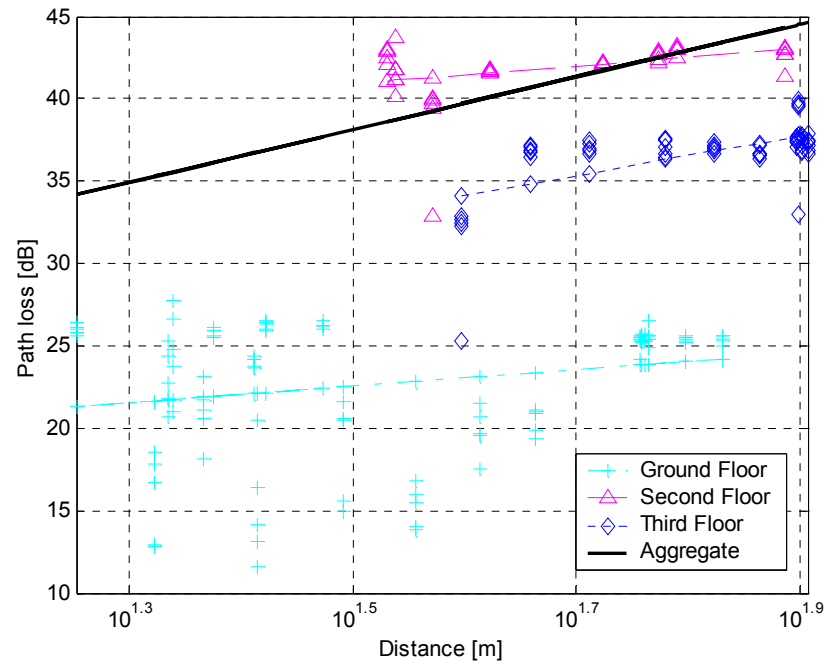


Figure 3.6. 900 MHz NLOS Path Loss in all floors of Stocker.

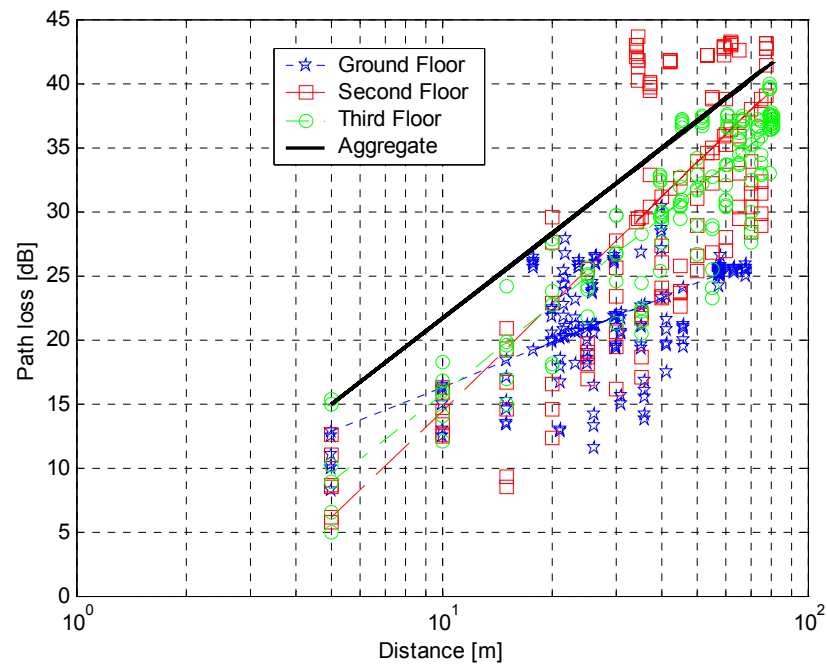


Figure 3.7. 900 MHz Path Loss in all floors of Stocker.

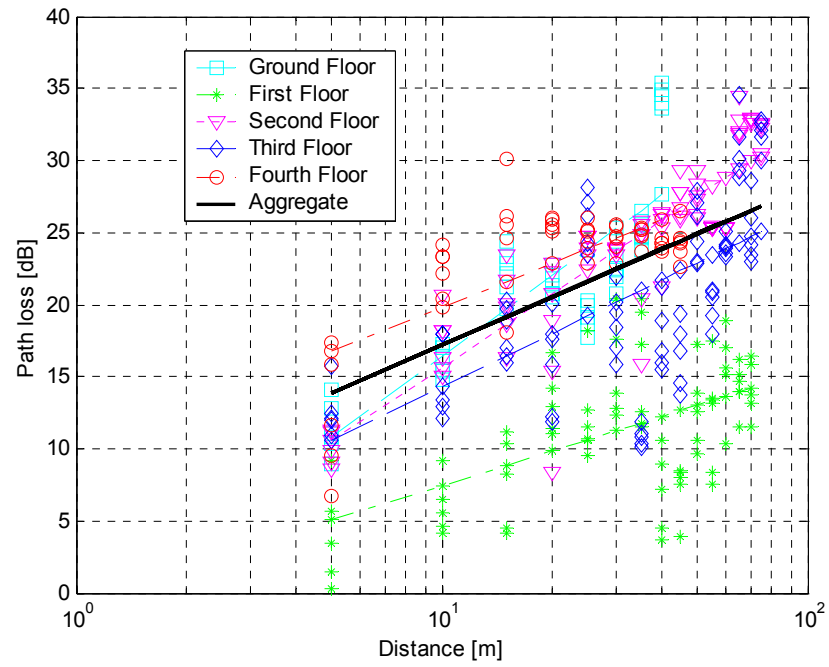


Figure 3.8. 2.4 GHz Path Loss LOS in all floors of Stocker.

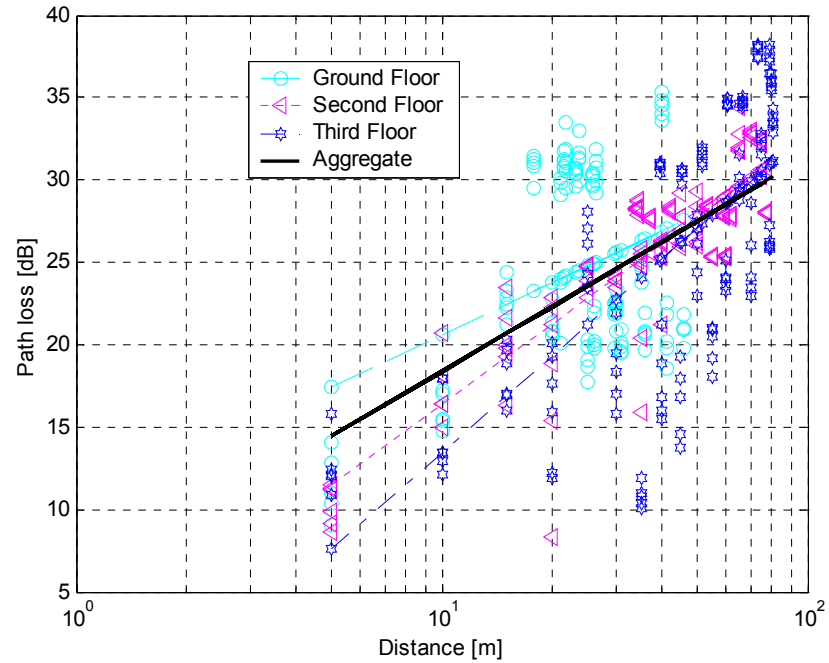


Figure 3.9. 2.4 GHz Path Loss in all floors of Stocker.

3.4. Data Analysis

As noted previously, our linear model can be summarized as follows: the path loss exponent n describes the rate at which the path loss increases with distance, and the precision of the path loss model is measured by the standard deviation σ of the random variable X_σ . We define the maximum and minimum spreads in path loss as the maximum and minimum variations of the path loss over a given data set, respectively. A data set for our purposes is described by the frequency band. Let the maximum variation of path loss be PLV_{max} , and the minimum variation be PLV_{min} . Then these spreads can be defined as

$$PLV_{max} = \max_d \max_l PL(d, l) \quad (3.1)$$

$$PLV_{min} = \min_d \min_l PL(d, l) \quad (3.2)$$

where $PL(d, l)$ represents the path loss with respect to the distance d and location l .

The mean path loss model statistically accounts for the clutter present in the environment at different locations with the same Tx/Rx separation distance. As the clutter changes from location to location, so does the received power, which introduces a random change in the path loss. This random change is modeled as Gaussian distributed.

3.4.1. Computation of Path Loss Exponent and Standard Deviation

The various parameters for the path loss model were calculated using Matlab programs. There are three programs: 1) PropagInStocker.m 2) PathLossModel and 3) PathLossGraph. These are given in Appendix E.

The Path Loss (PL) is calculated using the equation

$$PL = P_{d_0} - P_d \quad (3.3)$$

where P_{d_0} is the measured received power at distance $d_0 = 1$ m, and P_d is the measured received power at a distance d . The path loss exponent (n) and standard deviation (σ) is calculated using the least squares linear regression fit algorithm. Least Squares Regression is a method for finding the best fit of a model to data by minimizing the sum of squares of deviations between the data and model (the regression line) [7]. In regression analysis we have a dependent variable on the ordinate which is associated with an independent variable on the abscissa. If this association is linear, then the appropriate model is $Y = a + bX$. In our model, Y is the measured path loss, X is distance, and b represents the path loss exponent n .

Linear models can be fit by calculating the slope of the regression [7]:

$$n = I \sum_{i=1}^I \log d_i PL_i - \frac{(\sum_{i=1}^I \log d_i)(\sum_{i=1}^I PL_i)}{I \sum_{i=1}^I (\log d_i)^2 - (\sum_{i=1}^I \log d_i)^2} \quad (3.4)$$

where I is the total number of data points. Thus the value of n can be calculated using (3.4). After this has been done, the residual variation of data from the fitted model is assumed to be due to random variability. If PL_i is the actual value of the dependent variable associated with the value d_i of the independent variable, then expected value of PL_i according to the model is $E[PL_i] = a + n \log d_i$, and the variation of the observed value from this expectation is $PL_i - (a + n \log d_i)$. The "variance about the regression line" is, therefore,

$$s^2 = \sum_{i=1}^I [PL_i - (a + n \log d_i)]^2 / I - 2 \quad (3.5)$$

and the value of standard deviation (σ) is the square root of (3.5).

3.5. Discussion

In this experiment, after measuring the path loss at a number of locations, LOS as well as NLOS, we calculated propagation path loss exponents and standard deviations to characterize the path loss in this indoor wireless channel. The experimental results are satisfactory in the sense that they agree with the values calculated by other researchers in similar indoor environments [2]. The experimental values obtained for Stocker Center do not exactly agree with the values given in [2] because the structure of each building is unique, and path loss is a function of to a number of parameters that include physical ones (building material density, metal content in the structure etc.). Hence, exact agreement would not be realistic. Yet our results are also close to those in [3], and [8]

and so, given these agreements and the relative simplicity of the model, the path loss statistics we obtained are realistic and useful.

According to our observations, for the LOS case, the path loss increases as the distance between the transmitter and receiver increases. This is in agreement with the basic radio propagation concepts. For NLOS, the path loss values were sometimes inconsistent, i.e., the path loss sometimes decreased with distance. We attribute this to significant wave guiding in hallways, and diffraction around corridor corners.

Chapter 4

Dispersive Channel Measurements

The aims of this experiment were to obtain estimates of the magnitude of the transfer function, examples of its spatial variation, and amplitude frequency correlation functions from propagation measurements on all the floors of Stocker Center. The frequencies were again the Industrial, Scientific, and Medical (ISM) bands at 902 - 928 MHz and 2.4-2.5 GHz.

4.1. Measurement Description

4.1.1. Equipment Used

The equipment was the same as listed in Chapter 3. The experiment was conducted on all the five floors of Stocker Center. The simplified block diagram of the measurement set up is shown in Fig. 3.1. Signals were transmitted in the frequency range of 902-928 MHz with a power of -10 dBm using the signal generator.

Typically, the signal generator has a frequency accuracy of 0.005%. Table-3.1 from Chapter 3 gives the amplitude accuracy of the signal generator. The signal was received using the spectrum analyzer. The transmitted signal is a sinusoidal tone, whose amplitude was held constant and whose frequency is constant for some duration denoted as the dwell time T_d . The frequency was then “stepped.” The dwell time for the spectrum analyzer was set to 4 milliseconds; the span for each band was 26 MHz, and the

step dwell of the signal generator was 500 milliseconds. Figure 4.1 shows the transmitted signal for a single sweep.

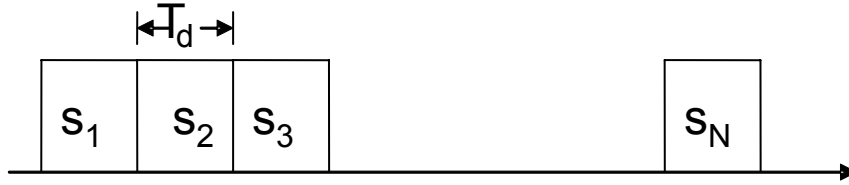


Figure 4.1. Transmitted signal for a single sweep

$$S(t) = \sum_{i=1}^N s_i(t) p(t - kT_d) \quad (4.1)$$

where T_d = dwell time of the signal

$$s_i(t) = A \cos(2\pi f_i t + \theta) \quad (4.2)$$

The sweep time, $T_{sweep} \cong NT_d$ and $S_k = S_i(t)$ for $i=k$. The total signal power is $P_s = A^2 / 2$ and, $f_i = 902\text{MHz} + i\text{MHz}$ where $i = 1, 2, \dots, 26$. That is, for the 900 MHz measurements, our frequency resolution was 1 MHz. This is convenient as the computations can be done in a reasonable amount of time and it also provides adequate frequency coverage. Also for wireless LAN applications, the frequency spectrum is

approximately larger or nearly equal to the signal bandwidth. If there is only a single path between transmitter and receiver, the received signal is given by

$$r_i(t) = \alpha s_i(t - \tau) + n_i(t) \quad (4.3)$$

where $S_i(t)$ is given by equation (4.2) and $n_i(t)$ is the additive white Gaussian noise. As in Chapter 3, the minimal SNR was approximately 11 dB. We are in effect *sampling* the channel transfer function amplitude (actually amplitude squared) at discrete frequency points. The steps involved for the experiment, for instance on the third floor, are as follows.

1. The transmitter was placed at the east end of the central corridor outside room number 323.
2. The first testing point was at a distance of 10 meters from the transmitter, and each successive measurement of received power was taken at a distance with an increment of 10 meters.
3. For every Rx location, the received signal power level was measured for a set of sample frequencies in the range of 902-928 MHz at intervals of 1 MHz (see eq. (4.2))
4. At every Rx location, the received signal power level was measured two times (for each frequency sample) in the same plane at a distance of approximately $\lambda/2$ apart. The average of the transfer function amplitude at these two spatial locations was computed for each frequency point. Figure 4.2 illustrates how we collect data for

a given distance. We define these two measurements as Measurement # 1 and Measurement # 2.

5. The signal level was recorded at intervals of 10 m until the receiver reached the west end of the main corridor.

6. A similar procedure was applied on all the other floors of Stocker. The table of measured data for all the floors is attached as Appendix D.

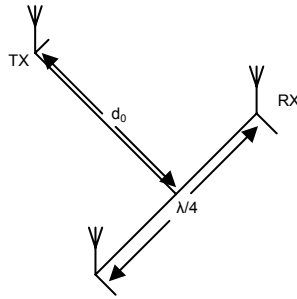


Figure 4.2. Data collection for a given distance d_0 .

4.2. Example $|H(f)|^2$ Results

The data for estimating the transfer function was measured at several points (locations) on all the floors of Stocker Center. The experimental data is presented in Appendix I.

The range of received power levels $(\Delta H^2)_{\max}$ is defined as follows:

$$(\Delta H^2)_{\max} = \max_f |H(f)|^2 - \min_f |H(f)|^2 \quad (4.4)$$

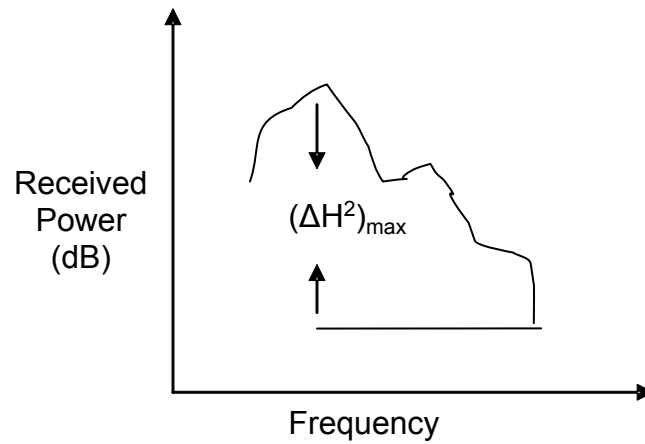


Figure 4.3. Example Plot showing $(\Delta H^2)_{\max}$

The (ΔH^2) values provide a measure of the range of signal powers in a particular frequency range. Conceptually, they can be related to the standard deviations of propagation path loss in Chapter 3. For instance, on the ground floor at a distance of 20 m from the transmitter there is almost flat fading between the frequency range from 905 MHz to 906 MHz. But there is a 8dB drop in the power level at a distance of 30 m on the ground Floor between 902 MHz to 903 MHz.

The values of $(\Delta H^2)_{\max}$ calculated at different distances for every floor are shown in Table 4.1. Given the relatively short range and fairly complex scattering environment, the values of $(\Delta H^2)_{\max}$ do not exhibit any regular trend vs. distance. For a much larger range of distance, more reflections and much larger path delays would be encountered. This could cause $(\Delta H^2)_{\max}$ to increase with distance.

Table 4.1 Range of received power levels (in dB) [$(\Delta H^2)_{\max}$]

Distances	10m	20m	30m	40m	50m	60m	70m
Ground Floor	3.83	6.04	14.03	1.77	-	-	-
First Floor	8.83	5.18	5.63	8.08	7.88	8.63	6.52
Second Floor	1.93	5.67	4.69	4.02	3.14	3.8	-
Third Floor	2.73	1.45	1.45	3.97	2.69	4.33	1.76
Fourth Floor	5.04	5.89	3.12	4.04	-	-	-

The plots of power vs. frequency for Measurement #1 and the frequency correlations computed from it are in Figures 4.4 through 4.17. The plots are arranged according to each floor. Each plot consists of transfer functions at various distances from the transmitter on a single floor for both Measurement #1 and #2. As mentioned, Measurement #1 and Measurement #2 are the two spatial locations of the receiver at the particular distance from the transmitter on every floor. For brevity, plots for Measurement 2 are placed in Appendix E. The MATLAB code used to generate these values and plots is attached as Appendix F. All plots are normalized for peak at 0 dB since we are interested in the variation with frequency only here.

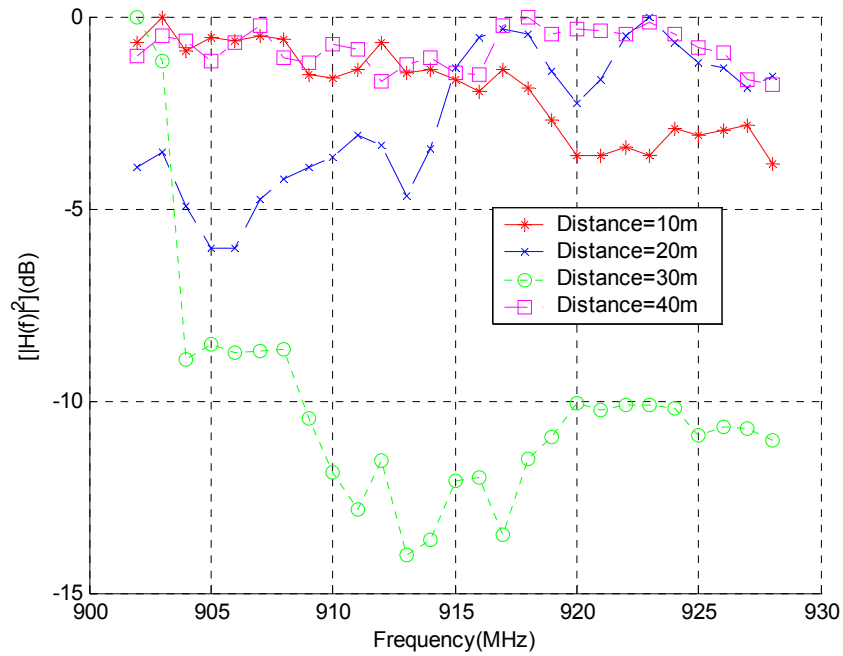


Figure 4.4. Variation of power with frequency for Measurement #1 on Ground Floor of Stocker center at various distances from the transmitter for 902-928 MHz.

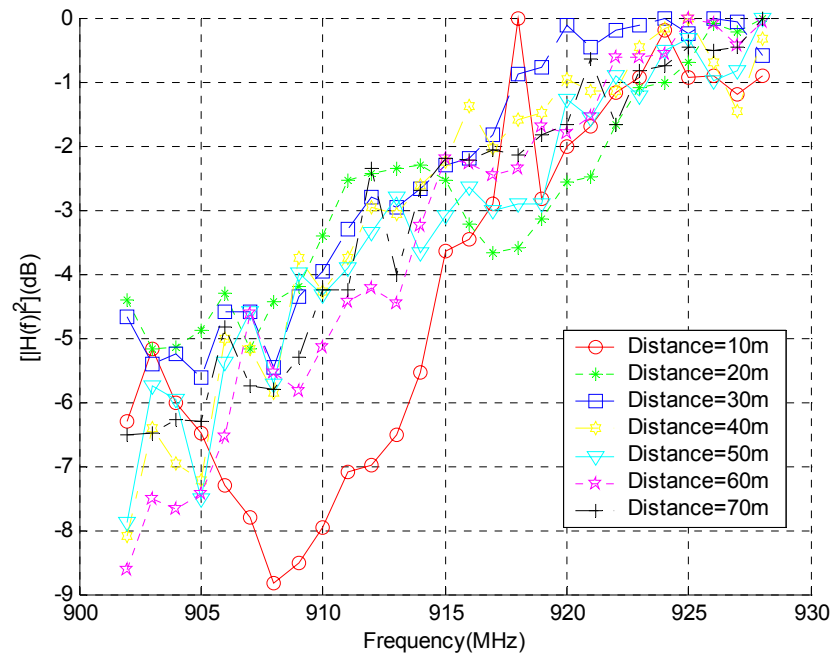


Figure 4.5. Variation of power with frequency for Measurement #1 on First Floor of Stocker center at various distances from the transmitter for 902-928 MHz.

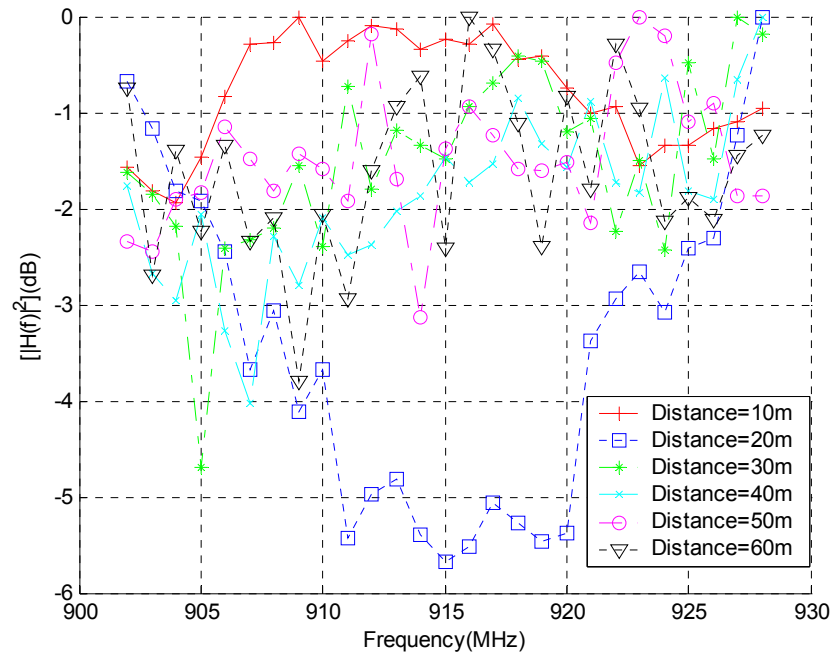


Figure 4.6. Variation of power with frequency for Measurement #1 on Second Floor of Stocker center at various distances from the transmitter for 902-928 MHz.

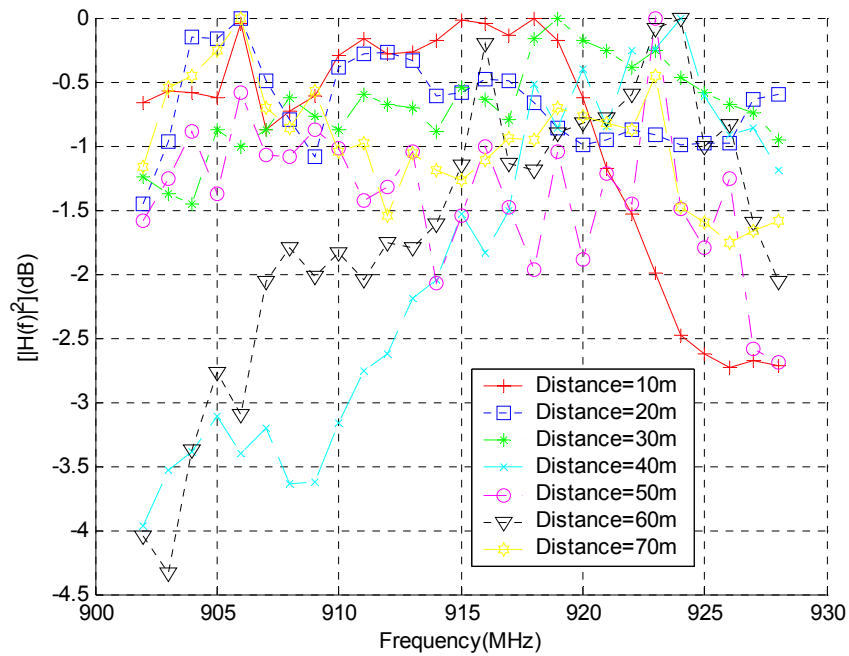


Figure 4.7. Variation of power with frequency for Measurement #1 on Third Floor of Stocker center at various distances from the transmitter for 902-928 MHz.

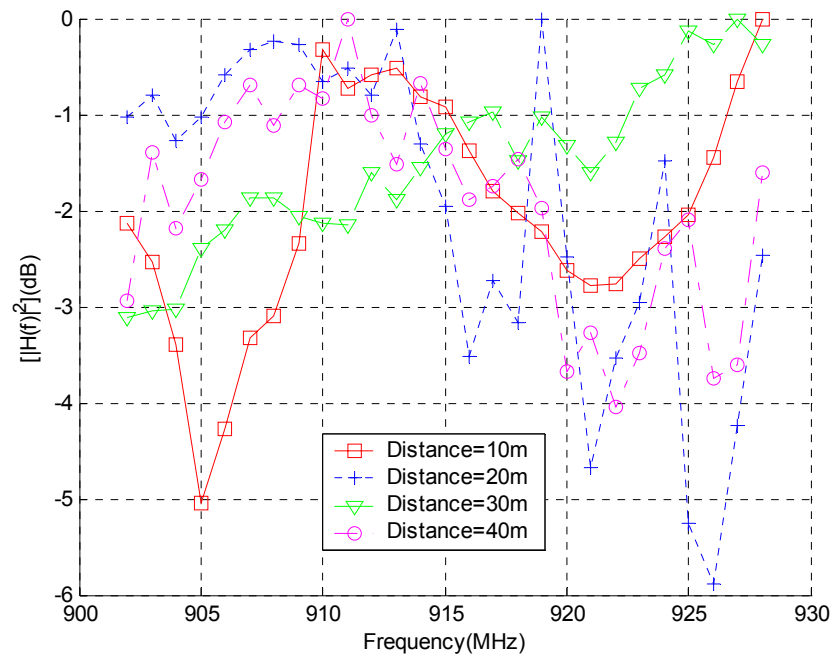


Figure 4.8. Variation of power with frequency for Measurement #1 on Fourth Floor of Stocker center at various distances from the transmitter for 902-928 MHz.

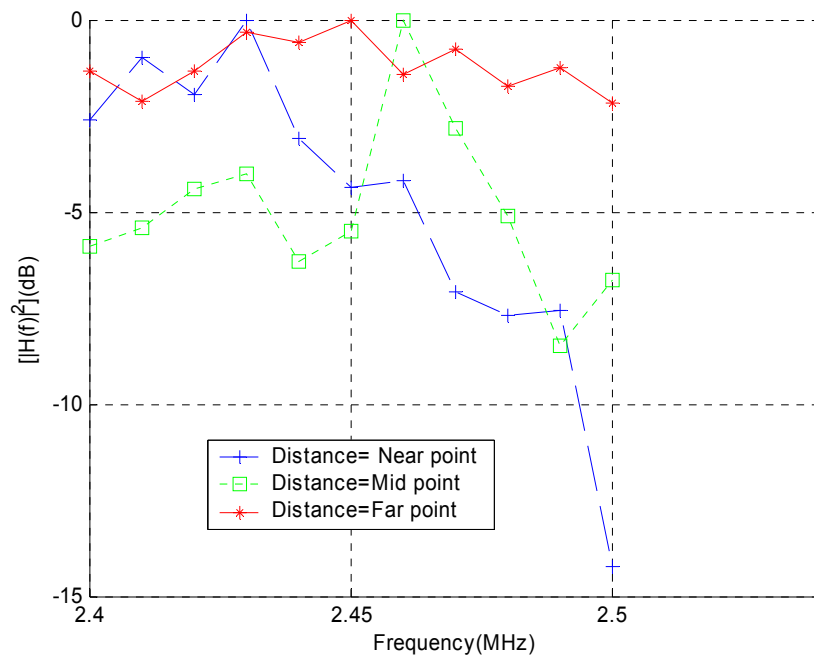


Figure 4.9. Variation of power with frequency for Measurement #1 on Third Floor of Stocker center at various distances from the transmitter for 2.4-2.5 GHz.

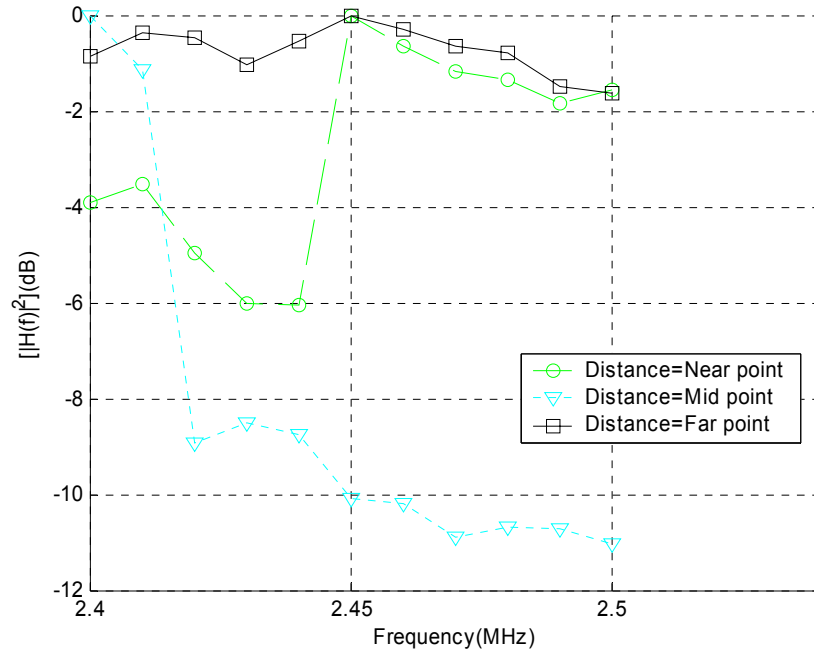


Figure 4.10. Variation of power with frequency for Measurement #1 on Second Floor of Stocker center at various distances from the transmitter for 2.4-2.5 GHz.

The autocorrelation function of a signal has been explained in detail in Section 2.5.2 of Chapter 2. The autocorrelation function we compute here is given by (refer equation 2.18):

$$\phi_{C^2}(f_1, f_2; \Delta t) = |C^*(f, t)|^2 \cdot |C(f + \Delta f, t)|^2 \quad (4.5)$$

This function is computed using the amplitude-squared transfer function data. Figures 4.11 to 4.17 are the spaced frequency amplitude autocorrelation function plots for different floors of Stocker for Measurement #1 and Measurement #2.

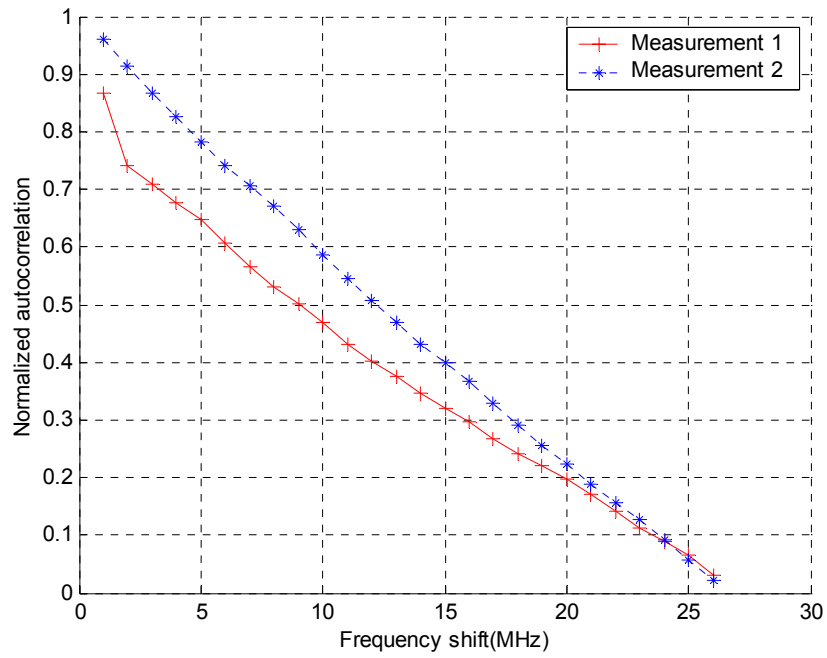


Figure 4.11. Spaced frequency amplitude autocorrelation (902-928 MHz) for Ground Floor.

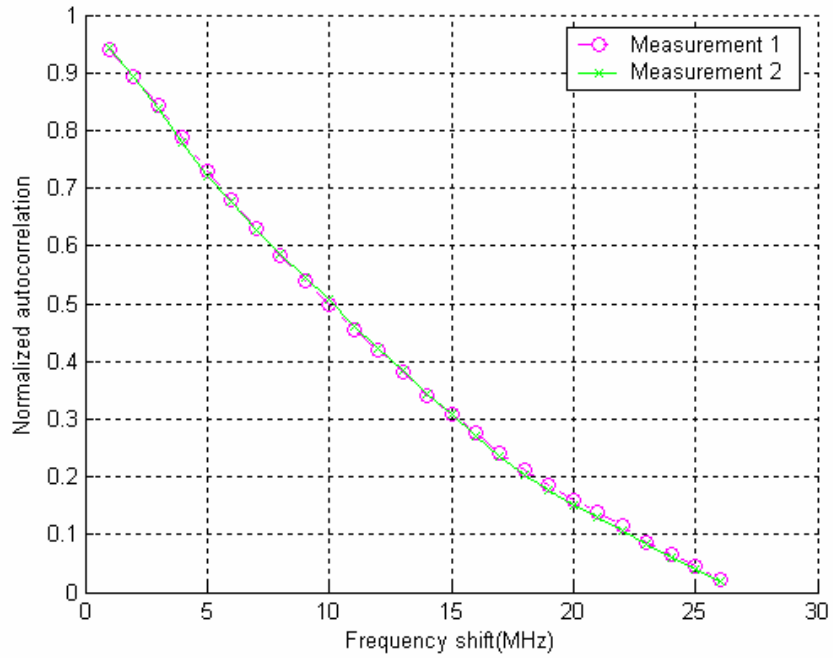


Figure 4.12. Spaced frequency amplitude autocorrelation (902-928 MHz) for First Floor.

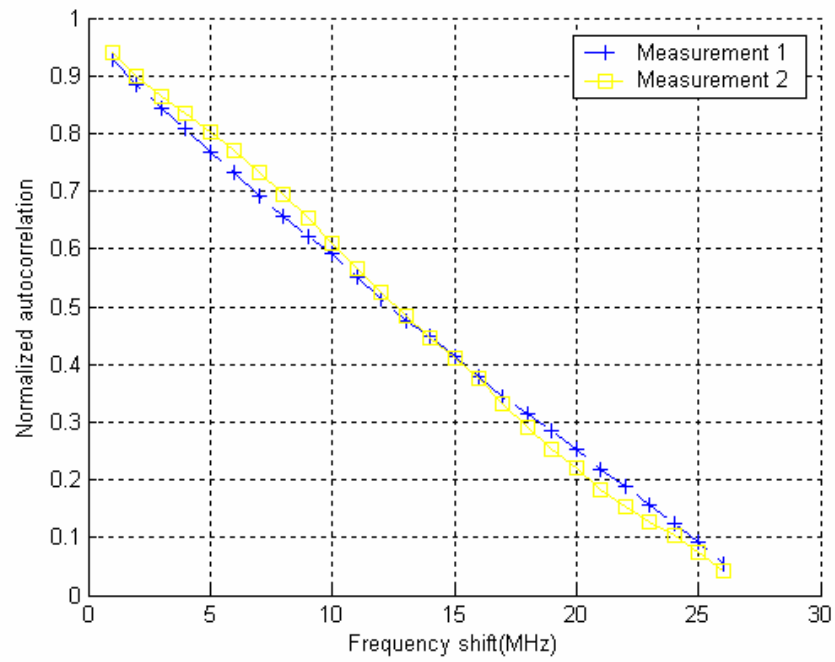


Figure 4.13. Spaced frequency amplitude autocorrelation (902-928 MHz) for Second Floor.

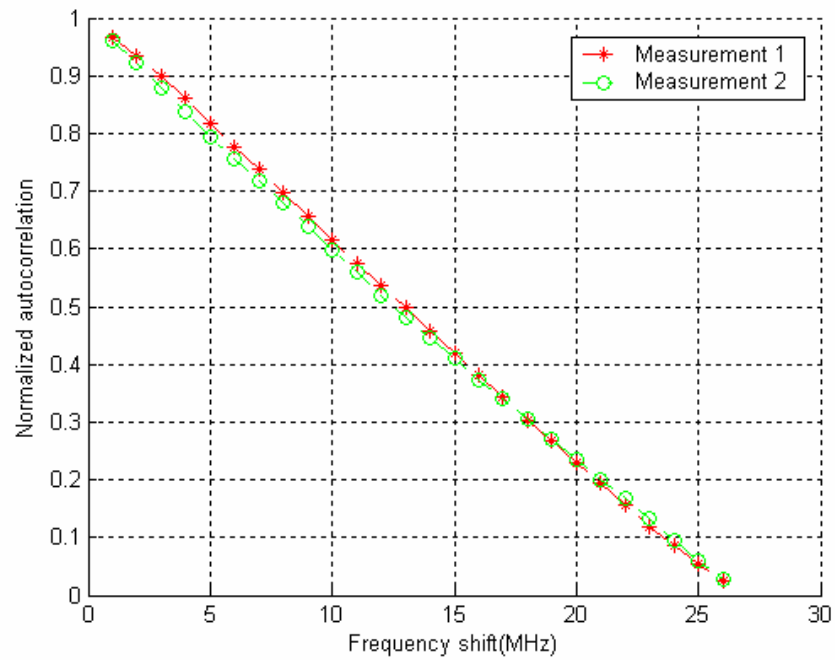


Figure 4.14. Spaced frequency amplitude autocorrelation (902-928 MHz) for Third Floor.

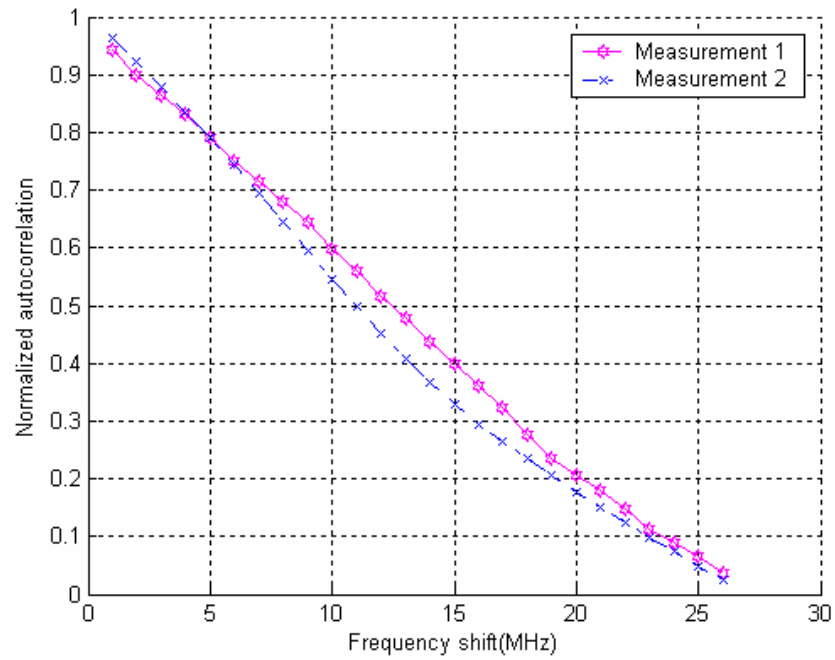


Figure 4.15. Spaced frequency amplitude autocorrelation (902-928 MHz) for Fourth Floor.

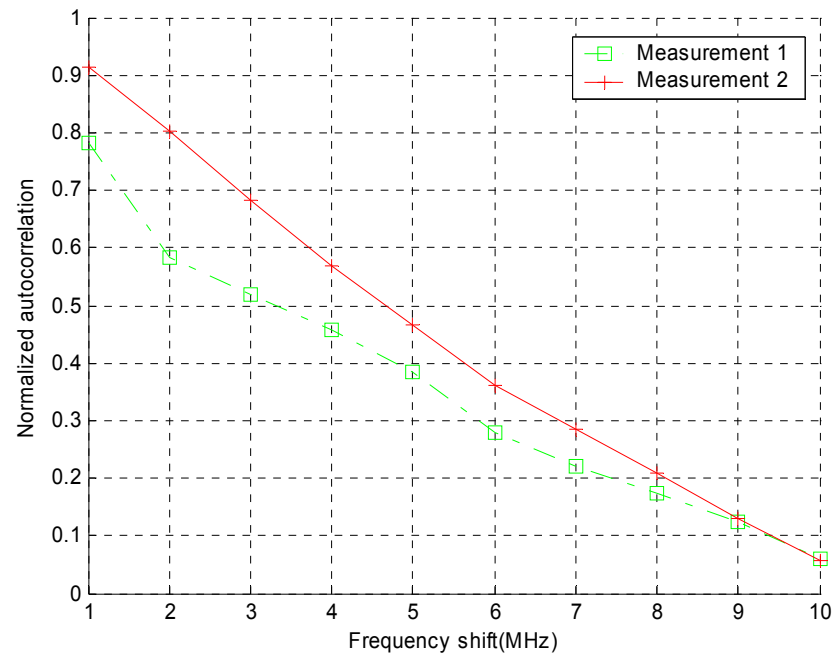


Figure 4.16. Spaced frequency amplitude autocorrelation (2.4-2.5 GHz) for Second Floor

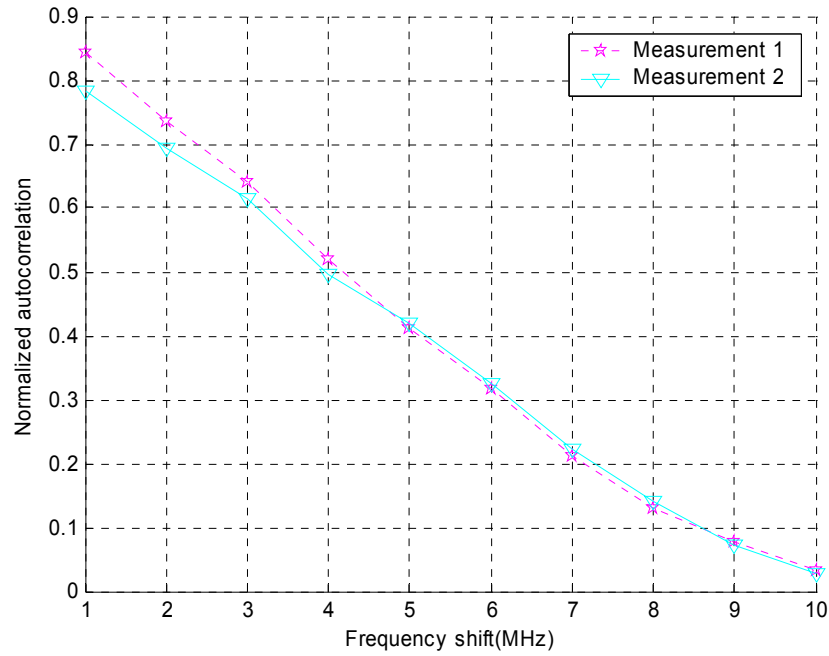


Figure 4.17. Spaced frequency amplitude autocorrelation (2.4-2.5 GHz) for Third Floor.

4.3. Data Analysis

4.3.1. Approximation of Frequency Correlation Functions

The function `correlation.m` takes the received power at each frequency as the input and calculates the autocorrelation, according to equation (4.6) and (2.18), i.e.,

$$\phi_{C^2}(f_1, f_2; \Delta t) = |C^*(f, t)|^2 \cdot |C(f + \Delta f, t)|^2 \quad (4.6)$$

The function `ChannelEstimation.m` is the main program. It takes in the measured data and calls the correlation function routine. It calculates the range of power for each

floor at every distance $[(\Delta H^2)_{\max}]$ and generates the power vs. frequency and spaced frequency correlation plots.

The frequency f_H^2 is approximately equal to f_c . For instance for $\phi_{H^2} = 0.5$, the value of f_H^2 is approximately between 9-12 MHz from Figure 4.9-4.13. Similarly for $\phi_{H^2} = 0.1$, f_H^2 is between 22-24 MHz. We cannot precisely say that $T_m \sim 1/f_H^2$, but it closely flows the relation.

4.4. Summary

Transfer function amplitude measurements in the ISM frequency bands were taken. The following data were obtained:

- (i) Received signal power vs. frequency, i.e., amplitude of channel transfer function.
- (ii) Spaced frequency amplitude squared correlation of the channel transfer function magnitude vs. Δf .
- (iii) The range of received power $(\Delta H^2)_{\max}$.

The value of the spaced-frequency correlation of the channel transfer function magnitude decreased with increasing Δf , which is in accordance with the expected result for fading multipath channels [9]. Future work involves devising a means to approximate calculating the multipath delay spread and the coherence bandwidth from this.

Chapter 5

Conclusion and Future Work

In this Chapter we summarize and conclude the research performed in this thesis. Future work in certain areas is also suggested.

5.1. Summary of Research

This thesis consisted of two parts. In the first part, we measured the path loss vs. distance on all the floors of Stocker Center. The propagation measurements were conducted in the ISM bands (900 MHz and 2.4 GHz) for both the LOS and NLOS cases. We observed, as expected, that the path loss increases as distance increases. The values for path loss exponent and standard deviation were calculated, and the results obtained matched well with results obtained by other researchers in similar environments [2]. In certain NLOS cases, for instance, the NLOS case on the ground floor for 2.4GHz, We observed that the path loss decreased with distance. This can be attributed to significant wave guiding in hallways, and diffraction around corridor corners.

The second part of the thesis involved estimating the magnitude (squared) of the transfer function, examples of its spatial variation and amplitude squared frequency correlation functions from propagation measurements.) Plots of the received signal power (amplitude square) vs. frequency and spaced frequency amplitude correlation of the channel transfer function magnitude vs. Δf were obtained. The values of range of

received power $(\Delta H^2)_{\max}$ were also obtained. The value of the spaced-frequency amplitude squared correlation of the channel transfer function magnitude decreased with increasing Δf , which is in accordance with the expected result for fading multipath channels [5]. We found $f_H^2(\sim f_c)$ was approximately 10 MHz.

A number of wireless networks have been set up in Stocker. The results obtained provide values one could expect for path loss and signal strength in the various floors. The results of this experiment help could be used to determine base station locations, number of base stations required, etc; in Stocker Center.

5.2. Future Work

Future work includes conducting more measurements and covering more data points on each floor, and also better averaging of the results. Additional data points would help to increase the accuracy of the model. We should also try to use more efficient equipment like the antennas used for collecting data. We have conducted experiments with only one transmitter location and within the building. In order to obtain a more efficient model, consider more transmitter locations, and also calculate the path loss between floors. In addition, we could perform propagation measurements from inside to the outside or just outside the building, to enable prediction for LAN users.

The experiments were performed taking caution that there were no obstacles between the receiver and the transmitter. For example, movement of people causes an effect on the results. Thus trying to come up with methods which would account for the presence or absence of obstacles would help. Calculating the Rician K-factors would be

useful. Time variations of fixed wireless channels result from the relative movement of scatterers in the propagating environment [13]. Finally implementing a method for estimating the Doppler spectrum from the received signal's power samples, without requiring the phase information would provide a more comprehensive characterization of the channel [13].

References

- [1] Bernard Sklar, *Digital Communications: Fundamentals and Applications*, Pearson Education, 2nd Edition, 2001.
- [2] Theodore S. Rappaport, "The Wireless Revolution", *IEEE Communications Magazine*, vol. 29, Issue: 11, pp.52, 61-71, November 1991.
- [3] Theodore S. Rappaport, *Wireless Communications Principles & Practice*, Prentice Hall, New Jersey, 1996.
- [4] J. D. Parsons, *The Mobile Radio Propagation Channel*, John Wiley & Sons Ltd, 2nd Edition, 2000.
- [5] John G. Proakis, *Digital Communications*. McGraw-Hill, 4th Edition, 2001.
- [6] Agilent Technologies, *ESG Family Signal Generators- User's and Programming Guide*, April 2000.
- [7] Eric W. Weisstein, *Mathworld.wolfram.com*, Wolfram Research, Inc, 1999-2004, November 22 2003.
- [8] "Wireless Communications Demo Edition", 1997© John Davis, II Jean Paul M. G. Linnartz, 1993, 1996.

- [9] Robert J. C. Bultitude, "Estimating frequency correlation functions from propagation measurements on fading radio channels: A critical review," *IEEE Journal on Selected Areas In Communications*, vol.20, no.6, pp.1133-1143, August 2002.
- [10] "An Introduction to Indoor Radio Propagation", Design Topics, *Spread Spectrum Scene*, January, 2001.
- [11] Gordon L. Stuber, *Principles of Mobile Communication*, Kluwer Academic Publishers, 2nd Edition, February 2001.
- [12] Chatterjee, S., Hadi, A., and Price, B. "Simple Linear Regression." Ch.2 in *Regression Analysis Example*, 3rd ed. New York, Wiley, pp. 21-50, 2000.
- [13] Andrej Domazetovic, Larry J. Greenstein, Narayan B. Mandayam, and Ivan Seskar, "Estimating the Doppler Spectrum of a Short-Range Fixed Wireless Channel", *IEEE Communications Letters*, vol 7, no. 5, May 2003.
- [14] Magdy F. Iskander, *Channel Characterization and Propagation Models for Wireless Communication Systems*, www.wtec.org/loyola/wireless/04_02.htm, July 2000.

Appendix A

Stocker Floor Plans

The layouts for the different floors of Stocker are presented with the transmitter and receiver locations. These plans help to understand the physical conditions of the measurement set up. Figure A.1 to A.5 shows the plans for the different floors. The transmitter location is labeled as TX . The LOS receiver locations are numbered 1,2,..... and the NLOS locations are labeled as N1, N2,.....and so on depending on the number of points measured. For ground floor the transmitter location for NLOS and LOS case is different. Thus we denote the LOS case by TX and NLOS case by TXN . The points 1 through 8 are common for both LOS and NLOS incase of ground floor.

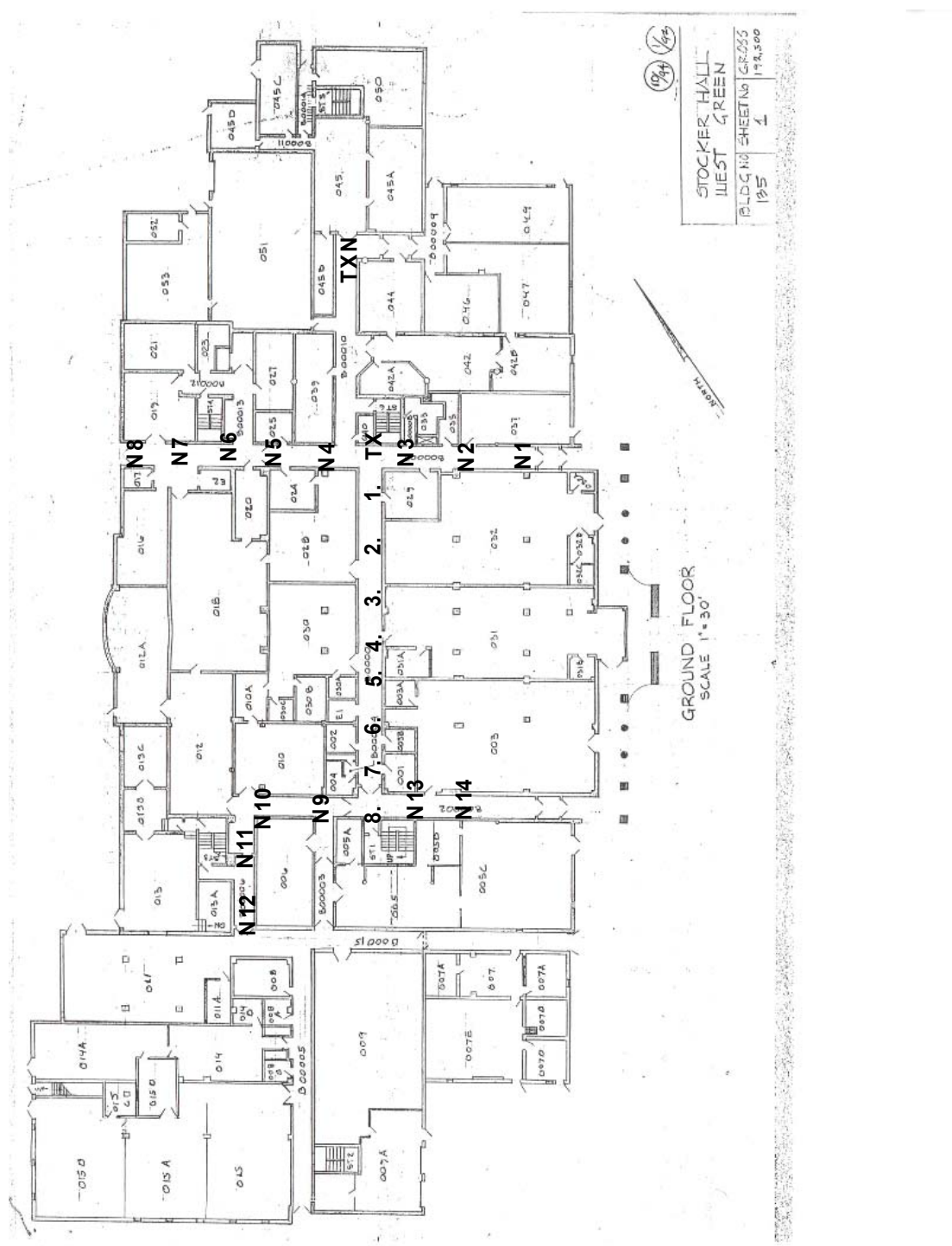


Figure A.1. Layout of floor plan of ground floor with transmitter and receiver locations.

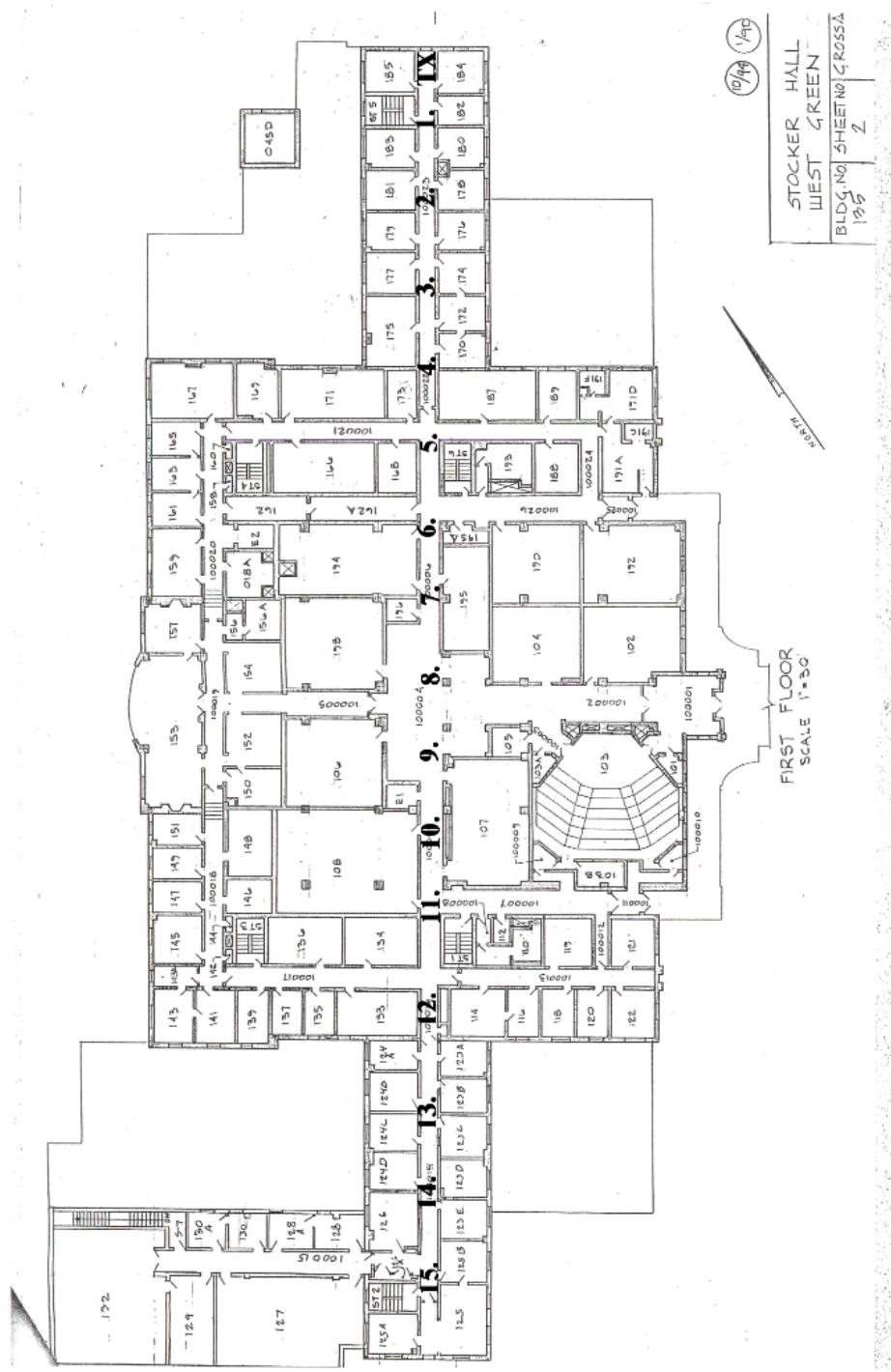


Figure A.2. Layout of floor plan of first floor with transmitter and receiver locations.

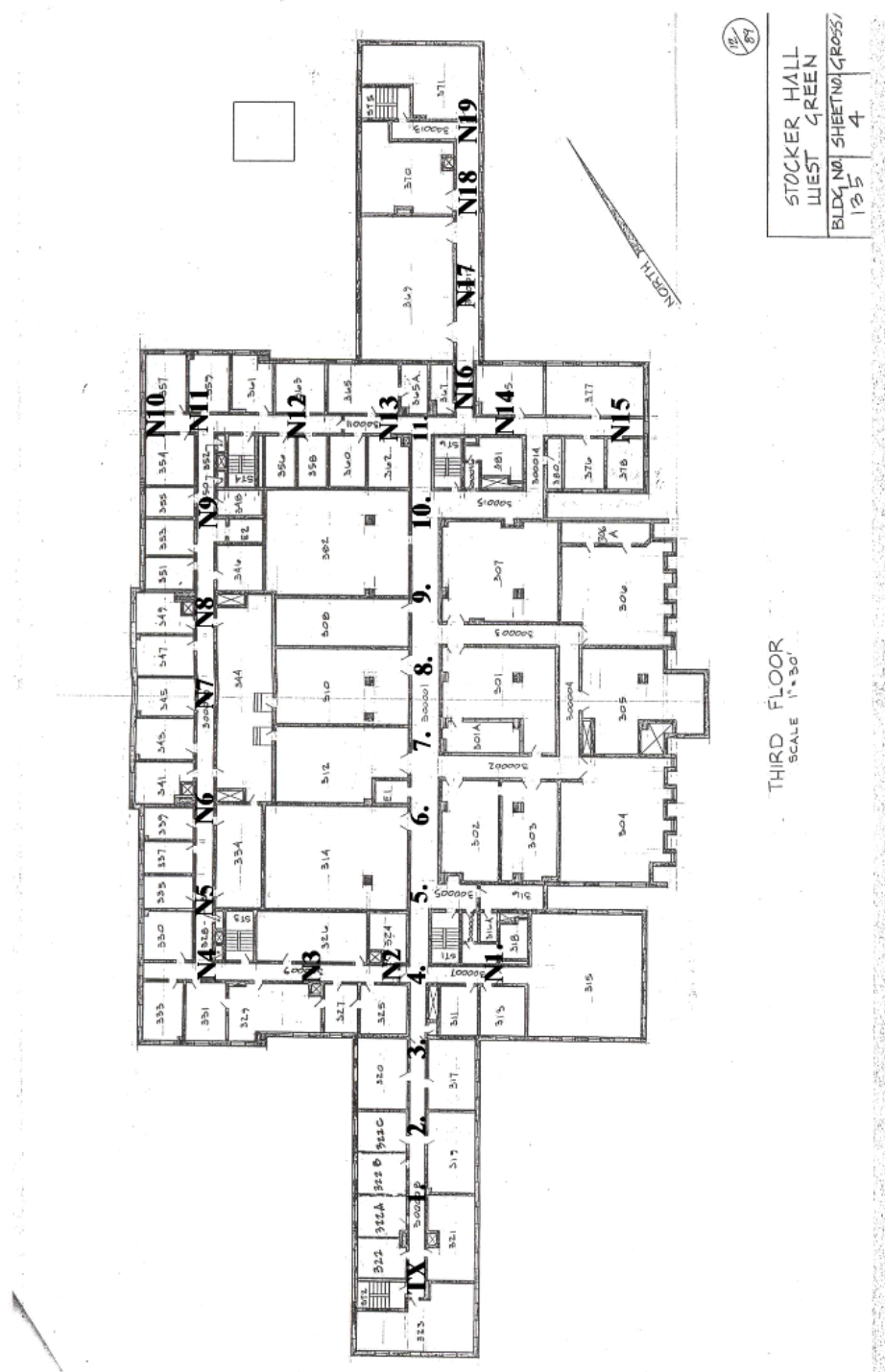


Figure A.3. Layout of floor plan of third floor with transmitter and receiver locations.

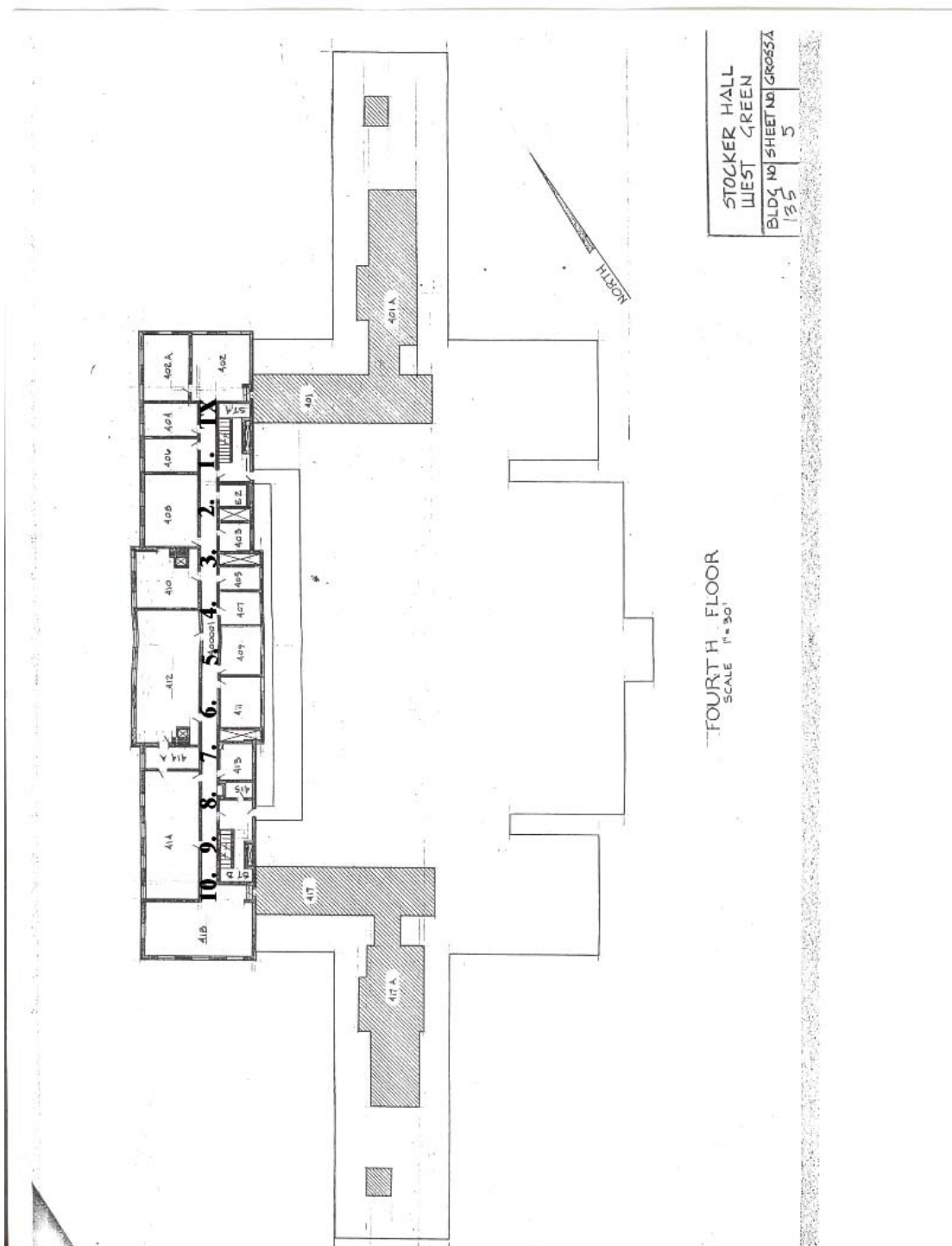


Figure A.4. Layout of floor plan of fourth floor with transmitter and receiver locations.

Appendix B

Experimental Data

Appendix B shows the data measured for path loss vs. distance on the various floors of Stocker. The data was collected for both LOS and NLOS cases in the frequencies 900MHz and 2.4 GHz.

Table B.1. LOS Measurements for 900 MHz on the Ground Floor

R' Location	'T' - 'R' Dist	Received signal Power (dBm) 900Mhz				
		Reading 1	Reading 2	Reading 3	Reading 4	Reading 5
Reference	1m	-61.3				
1	5m	-73.70	-72.32	-71.55	-71.23	-69.50
2	10m	-77.47	-77.62	-76.24	74.20	-73.67
3	15m	-78.40	-75.90	-74.60	-74.74	-76.50
4	20m	-81.70	-83.60	-83.78	-83.12	-81.20
5	25m	-82.40	-81.20	-80.30	-79.40	-79.80
6	30m	-82.30	-80.88	-80.55	-80.70	-83.20
7	35m	-82.30	-80.78	-80.62	-82.44	-88.02
8	40m	-91.60	-89.93	-88.38	-89.66	-91.66

Table B.2. LOS Measurements for 900 MHz on the First Floor

R' Location	'T' - 'R' Dist	Received signal Power (dBm) 900Mhz				
		Reading 1	Reading 2	Reading 3	Reading 4	Reading 5
Reference	1m	-47.23				
1	5m	-60.10	-55.75	-60.20	-62.30	-63.40
2	10m	-60.80	-61.70	-64.10	-61.80	-61.40
3	15m	-69.10	-71.30	-68.90	-65.20	-67.70
4	20m	-63.70	-66.70	-75.40	-78.10	-75.40
5	25m	-67.60	-69.80	-74.10	-74.50	-71.20
6	30m	-74.50	-72.40	-73.60	-72.10	-72.30
7	35m	-70.12	-72.30	-71.30	-74.72	-72.55
8	40m	-80.62	-74.53	-75.02	-71.10	-76.60
9	45m	-74.08	-80.10	-87.62	-80.08	-79.65
10	50m	-76.03	-79.42	-78.64	-77.60	-77.62
11	55m	-89.94	-83.05	-81.14	-81.92	-81.62
12	60m	-82.10	-81.30	-76.70	-87.20	-84.10
13	65m	-80.79	-79.50	-78.20	-80.30	-81.20
14	70m	-81.80	-82.40	-85.40	-83.30	-84.20

Table B.3. LOS Measurements for 900 MHz on the Second floor

R' Location	'T' - 'R' Dist	Received signal Power (dBm) 900Mhz				
		Reading 1	Reading 2	Reading 3	Reading 4	Reading 5
Reference	1m	-47.23				
1	5m	-55.81	-59.79	-55.78	-58.16	-53.00
2	10m	-63.43	-63.15	-60.83	-59.75	-59.72
3	15m	-56.57	-55.78	-63.87	-61.71	-68.13
4	20m	-59.59	-61.80	-74.77	-63.70	-76.81
5	25m	-66.24	-65.84	-66.90	-64.14	-65.36
6	30m	-63.39	-67.83	-72.84	-66.64	-70.55
7	35m	-69.19	-68.94	-69.19	-65.89	-64.30
8	40m	-70.63	-71.18	-70.50	-73.28	-74.55
9	45m	-69.74	-71.00	-70.93	-70.82	-72.99
10	50m	-73.68	-72.51	-78.22	-76.05	-80.05
11	55m	-79.42	-81.83	-86.03	-74.03	-86.13
12	60m	-80.12	-82.44	-86.01	-75.21	-74.18
13	65m	-76.67	-83.14	-89.74	-80.24	-77.52
14	70m	-75.53	-77.61	-79.44	-78.63	-81.07
15	75m	-79.55	-78.63	-76.14	-77.03	-84.85

Table B.4. LOS Measurements for 900 MHz on the Third Floor

R' Location	'T' - 'R' Dist	Received signal Power (dBm) 900Mhz				
		Reading 1	Reading 2	Reading 3	Reading 4	Reading 5
Reference	1m	-56.72				
1	5m	-72.10	-71.70	-66.90	-63.20	-61.70
2	10m	-70.73	-72.76	-74.90	-73.50	-68.70
3	15m	-80.80	-76.30	-71.70	-73.60	-75.90
4	20m	-84.60	-84.20	-80.50	-74.60	-74.80
5	25m	-81.80	-82.30	-78.50	-80.90	-80.60
6	30m	-83.40	-86.40	-86.40	-81.30	-78.00
7	35m	-81.10	-79.20	-78.10	-78.90	-77.20
8	40m	-86.30	-86.60	-86.50	-85.90	-84.30
9	45m	-89.40	-88.60	-87.20	-86.10	-87.10
10	50m	-90.90	-89.60	-88.40	-85.60	-83.40
11	55m	-85.40	-85.60	-82.20	-80.70	-79.90
12	60m	-88.70	-87.60	-87.60	-87.10	-87.20
13	65m	-92.20	-92.30	-92.90	-90.50	-90.40
14	70m	-89.20	-86.70	-85.70	-85.10	-84.30
15	75m	-93.70	-90.50	-89.60	-89.70	-91.10

Table B.5. LOS Measurements for 900 MHz on the Fourth Floor

R' Location	'T' - 'R' Dist	Received signal Power (dBm) 900Mhz				
		Reading 1	Reading 2	Reading 3	Reading 4	Reading 5
Reference	1m	-47.23				
1	5m	-54.67	-53.08	-63.71	-66.68	-65.68
2	10m	-69.14	-72.83	-63.48	-68.03	-66.36
3	15m	-64.18	-68.23	-67.86	-63.39	-70.35
4	20m	-67.43	-66.05	-76.23	-69.48	-66.75
5	25m	-84.88	-73.70	-67.71	-63.51	-78.23
6	30m	-78.13	-73.88	-68.49	-68.53	-74.80
7	35m	-68.81	-69.13	-69.45	-85.00	-77.01
8	40m	-73.85	-68.44	-72.27	-71.84	-72.77
9	45m	-79.04	-76.76	-67.67	-75.29	-77.64
10	47m	-78.67	-79.53	-72.40	-71.74	-75.82

Table B.6. LOS Measurements for 2.4 GHz on the Ground Floor

R' Location	'T' - 'R' Dist	Received signal Power (dBm) 2.4GHz				
		Reading 1	Reading 2	Reading 3	Reading 4	Reading 5
Reference	1m	-59.4				
E	5m	-73.47	-72.25	-70.40	-69.80	-68.40
B	10m	-76.40	-76.60	-74.80	-74.17	-74.90
C	15m	-80.60	-82.30	-83.80	-82.70	-81.60
D	20m	-80.17	-80.20	-79.88	-80.70	-82.12
F	25m	-78.50	-77.10	-78.10	-79.30	-79.70
G	30m	-82.80	-81.95	-81.30	-80.20	-81.80
H	35m	-85.20	-84.02	-83.18	-84.17	-84.86
I	40m	-94.79	-93.37	-93.02	-93.95	-94.28

Table B.7. LOS Measurements for 2.4 GHz on the First Floor

R' Location	'T' - 'R' Dist	Received signal Power (dBm) 2.4GHz				
		Reading 1	Reading 2	Reading 3	Reading 4	Reading 5
Reference	1m	-61.7				
1	5m	-70.90	-65.20	-62.00	-67.40	-63.18
2	10m	-67.20	-70.90	-66.30	-68.20	-65.90
3	15m	-72.90	-66.20	-65.80	-69.90	-72.10
4	20m	-74.60	-72.80	-75.90	-78.40	-73.10
5	25m	-71.20	-74.40	-73.20	-79.90	-72.40
6	30m	-75.60	-79.30	-74.50	-82.10	-74.00
7	35m	-81.20	-74.30	-73.20	-79.00	-82.10
8	40m	-70.70	-68.90	-66.20	-65.40	-72.30
9	45m	-70.10	-69.20	-69.70	-70.20	-65.60
10	50m	-74.30	-72.30	-71.40	-75.60	-79.00
11	55m	-75.20	-70.10	-69.20	-74.90	-79.20
12	60m	-77.30	-72.10	-76.90	-78.70	-80.60
13	65m	-76.90	-77.90	-76.40	-75.70	-73.20
14	70m	-74.90	-73.20	-75.40	-77.60	-78.10

Table B.8. LOS Measurements for 2.4 GHz on the Second Floor

R' Location	'T' - 'R' Dist	Received signal Power (dBm) 2.4GHz				
		Reading 1	Reading 2	Reading 3	Reading 4	Reading 5
Reference	1m	-61.70				
1	5m	-71.60	-70.33	-73.04	-70.80	-72.90
2	10m	-79.88	-78.06	-76.70	-82.39	-79.85
3	15m	-81.49	-77.96	-81.72	-83.38	-85.14
4	20m	-70.02	-83.95	-80.56	-77.09	-84.56
5	25m	-86.48	-86.44	-86.46	-85.56	-85.14
6	30m	-85.55	-85.56	-85.58	-85.54	-85.16
7	35m	-86.54	-87.21	-87.50	-77.60	-82.15
8	40m	-87.94	-82.89	-88.04	-87.06	-87.91
9	45m	-90.95	-87.62	-89.44	-89.44	-87.79
10	50m	-87.71	-91.01	-87.92	-89.00	-90.11
11	55m	-87.01	-87.09	-87.04	-87.01	-86.97
12	60m	-87.05	-87.07	-87.08	-87.06	-87.08
13	65m	-93.63	-93.47	-96.14	-93.61	-94.45
14	70m	-94.61	-94.51	-94.31	-94.45	-94.67
15	75m	-94.10	-94.22	-91.88	-94.11	-93.89

Table B.9. LOS Measurements for 2.4 GHz on the Third Floor

R' Location	'T' - 'R' Dist	Received signal Power (dBm) 2.4GHz				
		Reading 1	Reading 2	Reading 3	Reading 4	Reading 5
Reference	1m	-58.30				
1	5m	-70.40	-70.70	-70.30	-74.06	-69.20
2	10m	-70.40	-71.20	-71.70	-76.20	-76.20
3	15m	-77.20	-75.30	-74.30	-78.60	-78.00
4	20m	-78.40	-75.90	-74.20	-70.50	-70.20
5	25m	-81.80	-82.60	-85.40	-86.40	-84.40
6	30m	-77.80	-75.30	-74.10	-76.70	-80.20
7	35m	-68.70	-68.40	-69.30	-69.10	-70.20
8	40m	-79.50	-77.20	-75.10	-74.30	-73.80
9	45m	-77.60	-76.20	-75.10	-72.90	-72.10
10	50m	-81.30	-85.40	-86.20	-84.40	-82.70
11	55m	-79.20	-79.30	-78.80	-77.50	-76.30
12	60m	-83.40	-82.40	-82.30	-81.60	-81.90
13	65m	-88.40	-89.90	-92.90	-87.60	-87.10
14	70m	-86.90	-84.30	-82.40	-81.30	-81.80
15	75m	-91.10	-90.90	-90.40	-89.90	-88.30

Table B.10. LOS Measurements for 2.4 GHz on the Fourth Floor

R' Location	'T' - 'R' Dist	Received signal Power (dBm) 2.4GHz				
		Reading 1	Reading 2	Reading 3	Reading 4	Reading 5
Reference	1m	-61.70				
1	5m	-77.55	-71.24	-68.44	-73.35	-79.06
2	10m	-85.85	-84.99	-83.88	-82.12	-85.08
3	15m	-87.88	-86.32	-87.31	-91.84	-79.73
4	20m	-87.65	-86.83	-87.30	-87.02	-87.73
5	25m	-84.51	-86.03	-86.87	-87.78	-86.81
6	30m	-86.38	-87.30	-85.72	-84.57	-87.17
7	35m	-86.41	-86.92	-86.61	-86.91	-85.34
8	40m	-85.93	-86.35	-85.97	-85.67	-85.37
9	45m	-86.31	-84.32	-86.07	-85.98	-85.44
10	47m	-86.32	-85.42	-86.81	-86.07	-86.17

Table B.11. NLOS Measurements for 900 MHz on the Ground Floor

R' Location	'T' - 'R' Dist	Received signal Power (dBm) 900MHz				
		Reading 1	Reading 2	Reading 3	Reading 4	Reading 5
Reference	1m	-61.30				
1	21.02379604m	-74.08	-79.16	-78.01	-79.82	-74.20
2	21.84032967m	-82.32	-85.03	-89.08	-87.98	-86.12
3	23.70653918m	-87.20	-86.90	-87.40	-87.18	-86.85
4	26.40075756m	-87.30	-87.63	-87.79	-87.70	-87.20
5	29.69848481m	-87.48	-87.84	-87.29	-87.50	-87.53
6	17.88854382m	-87.33	-87.69	-87.14	-86.95	-87.41
7	21.58703314m	-86.60	-85.64	-83.14	-84.02	-81.97
8	23.2594067m	-79.41	-81.88	-82.40	-82.98	-84.42
9	25.8069758m	-85.48	-84.94	-85.05	-85.71	-85.48
10	26.01922366m	-74.47	-81.74	-75.47	-77.72	-72.86
11	31.01612484m	-81.75	-82.93	-81.94	-76.25	-76.91
12	36.01388621m	-77.32	-75.11	-75.38	-76.76	-78.13
13	41.01219331m	-80.86	-78.79	-82.03	-80.95	-82.84
14	46.01086828m	-81.19	-82.16	-80.71	-82.33	-82.40
15	57.14017851m	-86.75	-86.64	-86.86	-85.51	-86.85
16	57.70615219m	-86.61	-86.55	-86.56	-86.97	-86.74
17	62.80127387m	-86.57	-86.91	-86.72	-86.79	-86.45
18	67.74215822m	-86.91	-86.86	-86.25	-86.72	-86.62
19	57.31491952m	-86.45	-87.00	-86.62	-86.92	-86.47
20	58.05170109m	-86.17	-86.95	-86.88	-86.72	-87.86

Table B.12. NLOS Measurements for 900 MHz on the Second Floor

R' Location	'T' - 'R' Dist	Received signal Power (dBm) 900MHz				
		Reading 1	Reading 2	Reading 3	Reading 4	Reading 5
Reference	1m	-43.37				
1	33.96999m	-89.30	-89.71	-90.15	-90.20	-90.16
2	34.53925m	-89.01	-90.90	-88.96	-88.42	-87.40
3	37.21505m	-80.10	-86.95	-86.69	-87.18	-87.23
4	41.96093m	-88.90	-88.93	-88.96	-88.99	-89.01
5	52.96414m	-89.42	-89.35	-89.40	-89.43	-89.42
6	59.2871m	-89.44	-90.07	-90.12	-90.01	-89.95
7	61.60325m	-90.37	-90.23	-90.28	-90.26	-90.41
8	76.85337m	-88.62	-89.94	-89.91	-90.28	-90.30

Table B.13. NLOS Measurements for 900 MHz on the Third Floor

R' Location	'T' - 'R' Dist	Received signal Power (dBm) 900MHz				
		Reading 1	Reading 2	Reading 3	Reading 4	Reading 5
Reference	1m	-56.72				
334	39.597284m	-82.00	-89.00	-89.20	-89.40	-89.60
336	45.50535023m	-93.80	-93.90	-93.20	-93.60	-93.50
343	51.54206923m	-93.40	-93.60	-93.70	-94.00	-94.20
347	60.24832695m	-93.80	-93.40	-93.20	-94.30	-94.20
351	66.56912873m	-93.40	-93.80	-93.90	-93.70	-94.10
355	72.95763771m	-93.10	-93.40	-93.30	-93.40	-93.90
354	80.65194914m	-94.20	-94.10	-93.40	-93.60	-93.90
361a	79.55769542m	-93.90	-93.60	-93.50	-94.20	-94.40
363	78.7292633m	-93.80	-94.10	-94.30	-94.10	-94.20
365	78.08570228m	-89.04	-88.50	-90.60	-91.70	-92.80
367	78.4037429m	-88.60	-88.40	-88.50	-88.60	-88.50
369	83.90153098m	-88.70	-88.70	-88.80	-88.90	-88.80
370	96.39744239m	-88.02	-88.70	-88.80	-89.90	-89.00
371	104.8952187m	-88.70	-88.40	-88.50	-88.50	-88.80
375	78.24977252m	-88.90	-88.80	-88.70	-88.80	-88.60
376	79.04869955m	-96.20	-96.40	-96.70	-96.30	-89.70

Table B.14. NLOS Measurements for 2.4 GHz on the Ground Floor

R' Location	'T' - 'R' Dist	Received signal Power (dBm) 2.4 GHz				
		Reading 1	Reading 2	Reading 3	Reading 4	Reading 5
Reference	1m	-59.40				
1	21.02379604m	-79.50	-83.20	-88.50	-89.20	-89.50
2	21.84032967m	-92.90	-88.90	-90.40	-91.30	-89.92
3	23.70653918m	-89.30	-90.70	-90.72	-91.05	-92.42
4	26.40075756m	-91.30	-89.30	-90.09	-88.61	-90.50
5	29.69848481m	-81.80	-79.20	-81.20	-81.40	-82.00
6	17.88854382m	-90.20	-90.40	-88.90	-90.90	-90.70
7	21.58703314m	-90.70	-90.58	-91.20	-90.28	-90.15
8	23.2594067m	-89.80	-90.01	-90.13	-89.78	-89.00
9	25.8069758m	-89.88	-89.72	-89.60	-89.00	-89.13
10	26.01922366m	-81.70	-79.20	-81.30	-79.40	-79.60
11	31.01612484m	-80.30	-78.90	-79.50	-79.30	-79.00
12	36.01388621m	-79.10	-81.30	-79.97	-80.23	-80.14
13	41.01219331m	-81.20	-79.60	-78.00	-81.90	-79.20
14	46.01086828m	-80.40	-80.30	-79.20	-81.20	-80.30

Table B.15. NLOS Measurements for 2.4 GHz on the Second Floor

R' Location	'T' - 'R' Dist	Received signal Power (dBm) 2.4 GHz				
		Reading 1	Reading 2	Reading 3	Reading 4	Reading 5
Reference	1m	-59.40				
E	33.96999m	-89.92	-89.98	-89.95	-89.90	-89.96
B	34.53925m	-90.40	-90.48	-90.10	-90.02	-89.58
C	37.21505m	-89.31	-89.50	-89.42	-89.34	-89.26
D	41.96093m	-90.01	-90.13	-89.85	-89.88	-89.82
F	52.96414m	-90.04	-90.11	-90.05	-90.08	-90.19
G	59.2871m	-89.43	-89.56	-89.60	-89.57	-89.51
H	61.60325m	-89.47	-89.38	-89.57	-89.61	-89.54
I	76.85337m	-89.77	-89.70	-89.67	-89.76	-89.72

Table B.16. NLOS Measurements for 2.4 GHz on the Third Floor

R' Location	'T' - 'R' Dist	Received signal Power (dBm) 2.4 GHz				
		Reading 1	Reading 2	Reading 3	Reading 4	Reading 5
Reference	1m	-58.30				
334	39.597284m	-89.20	-89.12	-89.30	-89.10	-88.70
336	45.50535023m	-88.70	-88.90	-88.93	-88.01	-88.70
343	51.54206923m	-89.10	-89.30	-89.90	-90.07	-90.30
347	60.24832695m	-92.90	-92.78	-93.20	-93.26	-92.80
351	66.56912873m	-93.30	-92.90	-93.00	-93.09	-92.70
355	72.95763771m	-95.80	-96.40	-96.30	-96.50	-95.72
354	80.65194914m	-92.60	-92.06	-91.80	-91.69	-91.20
361a	79.55769542m	-93.70	-94.00	-94.40	-94.30	-94.80
363	78.7292633m	-96.50	-96.20	-95.70	-95.50	-94.80
365	78.08570228m	-91.90	-90.70	-90.70	-90.30	-90.04
367	78.4037429m	-84.90	-85.20	-85.00	-84.40	-84.60
369	83.90153098m	-84.80	-84.60	-84.90	-84.50	-84.00
370	96.39744239m	-85.10	-85.90	-84.80	-85.30	-84.20
371	104.8952187m	-85.10	-85.40	-85.10	-85.90	-85.60
375	78.24977252m	-84.80	-85.30	-85.60	-85.70	-85.90
376	79.04869955m	-84.20	-84.50	-84.10	-85.60	-84.30

Table B.17. Measurements for 900 MHz between Walls

Wall Number	Received signal Power 900 MHz (reference power -47.23dbm at 1m) (dBm)					
	Reading 1	Reading 2	Reading 3	Reading 4	Reading 5	Average
1	-71.66	-72.22	-72.51	-71.37	-69.87	-71.526
2	-81.68	-82.11	-80.42	-73.83	-73.51	-78.310
3	-84.46	-84.67	-83.32	-82.23	-81.63	-83.262
4	-82.25	-86.51	-91.05	-91.36	-91.72	-88.578

Table B.18. Measurements for 2.4 GHz between Walls

Wall Number	Received signal Power (dBm) 2.4 GHz (reference power -61.7dbm at 1m)					
	Reading 1	Reading 2	Reading 3	Reading 4	Reading 5	Average
1	-76.28	-77.82	-78.61	-78.31	-78.39	-77.882
2	-77.14	-79.84	-79.38	-79.26	-79.91	-79.106
3	-87.08	-85.75	-85.96	-86.97	-97.97	-88.746
4	-93.12	-92.52	-92.91	-93.01	-92.47	-92.806

Appendix C

Path Loss vs. Distance Plots

Figure C.1 to C.22 show the plots of path loss vs. distance in different floors of Stocker. The plots are for LOS, NLOS and overall path loss cases, both in the 900 MHz and 2.4 GHz frequency band.

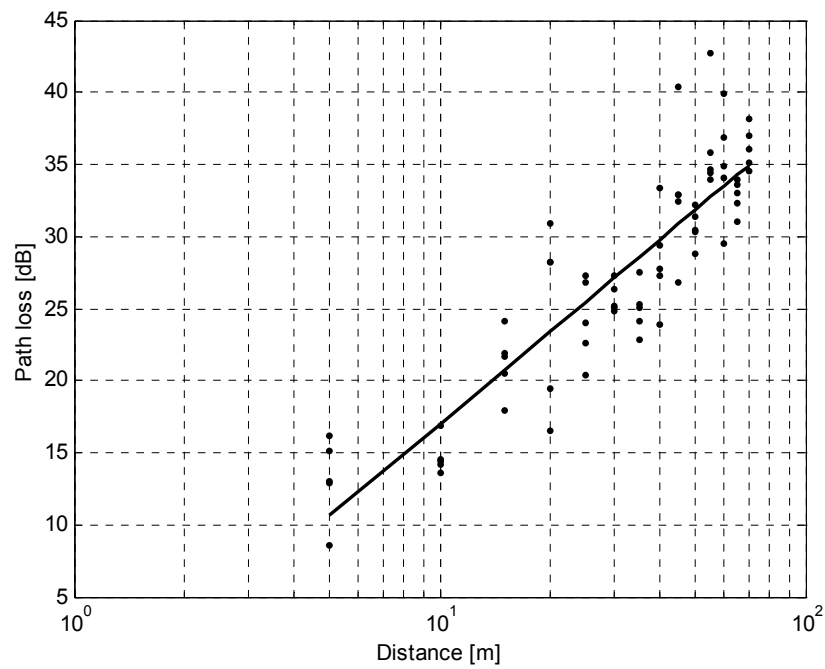


Figure C.1. 900MHz LOS Path Loss in First Floor of Stocker

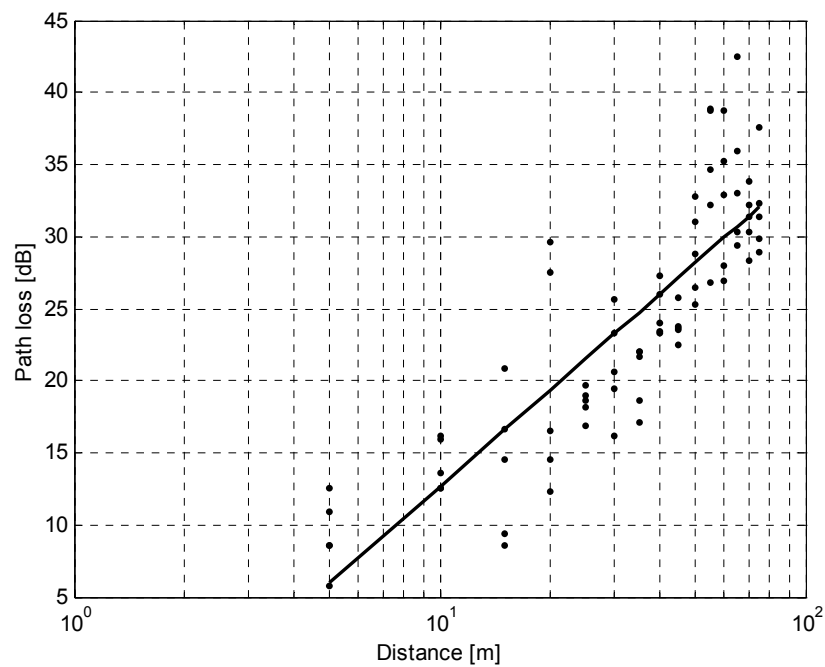


Figure C.2. 900MHz LOS Path Loss in Second Floor of Stocker

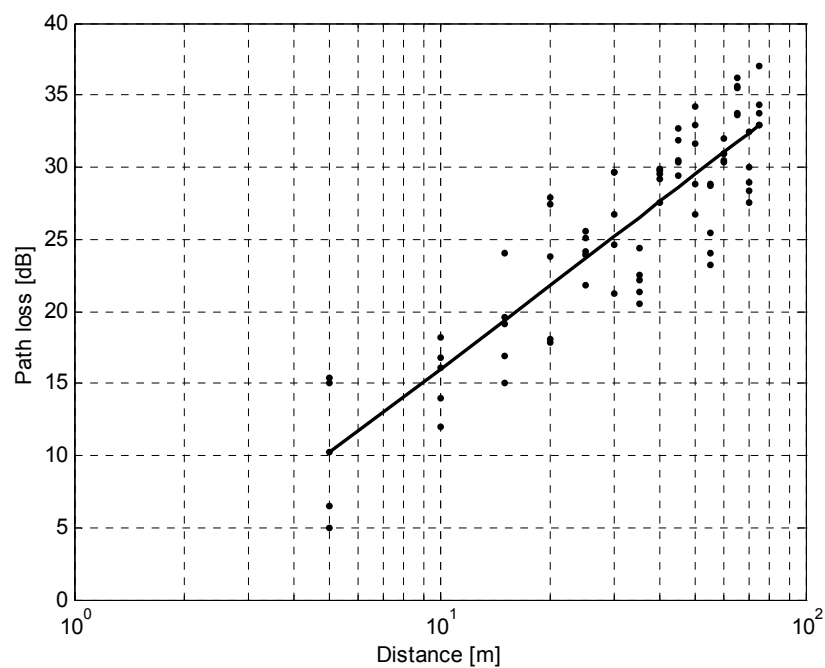


Figure C.3. 900MHz LOS Path Loss in Third Floor of Stocker

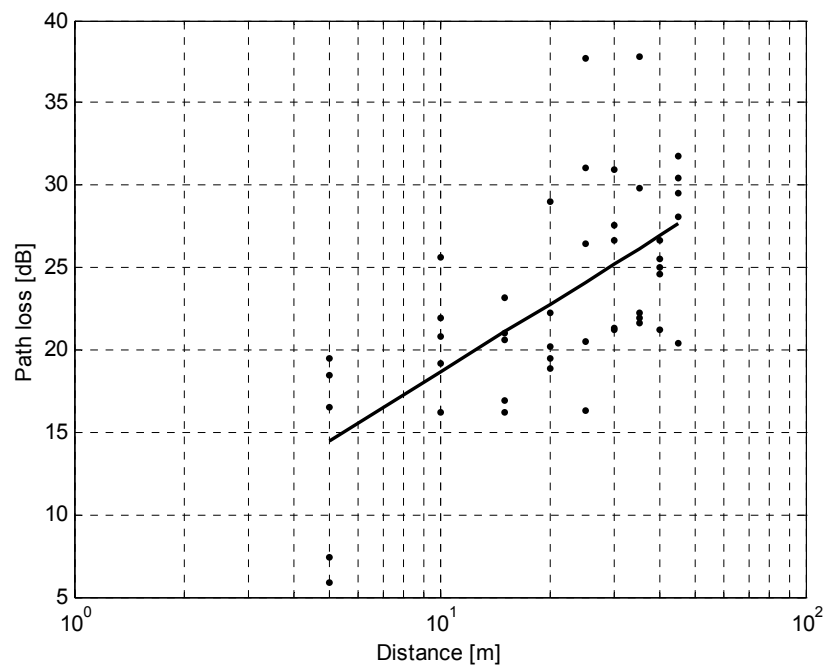


Figure C.4. 900MHz LOS Path Loss in Fourth Floor of Stocker

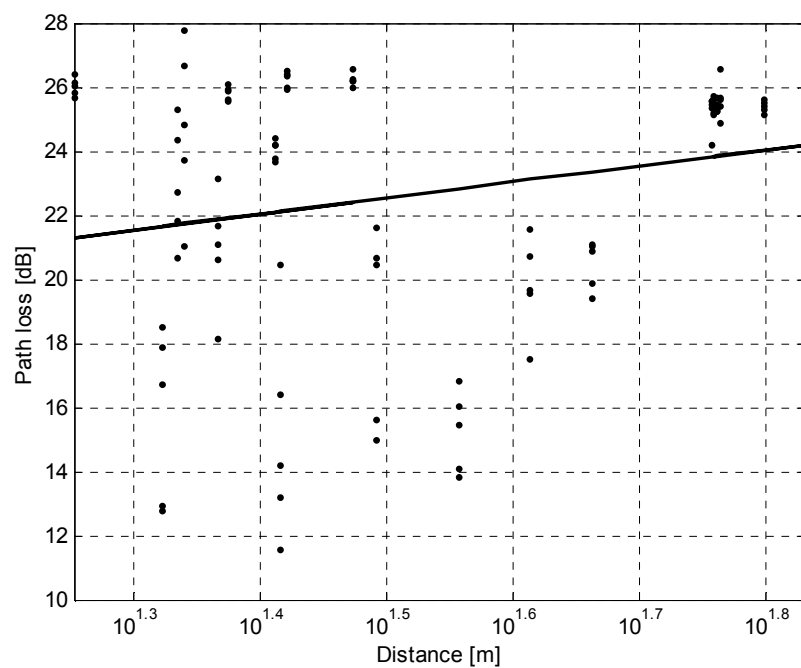


Figure C.5. 900MHz NLOS Path Loss in Ground Floor of Stocker

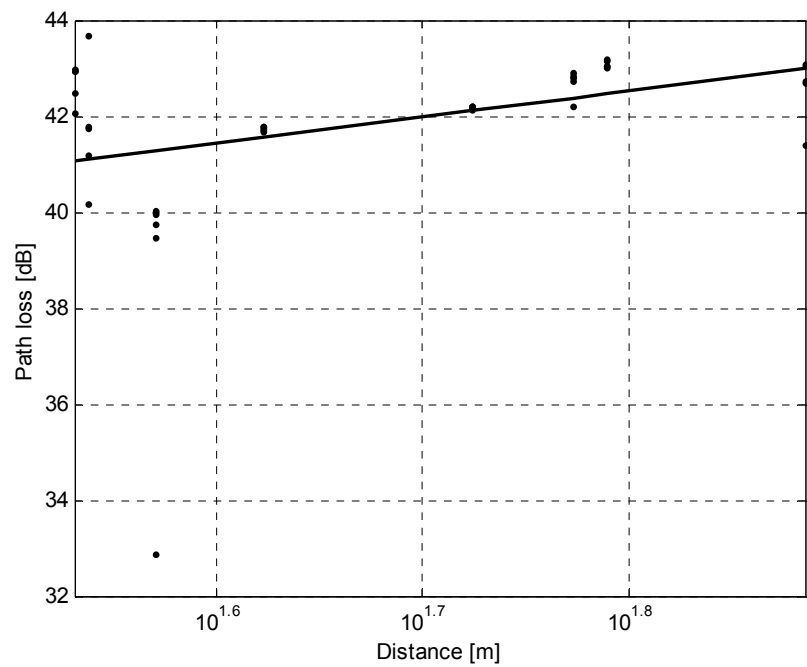


Figure C.6. 900MHz NLOS Path Loss in Second Floor of Stocker

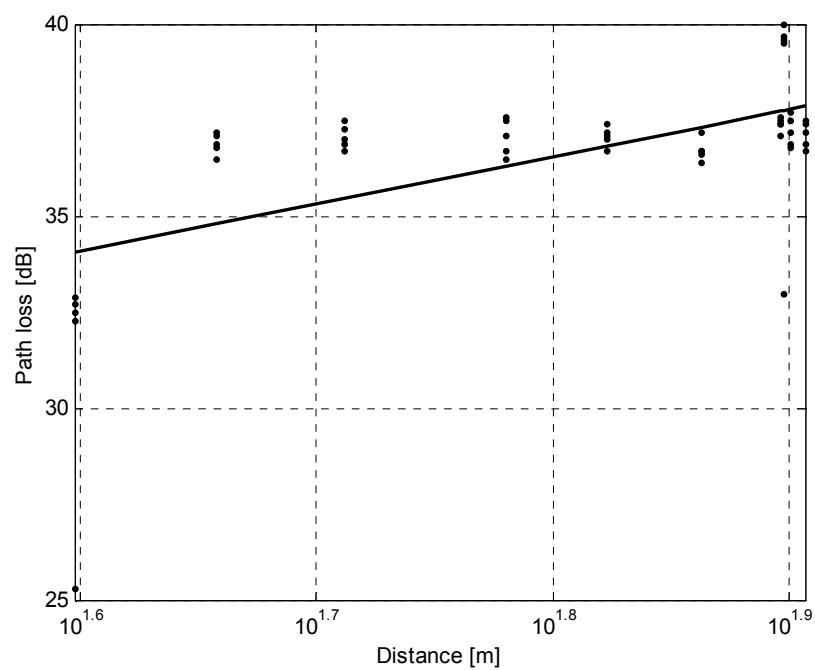


Figure C.7. 900MHz NLOS Path Loss in Third Floor of Stocker

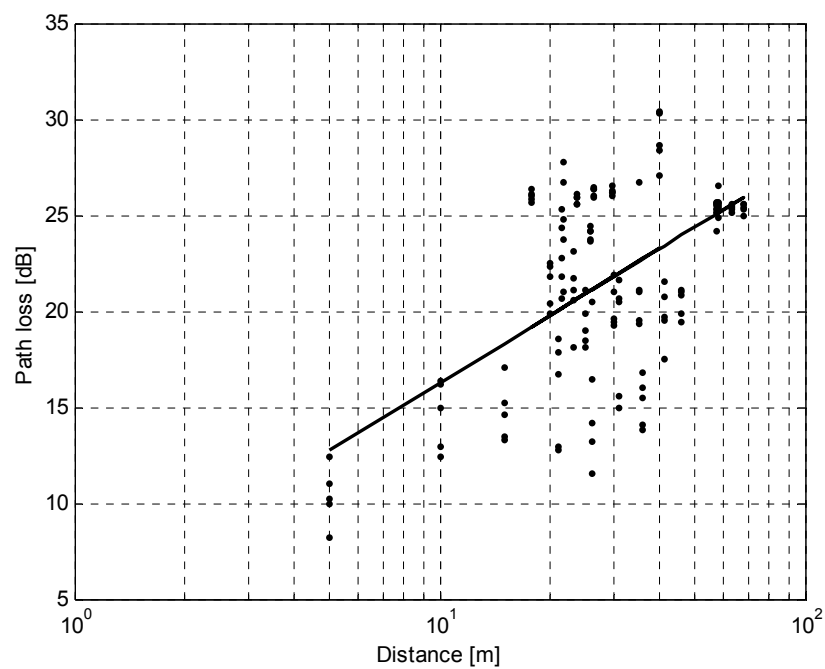


Figure C.8. 900MHz Path Loss in Ground Floor of Stocker

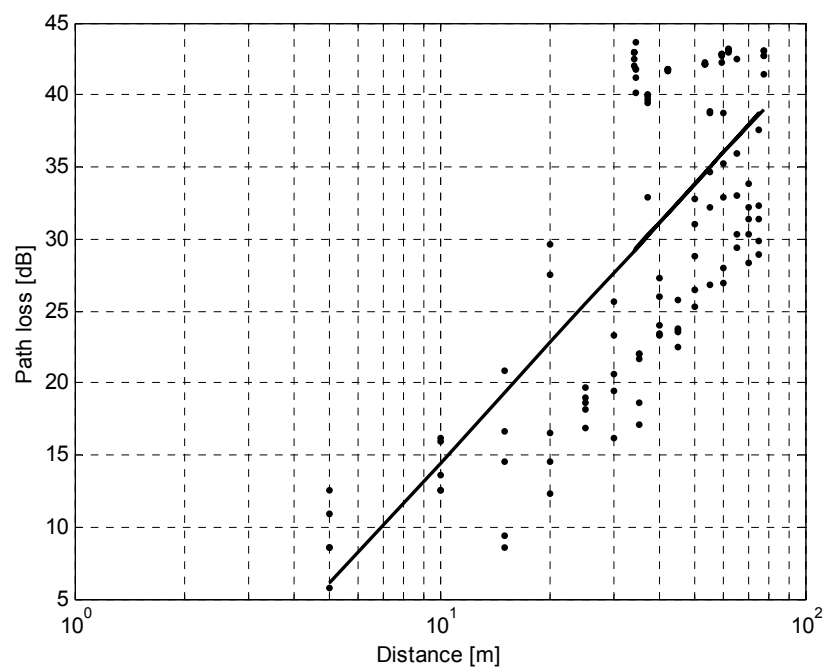


Figure C.9. 900MHz Path Loss in Second Floor of Stocker

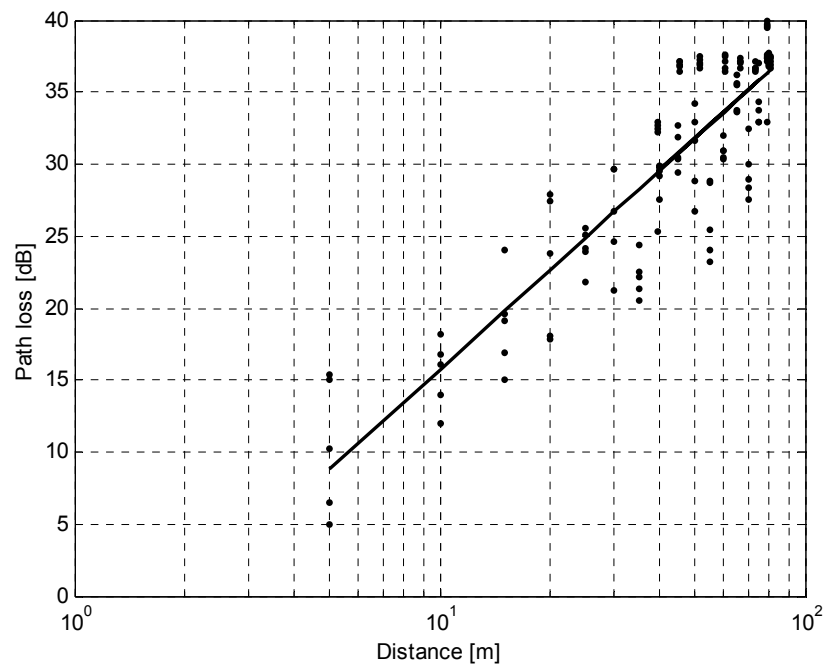


Figure C.10. 900MHz Path Loss in Third Floor of Stocker

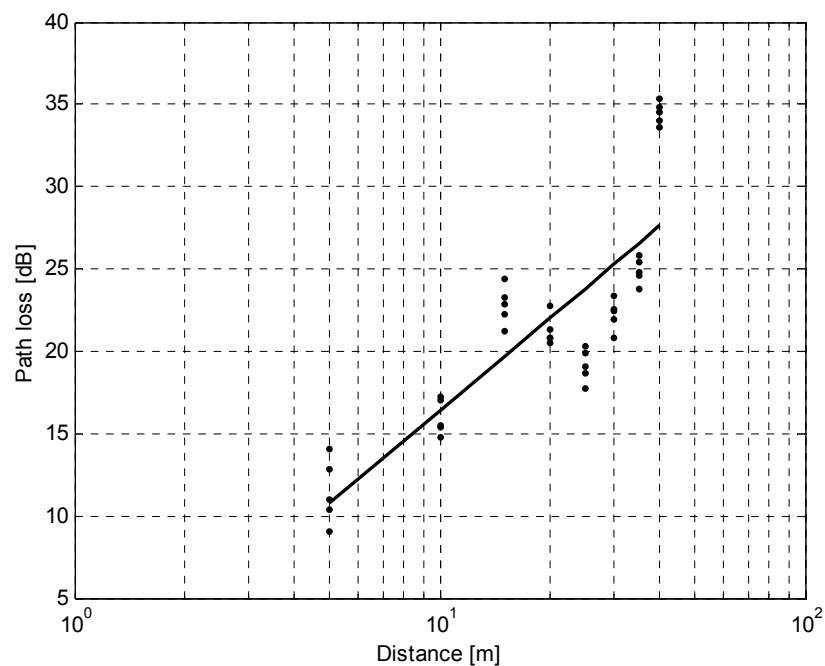


Figure C.11. 2.4 GHz LOS Path Loss in Ground Floor of Stocker

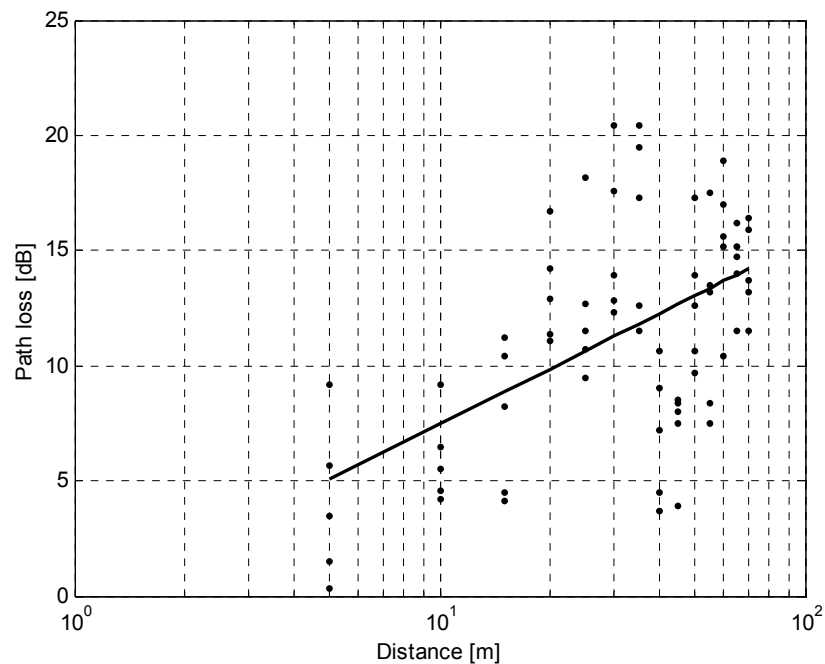


Figure C.12. 2.4 GHz LOS Path Loss in First Floor of Stocker

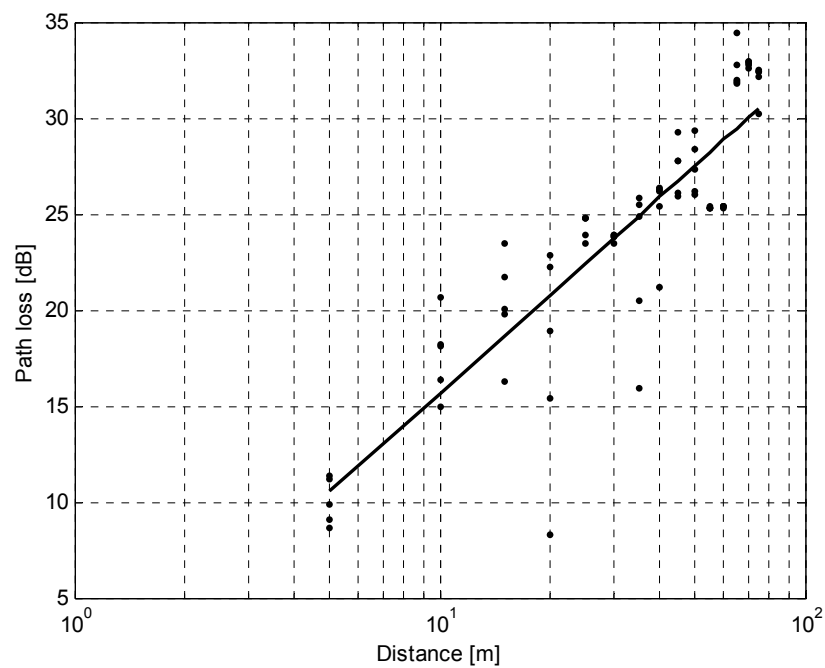


Figure C.13. 2.4 GHz LOS Path Loss in Second Floor of Stocker

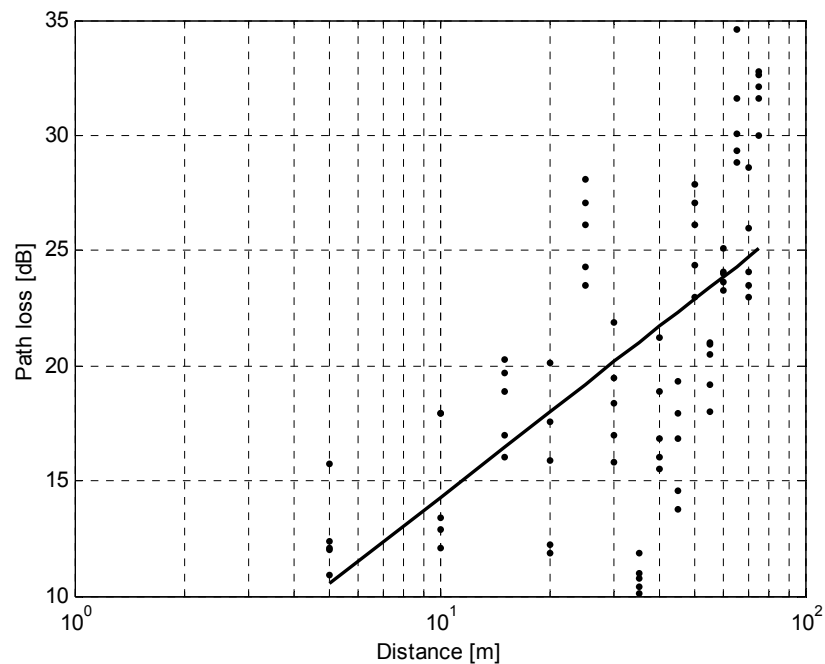


Figure C.14. 2.4 GHz LOS Path Loss in Third Floor of Stocker

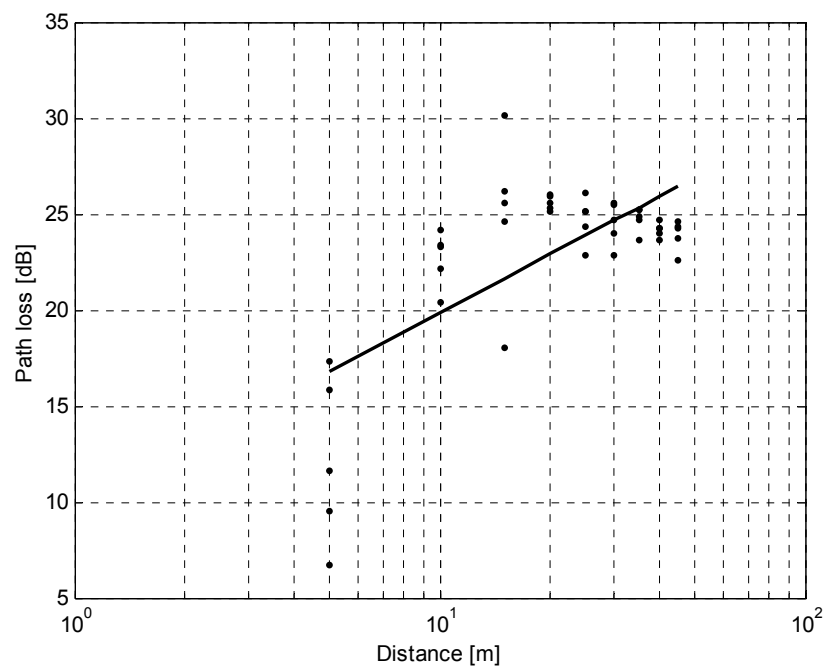


Figure C.15. 2.4 GHz LOS Path Loss in Fourth Floor of Stocker

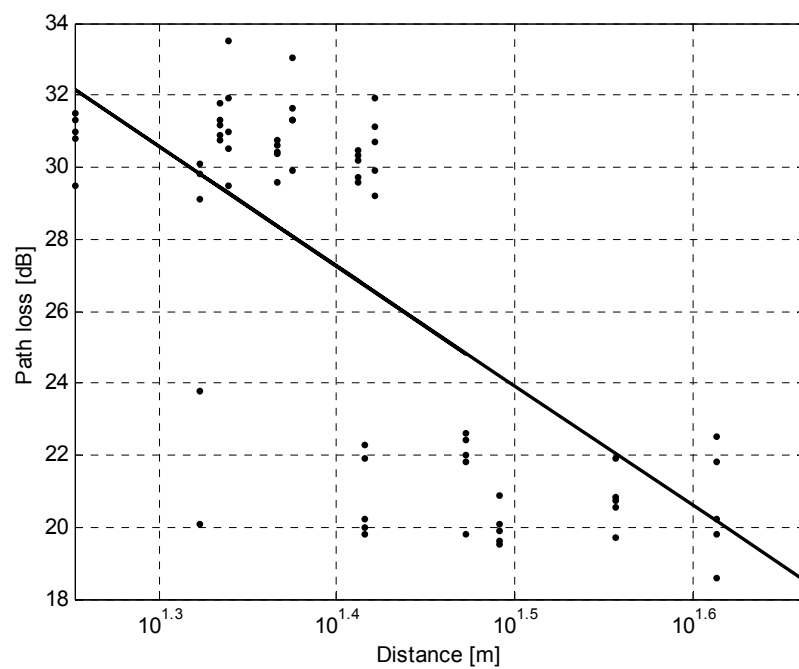


Figure C.16. 2.4 GHz NLOS Path Loss in Ground Floor of Stocker

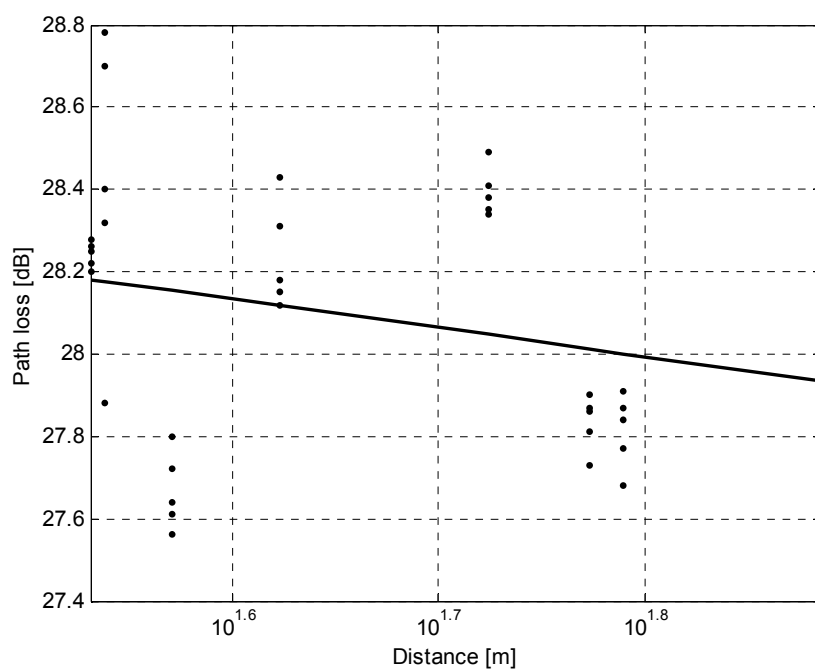


Figure C.17. 2.4 GHz NLOS Path Loss in Second Floor of Stocker

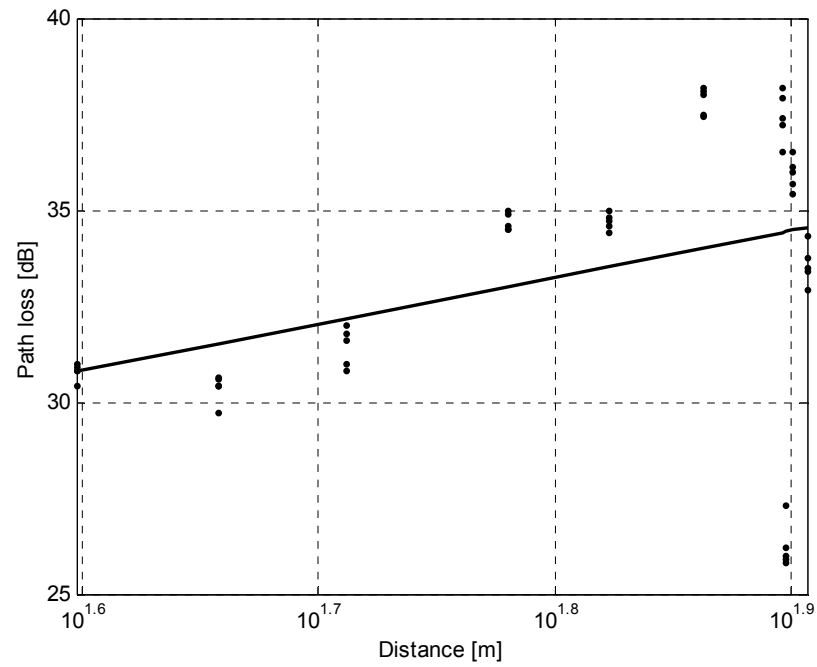


Figure C.18. 2.4 GHz NLOS Path Loss in Third Floor of Stocker

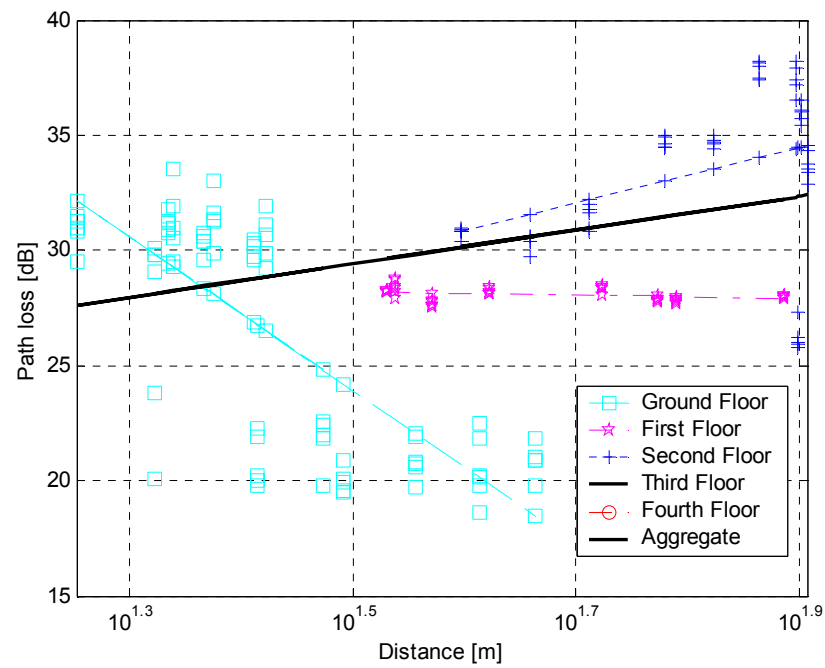


Figure C.19. 2.4 GHz NLOS Path Loss in all floors of Stocker

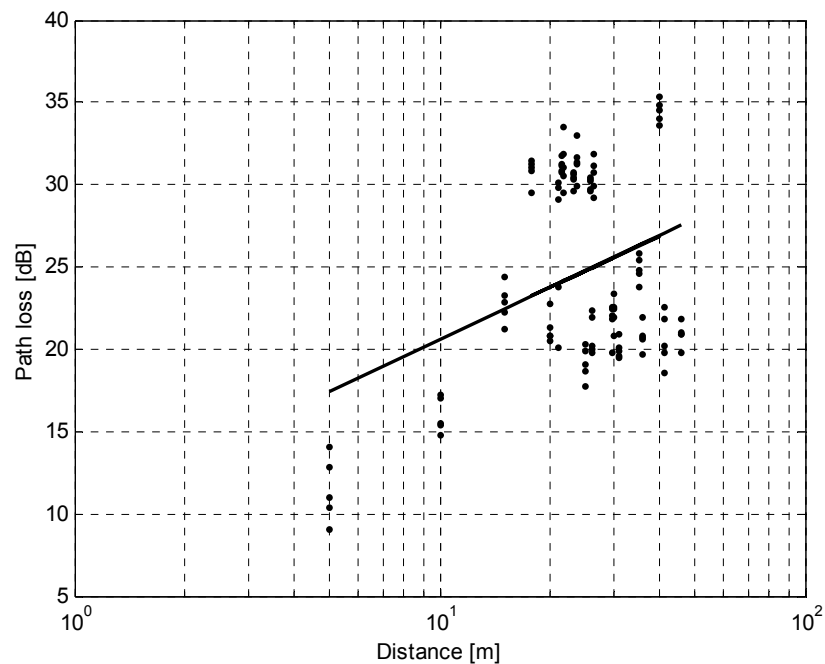


Figure C.20. Path Loss of 2.4 GHz in Ground Floor of Stocker

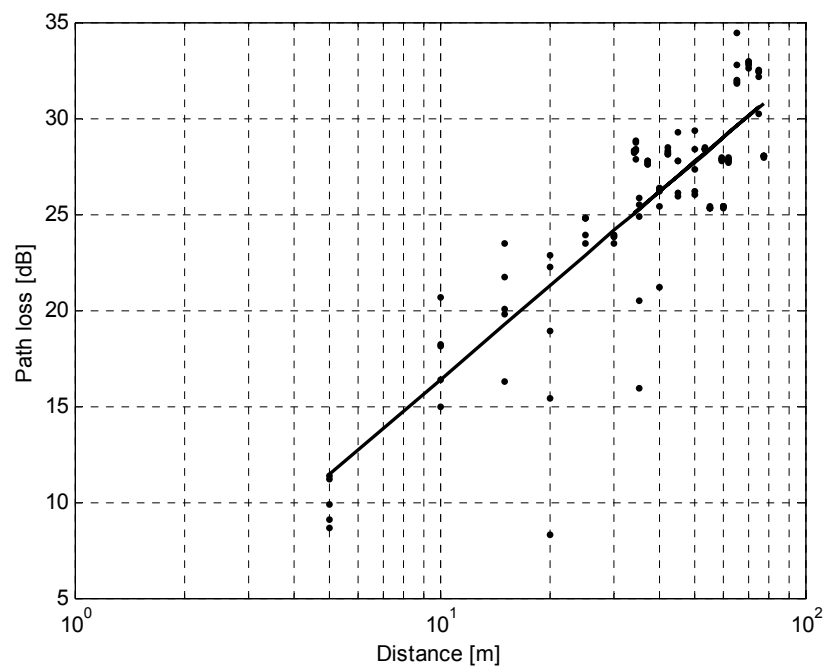


Figure C.21. 2.4 GHz Path Loss in Second Floor of Stocker

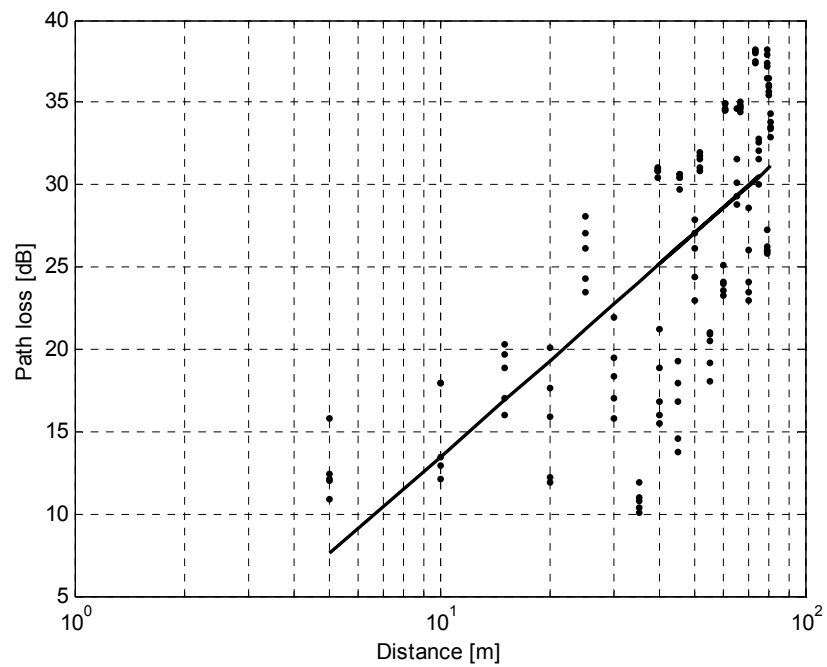


Figure C.22. 2.4 GHz Path Loss in Third Floor of Stocker

Appendix D

Experimental Data

The data for estimating the transfer function was measured at several locations on all the floors of Stocker Center. The experimental data is presented in Table D.1. to D.5. *M 1* and *M 2* represent Measurement #1 and Measurement #2.

Table D.1. Power Measurements on the Ground Floor of Stocker Center

Frequency	Distance between the Transmitter and Receiver							
	10m		20m		30m		40m	
	M 1	M 2	M 1	M 2	M 1	M 2	M 1	M 2
902	-54.95	-54.56	-61.65	-61.35	-53.47	-58.95	-61.16	-64.72
903	-54.29	-54.59	-61.24	-60.42	-54.62	-58.99	-60.65	-63.95
904	-55.2	-54.01	-62.68	-60.61	-62.41	-58.18	-60.77	-64.86
905	-54.84	-55.03	-63.74	-62.55	-61.99	-57.87	-61.31	-65.46
906	-54.91	-55.78	-63.77	-62.23	-62.21	-57.95	-60.84	-64.5
907	-54.81	-55.03	-62.47	-60.65	-62.19	-58.02	-60.38	-63.4
908	-54.87	-55.51	-61.97	-59	-62.13	-57.43	-61.22	-63.94
909	-55.82	-56.38	-61.64	-59.26	-63.94	-58.09	-61.35	-63.49
910	-55.9	-55.75	-61.4	-59.11	-65.32	-58.93	-60.89	-63.1
911	-55.68	-55.46	-60.81	-58.81	-66.3	-58.76	-61	-63.26
912	-54.99	-56.1	-61.09	-59.49	-65.02	-58.27	-61.86	-63.56
913	-55.74	-56.17	-62.38	-59.91	-67.5	-59.89	-61.38	-63.31
914	-55.68	-56.24	-61.19	-59.32	-67.07	-60.95	-61.23	-62.85
915	-55.94	-56.63	-59.06	-58.1	-65.54	-59.03	-61.6	-62.28
916	-56.24	-56.47	-58.26	-57.73	-65.46	-58.74	-61.65	-62.69
917	-55.68	-57.33	-58.07	-57.54	-66.94	-59.44	-60.39	-62.09
918	-56.16	-57.68	-58.17	-57.1	-64.98	-59.56	-60.15	-61.93
919	-56.99	-57.79	-59.17	-57.47	-64.41	-59.03	-60.59	-62.12
920	-57.92	-58.01	-59.97	-58.03	-63.53	-59.23	-60.47	-61.91
921	-57.9	-58.63	-59.37	-58.82	-63.71	-58.74	-60.53	-62.36
922	-57.68	-58.66	-58.23	-58.02	-63.56	-59.08	-60.62	-62.28
923	-57.92	-57.02	-57.73	-57.51	-63.56	-59.23	-60.29	-62.08
924	-57.21	-57.13	-58.39	-57.49	-63.65	-59.74	-60.6	-61.82
925	-57.39	-57.2	-58.92	-57.01	-64.38	-60.12	-60.95	-61.41
926	-57.23	-57.33	-59.07	-56.86	-64.14	-59.93	-61.08	-61.7
927	-57.13	-55.85	-59.58	-57.67	-64.2	-59.79	-61.78	-62.35
928	-58.12	-59.51	-59.3	-58.87	-64.52	-60.83	-61.92	-62.5

Table D.2(i). Power Measurements on the First Floor of Stocker Center

Frequency	Distance between the Transmitter and Receiver							
	10m		20m		30m		40m	
	M 1	M 2	M 1	M 2	M 1	M 2	M 1	M 2
902	-66.41	-65.86	-66.7	-66.33	-69.96	-71.53	-72.55	-71.1
903	-65.29	-66.13	-67.44	-66.06	-70.7	-70.91	-70.87	-69.74
904	-66.12	-66.67	-67.43	-66.58	-70.53	-69.45	-71.43	-68.89
905	-66.6	-67.28	-67.15	-66.61	-70.91	-69.74	-71.7	-69.28
906	-67.42	-67.67	-66.58	-66.1	-69.88	-68.98	-69.49	-68.69
907	-67.93	-67.05	-67.46	-65.97	-69.86	-67.74	-69.65	-68.2
908	-68.95	-66.69	-66.71	-66.42	-70.75	-68.8	-70.32	-67.48
909	-68.62	-65.57	-66.47	-65.6	-69.63	-68.71	-68.21	-67.2
910	-68.08	-64.82	-65.69	-66.71	-69.24	-66.97	-68.74	-66.46
911	-67.22	-63.86	-64.83	-65.34	-68.58	-67.09	-68.21	-66.3
912	-67.1	-63.41	-64.71	-64.32	-68.08	-66.49	-67.42	-65.94
913	-66.62	-62.99	-64.64	-64.37	-68.23	-66.27	-67.53	-65.35
914	-65.67	-62.4	-64.59	-64.68	-67.95	-65.93	-67.1	-65.29
915	-63.76	-61.47	-64.82	-64.07	-67.58	-65.73	-66.71	-64.4
916	-63.57	-60.51	-65.5	-64.48	-67.48	-66.04	-65.86	-64.66
917	-63.04	-59.77	-65.95	-64.82	-67.11	-66	-66.5	-64.62
918	-60.12	-59.33	-65.86	-64.43	-66.15	-65.49	-66.06	-64.43
919	-62.96	-58.74	-65.43	-64.87	-66.05	-66.06	-65.95	-63.97
920	-62.13	-58.52	-64.85	-64.19	-65.4	-65.95	-65.44	-63.53
921	-61.83	-58.76	-64.76	-63.38	-65.73	-65.69	-65.61	-63.42
922	-61.3	-57.3	-63.96	-63	-65.48	-65.3	-65.61	-63.2
923	-61.06	-57.43	-63.38	-63.15	-65.41	-65.64	-64.94	-62.62
924	-60.33	-56.94	-63.28	-62.75	-65.29	-64.85	-64.65	-61.84
925	-61.06	-56.72	-62.97	-62.4	-65.52	-64.6	-64.47	-62.42
926	-61.04	-56.82	-62.37	-62.96	-65.28	-64.92	-65.17	-61.96
927	-61.33	-56.49	-62.5	-62.38	-65.34	-65.19	-65.94	-62.32
928	-61.03	-56.72	-62.28	-62.81	-65.86	-64.81	-64.79	-62.8

Table D.2(ii). Power Measurements on the First Floor of Stocker Center (continued)

Frequency	Distance between the Transmitter and Receiver					
	50m		60m		70m	
	M 1	M 2	M 1	M 2	M 1	M 2
902	-75.37	-73.83	-76.05	-74.46	-74.52	-74.18
903	-73.23	-72.86	-74.92	-75.02	-74.49	-75.26
904	-73.46	-73.5	-75.08	-75.43	-74.28	-74.33
905	-74.99	-72.48	-74.85	-75.86	-74.31	-74.29
906	-72.88	-73.2	-73.96	-75.51	-72.83	-73.55
907	-72.07	-72.24	-72.04	-74.46	-73.75	-73.27
908	-73.22	-71.01	-72.95	-74.25	-73.81	-73.78
909	-71.48	-70.34	-73.26	-74.96	-73.29	-73.12
910	-71.81	-69.51	-72.57	-74.05	-72.25	-72.98
911	-71.39	-67.73	-71.86	-73.6	-72.24	-71.51
912	-70.84	-68.76	-71.64	-73.25	-70.35	-71.03
913	-70.28	-68.31	-71.89	-73.37	-72	-70.83
914	-71.17	-68.28	-70.68	-73.55	-70.7	-71.22
915	-70.58	-68.57	-69.63	-71.8	-70.2	-70.29
916	-70.13	-68.47	-69.69	-72.89	-70.22	-70.12
917	-70.5	-68.11	-69.89	-72.99	-70.07	-69.81
918	-70.41	-68.06	-69.78	-71.73	-70.14	-68.28
919	-70.39	-68.07	-69.11	-73.1	-69.83	-69.46
920	-68.76	-67.82	-69.21	-72.21	-69.66	-69.31
921	-69.06	-67.71	-68.95	-71.62	-68.64	-69.03
922	-68.39	-67.18	-68.05	-72.38	-69.67	-69.05
923	-68.72	-68.61	-68.04	-71.66	-68.83	-67.76
924	-68	-66.53	-67.98	-70.82	-68.74	-67.11
925	-67.81	-66	-67.42	-70.84	-68.45	-67.76
926	-68.47	-65.92	-67.51	-71.35	-68.51	-67.12
927	-68.32	-65.76	-67.85	-72.57	-68.47	-67.54
928	-67.49	-65.16	-67.49	-72.66	-68	-67.1

Table D. 3(i). Power Measurements on the Second Floor of Stocker Center

Frequency	Distance between the Transmitter and Receiver							
	10m		20m		30m		40m	
	M 1	M 2	M 1	M 2	M 1	M 2	M 1	M 2
902	-58.21	-61.24	-63.68	-60.1	-65.61	-66.14	-69.72	-68.91
903	-58.45	-62.58	-64.17	-60.68	-65.84	-66.96	-70.64	-68.94
904	-58.57	-62.29	-64.82	-60.95	-66.17	-67.09	-70.92	-69.27
905	-58.11	-61.87	-64.92	-61.2	-68.68	-67.06	-70.03	-69.73
906	-57.48	-61.95	-65.44	-61.23	-66.4	-67.03	-71.23	-69.61
907	-56.93	-60.91	-66.67	-61.79	-66.31	-66.41	-71.98	-69.86
908	-56.92	-59.54	-66.06	-61.54	-66.2	-66.26	-70.25	-69.66
909	-56.64	-59.48	-67.11	-61.72	-65.54	-66.17	-70.75	-69.42
910	-57.1	-58.58	-66.68	-61.71	-66.38	-66.13	-70.06	-68.36
911	-56.9	-58.13	-68.43	-61.69	-64.71	-65.7	-70.44	-67.85
912	-56.73	-57.74	-67.98	-61.92	-65.78	-65.88	-70.34	-67.88
913	-56.78	-57.61	-67.82	-61.93	-65.18	-66.31	-69.98	-67.81
914	-56.99	-57.69	-68.4	-61.86	-65.34	-65.13	-69.82	-67.99
915	-56.87	-57.98	-68.67	-61.61	-65.48	-65.91	-69.43	-67.4
916	-56.93	-57.05	-68.52	-61.38	-64.92	-65.69	-69.68	-67.83
917	-56.72	-57.01	-68.07	-61.08	-64.68	-65.88	-69.5	-66.53
918	-57.08	-57.19	-68.28	-60.84	-64.41	-65.54	-68.81	-67.02
919	-57.05	-57.71	-68.47	-60.69	-64.46	-66	-69.29	-67.06
920	-57.38	-57.65	-68.38	-60.67	-65.2	-65.74	-69.53	-67.27
921	-57.64	-57.64	-66.37	-60.98	-65.06	-66.09	-68.84	-67.43
922	-57.57	-58.05	-65.93	-60.98	-66.23	-66.03	-69.69	-66.69
923	-58.19	-58.21	-65.65	-61.31	-65.49	-67.36	-69.79	-66.62
924	-57.99	-58.03	-66.08	-61.29	-66.42	-66.89	-68.6	-67.09
925	-57.99	-58.29	-65.41	-60.64	-64.48	-67.6	-69.77	-66.52
926	-57.8	-58.13	-65.31	-60.38	-65.48	-67.76	-69.87	-67.24
927	-57.73	-57.08	-64.24	-60.12	-63.99	-67.28	-68.62	-66.45
928	-57.6	-57.14	-63	-60.01	-64.18	-66.4	-67.96	-66.31

Table D. 3(ii). Power Measurements on the Second Floor of Stocker Center (continued)

Frequency	Distance between the Transmitter and Receiver			
	50m		60m	
	M 1	M 2	M 1	M 2
902	-75.29	-72.5	-71.71	-72.85
903	-75.4	-73.9	-73.67	-72.39
904	-74.85	-71.8	-72.36	-72.84
905	-74.79	-73.94	-73.21	-72.59
906	-74.1	-73.64	-72.32	-72.4
907	-74.43	-74.09	-73.31	-73.15
908	-74.77	-72.35	-73.06	-71.01
909	-74.38	-74.28	-74.77	-72.75
910	-74.54	-72.62	-73.04	-73.59
911	-74.87	-71.96	-73.9	-72.18
912	-73.14	-72.72	-72.58	-71.07
913	-74.64	-73.95	-71.9	-73.23
914	-76.09	-73.92	-71.6	-72.15
915	-74.33	-71.79	-73.39	-72.86
916	-73.88	-72.87	-70.97	-72.49
917	-74.19	-73.41	-71.31	-70.77
918	-74.53	-72.14	-72.09	-71.61
919	-74.55	-72.03	-73.37	-70.82
920	-74.46	-71.84	-71.8	-71.26
921	-75.1	-71.43	-72.76	-72.12
922	-73.43	-72.17	-71.26	-72.2
923	-72.95	-71.81	-71.93	-71.62
924	-73.16	-73.7	-73.11	-71.62
925	-74.04	-73.45	-72.86	-72.61
926	-73.85	-74	-73.09	-71.18
927	-74.82	-72.89	-72.42	-70.79
928	-74.82	-71.47	-72.2	-70.51

Table D.4(i). Power Measurements on the Third Floor of Stocker Center

Frequency	Distance between the Transmitter and Receiver							
	10m		20m		30m		40m	
	M 1	M 2	M 1	M 2	M 1	M 2	M 1	M 2
902	-53.99	-53.79	-56.87	-55.77	-63.66	-62.19	-63.43	-62.16
903	-53.9	-53.69	-56.39	-55.37	-63.8	-62.25	-62.99	-61.4
904	-53.92	-53.51	-55.57	-54.78	-63.87	-61.35	-62.85	-61.39
905	-53.96	-53.67	-55.59	-54.14	-63.29	-60.77	-62.57	-61.26
906	-53.38	-54.13	-55.42	-53.98	-63.43	-61.52	-62.86	-61.38
907	-54.2	-55.35	-55.91	-53.46	-63.3	-61.26	-62.67	-61.06
908	-54.06	-55.53	-56.21	-53.37	-63.04	-61.27	-63.1	-60.99
909	-53.94	-55.21	-56.5	-53.16	-63.19	-61.5	-63.08	-60.65
910	-53.63	-55.37	-55.81	-53.13	-63.29	-60.85	-62.62	-60.63
911	-53.5	-54.97	-55.7	-52.9	-63.02	-61.28	-62.21	-60.73
912	-53.61	-55.06	-55.69	-52.85	-63.1	-61.59	-62.08	-60.12
913	-53.6	-55.22	-55.75	-52.73	-63.13	-61.24	-61.65	-60.32
914	-53.51	-55.4	-56.03	-52.11	-63.31	-60.84	-61.5	-60.73
915	-53.35	-55.37	-56.01	-52.02	-62.97	-61.12	-60.99	-60.26
916	-53.38	-55.14	-55.9	-51.74	-63.06	-60.26	-61.3	-60.03
917	-53.47	-54.6	-55.91	-51.66	-63.22	-59.49	-60.97	-60.04
918	-53.33	-54.46	-56.09	-51.74	-62.58	-62.26	-59.98	-60.03
919	-53.51	-53.82	-56.28	-51.68	-62.42	-60.81	-60.32	-60.29
920	-53.95	-53.62	-56.41	-51.78	-62.6	-60.74	-59.86	-59.99
921	-54.51	-53.17	-56.37	-51.94	-62.68	-59.92	-60.31	-60.1
922	-54.86	-53.41	-56.29	-52.03	-62.81	-60.12	-59.72	-60.33
923	-55.32	-53.51	-56.34	-52.18	-62.67	-59.77	-59.7	-60.53
924	-55.81	-53.54	-56.41	-52.2	-62.89	-59.39	-59.46	-60.1
925	-55.96	-53.53	-56.4	-52.12	-63	-60.33	-60.07	-60
926	-56.06	-53.49	-56.4	-52.03	-63.1	-60.07	-60.38	-60.15
927	-56.01	-53.57	-56.06	-51.94	-63.16	-60.71	-60.32	-60.26
928	-56.05	-53.65	-56.02	-52.04	-63.37	-61.29	-60.65	-60.15

Table D.4(ii). Power Measurements on the Third Floor of Stocker Center (continued)

Frequency	Distance between the Transmitter and Receiver					
	500m		60m		70m	
	M 1	M 2	M 1	M 2	M 1	M 2
902	-66.9	-68.08	-69.92	-72.01	-67.86	-67.89
903	-66.57	-68.79	-70.2	-71.81	-67.24	-67.27
904	-66.2	-68.04	-69.25	-71.32	-67.16	-67.24
905	-66.69	-67.7	-68.64	-71.29	-66.96	-67.73
906	-65.9	-67.06	-68.97	-72.17	-66.7	-67.51
907	-66.38	-68.22	-67.93	-71.48	-67.4	-67.69
908	-66.4	-67.58	-67.67	-71.5	-67.56	-67.71
909	-66.19	-68.71	-67.89	-71.77	-67.27	-67.72
910	-66.33	-68.13	-67.71	-71.28	-67.74	-67.76
911	-66.74	-69.04	-67.92	-70.68	-67.68	-67.32
912	-66.63	-68.53	-67.63	-72.69	-68.25	-67.53
913	-66.35	-68.39	-67.66	-71.65	-67.76	-67.26
914	-67.38	-68.26	-67.48	-71.43	-67.89	-67.48
915	-66.86	-68.22	-67.02	-71.41	-67.97	-67.38
916	-66.32	-67.77	-66.08	-70.42	-67.81	-67.04
917	-66.79	-68.18	-67.01	-68.88	-67.64	-67.14
918	-67.28	-68.42	-67.06	-68.78	-67.65	-67.38
919	-66.35	-69.21	-66.77	-68.78	-67.41	-67.01
920	-67.2	-69.57	-66.69	-68.43	-67.47	-67.25
921	-66.53	-69.91	-66.65	-69.13	-67.52	-67.55
922	-66.77	-69.9	-66.47	-68.47	-67.58	-67.37
923	-65.31	-70.19	-65.96	-68.56	-67.16	-67.26
924	-66.8	-70.88	-65.87	-68.14	-68.18	-66.92
925	-67.11	-69.91	-66.88	-68.2	-68.3	-66.8
926	-66.56	-70.89	-66.71	-67.81	-68.46	-67.2
927	-67.89	-70.65	-67.47	-68.16	-68.36	-66.54
928	-68	-71.81	-67.93	-67.99	-68.28	-67.43

Table D.5(i). Power Measurements on the Fourth Floor of Stocker Center

Frequency	Distance between the Transmitter and Receiver							
	10m		20m		30m		40m	
	M 1	M 2	M 1	M 2	M 1	M 2	M 1	M 2
902	-64.21	-60.2	-68.01	-66.16	-64.03	-62.93	-69.32	-67.27
903	-64.61	-60.26	-67.77	-65.33	-63.95	-62.16	-67.79	-67.54
904	-65.46	-59.89	-68.26	-64.67	-63.93	-62.39	-68.58	-67.38
905	-67.11	-60.01	-68	-65.6	-63.3	-62.65	-68.07	-67.03
906	-66.35	-60.09	-67.57	-64.73	-63.12	-61.99	-67.47	-67.3
907	-65.4	-59.39	-67.31	-63.89	-62.77	-61.8	-67.09	-66.89
908	-65.16	-59.34	-67.21	-63.45	-62.78	-61.81	-67.5	-66.24
909	-64.42	-58.94	-67.25	-62.71	-62.97	-61.73	-67.08	-66.18
910	-62.39	-59.11	-67.64	-62.76	-63.04	-62.15	-67.22	-65.89
911	-62.8	-59.06	-67.5	-62.97	-63.06	-62.08	-66.39	-65.55
912	-62.65	-59.63	-67.77	-63.19	-62.52	-62.92	-67.4	-65.64
913	-62.58	-60.06	-67.09	-62.9	-62.8	-62.99	-67.91	-64.96
914	-62.89	-61.08	-68.28	-62.76	-62.46	-63.1	-67.06	-65.74
915	-62.99	-62.01	-68.94	-63.01	-62.11	-62.81	-67.75	-65.41
916	-63.45	-63.42	-70.5	-62.55	-61.99	-62.03	-68.27	-65.22
917	-63.87	-65.38	-69.7	-63.16	-61.88	-62.67	-68.13	-65.09
918	-64.1	-67.81	-70.15	-64.36	-62.39	-62.18	-67.85	-65.94
919	-64.29	-70.74	-66.98	-63.96	-61.93	-62.14	-68.36	-66.61
920	-64.69	-72.96	-69.47	-64.8	-62.24	-62.3	-70.07	-66.68
921	-64.85	-71.81	-71.66	-65.36	-62.52	-62.7	-69.67	-67.05
922	-64.84	-70.78	-70.52	-65.48	-62.2	-62.45	-70.43	-66.71
923	-64.57	-68.97	-69.94	-65.24	-61.64	-62.34	-69.87	-66.62
924	-64.35	-68.29	-68.46	-66.07	-61.5	-61.63	-68.79	-66.47
925	-64.11	-68.14	-72.24	-65.07	-61.05	-60.94	-68.48	-66.84
926	-63.52	-72.5	-72.87	-64.94	-61.19	-60.67	-70.13	-67
927	-62.72	-70.17	-71.21	-64.27	-60.91	-61.09	-70	-66.87
928	-62.07	-68.12	-69.44	-64.28	-61.18	-60.8	-68	-66.53

Appendix E

Amplitude Transfer Function Plots

Figure E.1 to E.7 shows the plots for power vs. frequency for Measurement #2 on different floors of Stocker. The figures are arranged in increasing order of floors for both 902-928 MHz and 2.4-2.5 GHz frequency bands.

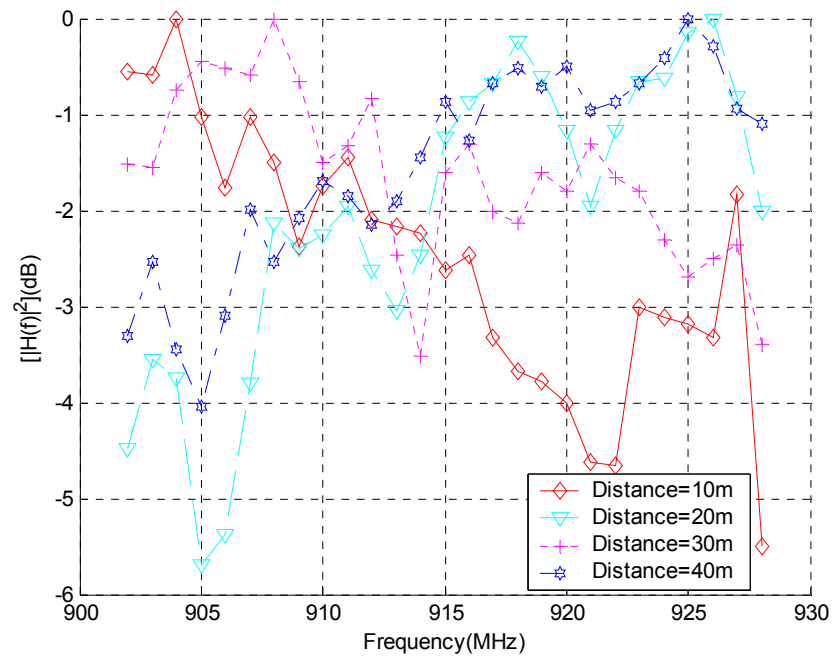


Figure E.1. Variation of power with frequency for Measurement #2 on Ground Floor of Stocker center at various distances from the transmitter for 902-928 MHz.

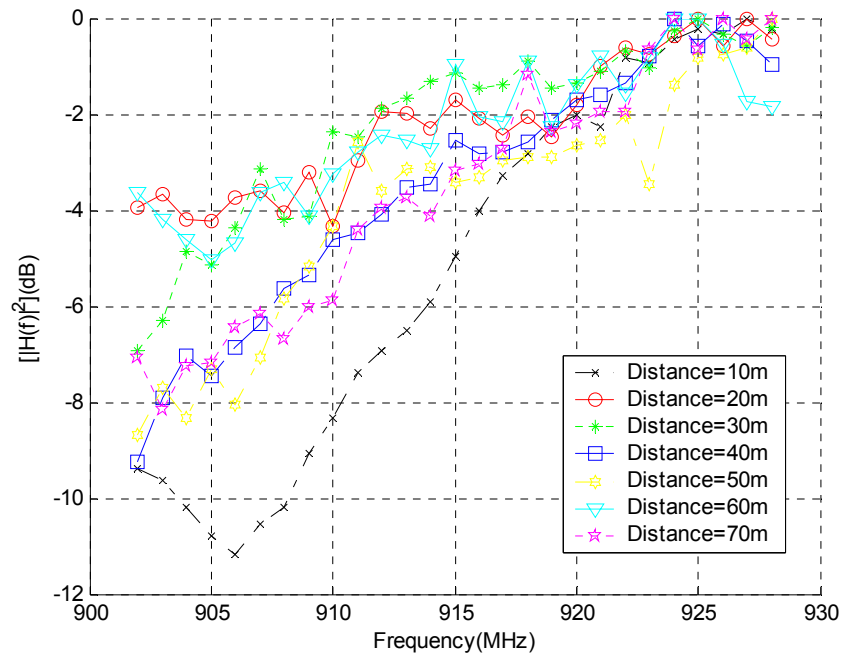


Figure E.2. Variation of power with frequency for Measurement #2 on First Floor of Stocker center at various distances from the transmitter for 902-928 MHz.

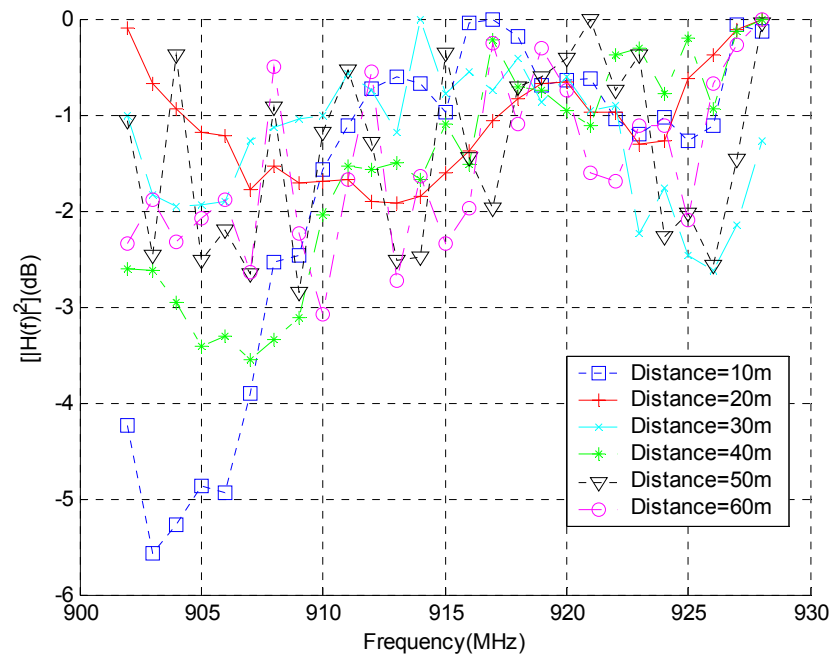


Figure E.3. Variation of power with frequency for Measurement #2 on Second Floor of Stocker center at various distances from the transmitter for 902-928 MHz.

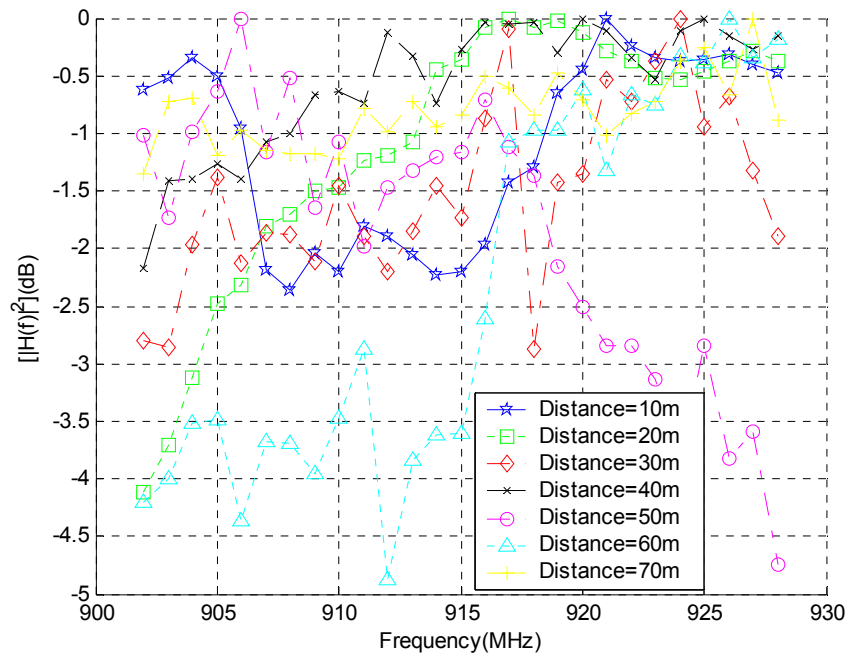


Figure E.4. Variation of power with frequency for Measurement #2 on Third Floor of Stocker center at various distances from the transmitter for 902-928MHz.

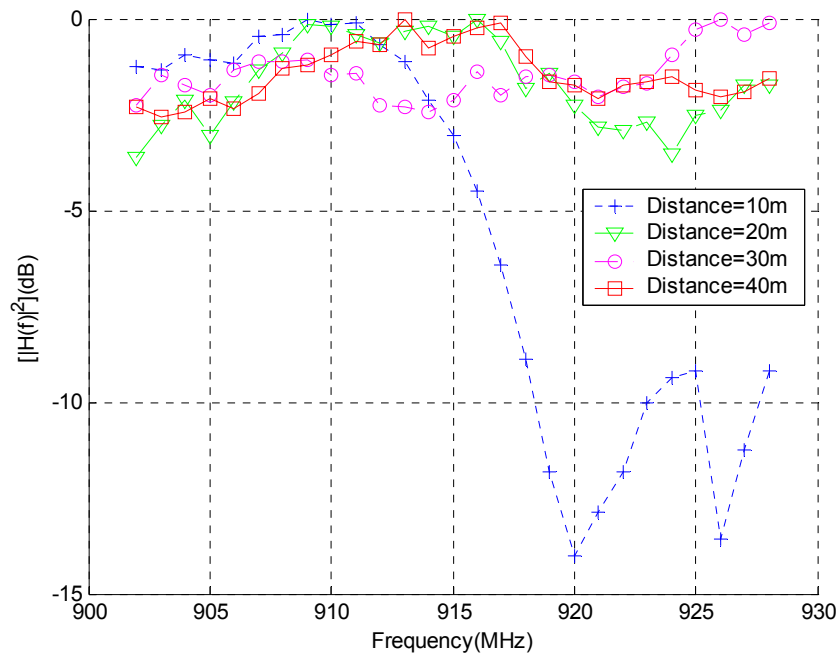


Figure E.5. Variation of power with frequency for Measurement #2 on Fourth Floor of Stocker center at various distances from the transmitter for 902-928 MHz.

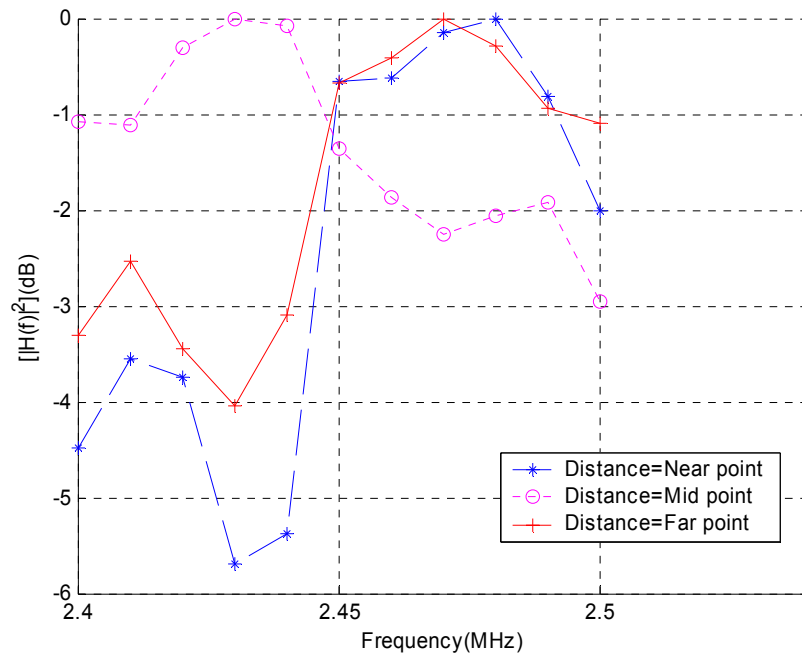


Figure E.6. Variation of power with frequency for Measurement #2 on Second Floor of Stocker center at various distances from the transmitter for 2.4-2.5 GHz.

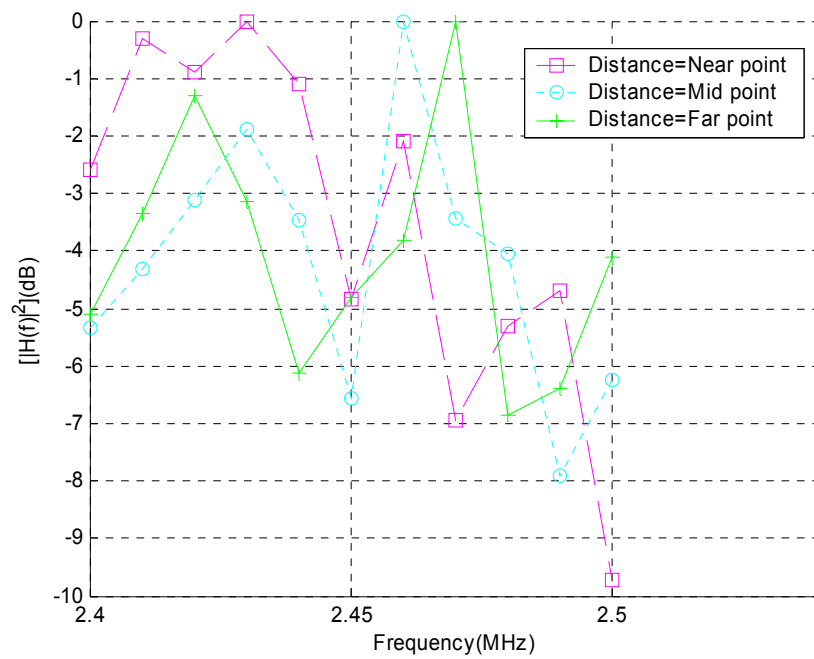


Figure E.7. Variation of power with frequency for Measurement #2 on Third Floor of Stocker center at various distances from the transmitter for 2.4-2.5 GHz.

Appendix F

Matlab Programs

F.1. Matlab program for Path loss vs. Distance

Function PathLossModel takes the measurement data of received power, Tx-Rx separated distance, reference power and reference distance as inputs. It calculates path loss, computes propagation component n using least squares linear regression fit algorithm, and finds the standard deviation and spread of the measured data.

Function PathLossGraph plots the figure of path loss vs Tx-Rx separated distance.

PropagInStocker.m is the main program. It reads in the measurement data in Stocker building and calls functions PathLossModel and PathLossGraph to model the propagations with different transmission frequencies in different floors of Stocker building.

PathLossModel.m

```
%*****
%Indoor propagation path loss modeling
%*****

%Pr[dBm]: Matrix of received power
%Pr0[dBm]: Received power at reference distance
%d[m]: Tx-Rx seperation
%d0[m]: Reference distance
function [n,rou,PL,yhat,D,MaxSprd,MinSprd]=PathLossModel(Pr,d,Pr0,d0)
PL=Pr0-Pr;
D=10*log10(d/d0);
```

```

%-----
%least squares linear regression fit
%-----

[row,col]=size(PL);

X=(D')*ones(1,row);
Y=PL;

s1=sum(diag(X*Y));
s2=sum(sum(X));
s3=sum(sum(Y));
s4=sum(sum(X.^2));

m=row*col;
n=(m*s1-s2*s3)/(m*s4-s2^2);
b=(s3*s4-s2*s1)/(m*s4-s2^2);
yhat=n.*D+b;

e=Y-n*(X')-b;
z=1/m*sum(sum(e.^2));
rou=sqrt(z);          %standard variance

upper=max(PL);
lower=min(PL);
MaxSprd=max(upper-lower);
MinSprd=min(upper-lower);

```

PathLossGraph.m

```

function linep=PathLossGraph(n,rou,MaxSprd,MinSprd,PL,yhat,d,
                             line_color,line_width,newPlot,drawPnts)

if newPlot >0
    figure;
else
    hold on;
end

if drawPnts
    semilogx(d,PL, strcat(line_color,'.'));
    hold on,

```



```

end
linep=semilogx(d,yhat, strcat(line_color,'-'),'LineWidth',line_width);

leg=strcat('n=',num2str(n),', \sigma=',num2str(rou),'[dB]', ...
           ', MaxSprd=',num2str(MaxSprd),' MinSprd=',num2str(MinSprd));
xlabel('Distance [m]');
ylabel('Path loss [dB]')
legend(leg,2);

grid on;
hold off;

```

PropagInStocker.m

```

%*****
% Indoor Wireless Propagation Modeling in Stocker Building
%*****

clear;

%*****
% measurements
%*****

%Raw measurement data from different floors in Stocker Center
%Distance in meter
%Received power in dBm
%Take 5 readings at the same distance

d0=1;

%=====
% 900MHZ
%=====

Pr0_dbm_grd_900mhz=-61.3;
Pr0_dbm_1st_900mhz=-47.23;
Pr0_dbm_2nd_900mhz=-47.23;
Pr0_dbm_3rd_900mhz=-56.72;
Pr0_dbm_4th_900mhz=-47.23;
Pr0_dbm_900mhz=-47.23;

%-----
% LOS / 900MHz / Stocker

```

%-----

d_grd_900mhz_los=[5,10,15,20,25,30,35,40];

Pr_dbm_grd_900mhz_los=[
 -73.70 -72.32 -71.55 -71.23 -69.50;
 -77.47 -77.62 -76.24 -74.20 -73.67;
 -78.40 -75.90 -74.60 -74.74 -76.50;
 -81.70 -83.60 -83.78 -83.12 -81.20;
 -82.40 -81.20 -80.30 -79.40 -79.80;
 -82.30 -80.88 -80.55 -80.70 -83.20;
 -82.30 -80.78 -80.62 -82.44 -88.02;
 -91.60 -89.93 -88.38 -89.66 -91.66
]';

d_1st_900mhz_los=[5,10,15,20,25,30,35,40,45,50,55,60,65,70];

Pr_dbm_1st_900mhz_los=-[
 60.10 55.75 60.20 62.30 63.40;
 60.80 61.70 64.10 61.80 61.40;
 69.10 71.30 68.90 65.20 67.70;
 63.70 66.70 75.40 78.10 75.40;
 67.60 69.80 74.10 74.50 71.20;
 74.50 72.40 73.60 72.10 72.30;
 70.12 72.30 71.30 74.72 72.55;
 80.62 74.53 75.02 71.10 76.60;
 74.08 80.10 87.62 80.08 79.65;
 76.03 79.42 78.64 77.60 77.62;
 89.94 83.05 81.14 81.92 81.62;
 82.10 81.30 76.70 87.20 84.10;
 80.79 79.50 78.20 80.30 81.20;
 81.80 82.40 85.40 83.30 84.20
]';

d_2nd_900mhz_los=[5,10,15,20,25,30,35,40,45,50,55,60,65,70,75];

Pr_dbm_2nd_900mhz_los=[
 -55.81 -59.79 -55.78 -58.16 -53;
 -63.43 -63.15 -60.83 -59.75 -59.72;
 -56.57 -55.78 -63.87 -61.71 -68.13;
 -59.59 -61.8 -74.77 -63.7 -76.81;
 -66.24 -65.84 -66.9 -64.14 -65.36;
 -63.39 -67.83 -72.84 -66.64 -70.55;
 -69.19 -68.94 -69.19 -65.89 -64.3;
 -70.63 -71.18 -70.5 -73.28 -74.55;
 -69.74 -71 -70.93 -70.82 -72.99;
 -73.68 -72.51 -78.22 -76.05 -80.05;
 -79.42 -81.83 -86.03 -74.03 -86.13;

```
-80.12 -82.44 -86.01 -75.21 -74.18;
-76.67 -83.14 -89.74 -80.24 -77.52;
-75.53 -77.61 -79.44 -78.63 -81.07;
-79.55 -78.63 -76.14 -77.03 -84.85
]';
```

```
d_3rd_900mhz_los=[5,10,15,20,25,30,35,40,45,50,55,60,65,70,75];
Pr_dbm_3rd_900mhz_los=[
-72.10 -71.70 -66.90 -63.20 -61.70;
-70.73 -72.76 -74.90 -73.50 -68.70;
-80.80 -76.30 -71.70 -73.60 -75.90;
-84.60 -84.20 -80.50 -74.60 -74.80;
-81.80 -82.30 -78.50 -80.90 -80.60;
-83.40 -86.40 -86.40 -81.30 -78.00;
-81.10 -79.20 -78.10 -78.90 -77.20;
-86.30 -86.60 -86.50 -85.90 -84.30;
-89.40 -88.60 -87.20 -86.10 -87.10;
-90.90 -89.60 -88.40 -85.60 -83.40;
-85.40 -85.60 -82.20 -80.70 -79.90;
-88.70 -87.60 -87.60 -87.10 -87.20;
-92.20 -92.30 -92.90 -90.50 -90.40;
-89.20 -86.70 -85.70 -85.10 -84.30;
-93.70 -90.50 -89.60 -89.70 -91.10
]';
```

```
d_4th_900mhz_los=[5,10,15,20,25,30,35,40,45];
Pr_dbm_4th_900mhz_los=[
-54.67 -53.08 -63.71 -66.68 -65.68;
-69.14 -72.83 -63.48 -68.03 -66.36;
-64.18 -68.23 -67.86 -63.39 -70.35;
-67.43 -66.05 -76.23 -69.48 -66.75;
-84.88 -73.7 -67.71 -63.51 -78.23;
-78.13 -73.88 -68.49 -68.53 -74.8;
-68.81 -69.13 -69.45 -85 -77.01;
-73.85 -68.44 -72.27 -71.84 -72.77;
-79.04 -76.76 -67.67 -75.29 -77.64
]';
```

```
%-----
% NLOS / 900MHz / Stocker
%-----
```

```
d_grd_900mhz_nlos=[
21.02379604;
21.84032967;
```

```

23.70653918;
26.40075756;
29.69848481;
17.88854382;
21.58703314;
23.2594067;
25.8069758;
26.01922366;
31.01612484;
36.01388621;
41.01219331;
46.01086828;
57.14017851;
57.70615219;
62.80127387;
67.74215822;
57.31491952;
58.05170109
]';

```

```

Pr_dbm_grd_900mhz_nlos=-[
74.08 79.16 78.01 79.82 74.20;
82.32 85.03 89.08 87.98 86.12;
87.20 86.90 87.40 87.18 86.85;
87.30 87.63 87.79 87.70 87.20;
87.48 87.84 87.29 87.50 87.53;
87.33 87.69 87.14 86.95 87.41;
86.60 85.64 83.14 84.02 81.97;
79.41 81.88 82.40 82.98 84.42;
85.48 84.94 85.05 85.71 85.48;
74.47 81.74 75.47 77.72 72.86;
81.75 82.93 81.94 76.25 76.91;
77.32 75.11 75.38 76.76 78.13;
80.86 78.79 82.03 80.95 82.84;
81.19 82.16 80.71 82.33 82.40;
86.75 86.64 86.86 85.51 86.85;
86.61 86.55 86.56 86.97 86.74;
86.57 86.91 86.72 86.79 86.45;
86.91 86.86 86.25 86.72 86.62;
86.45 87 86.62 86.92 86.47;
86.17 86.95 86.88 86.72 87.86
]';

```

```

d_2nd_900mhz_nlos=[
33.96998675;

```

```

34.53925303;
37.21505072;
41.96093421;
52.96413881;
59.28709809;
61.60324667;
76.85336687
]';

```

```

Pr_dbm_2nd_900mhz_nlos=[
-89.3 -89.71 -90.15 -90.2 -90.16;
-89.01 -90.9 -88.96 -88.42 -87.4;
-80.1 -86.95 -86.69 -87.18 -87.23;
-88.9 -88.93 -88.96 -88.99 -89.01;
-89.42 -89.35 -89.4 -89.43 -89.42;
-89.44 -90.07 -90.12 -90.01 -89.95;
-90.37 -90.23 -90.28 -90.26 -90.41;
-88.62 -89.94 -89.91 -90.28 -90.3
]';

```

```

d_3rd_900mhz_nlos=[
39.597284;
45.50535023;
51.54206923;
60.24832695;
66.56912873;
72.95763771;
78.7292633;
79.04869955;
79.55769542;
80.65194914;
]';

```

```

Pr_dbm_3rd_900mhz_nlos=-[
82      89      89.2    89.4    89.6;
93.8    93.9    93.2    93.6    93.5;
93.4    93.6    93.7    94      94.2;
93.8    93.4    93.2    94.3    94.2;
93.4    93.8    93.9    93.7    94.1;
93.1    93.4    93.3    93.4    93.9;
93.8    94.1    94.3    94.1    94.2;
96.2    96.4    96.7    96.3    89.7
93.9    93.6    93.5    94.2    94.4;
94.2    94.1    93.4    93.6    93.9;
]';

```

```

%=====
% 2.4GHZ
%=====

Pr0_dbm_grd_24ghz=-59.4;
Pr0_dbm_1st_24ghz=-61.7;
Pr0_dbm_2nd_24ghz=-61.7;
Pr0_dbm_3rd_24ghz=-58.3;
Pr0_dbm_4th_24ghz=-61.7;
Pr0_dbm_24ghz=-58.3;

%-----
% LOS / 2.4GHz / Stocker
%-----

d_grd_24ghz_los=[5,10,15,20,25,30,35,40];
Pr_dbm_grd_24ghz_los=[
-73.47 -72.25 -70.40 -69.80 -68.40;
-76.40 -76.60 -74.80 -74.17 -74.90;
-80.60 -82.30 -83.80 -82.70 -81.60;
-80.17 -80.20 -79.88 -80.70 -82.12;
-78.50 -77.10 -78.10 -79.30 -79.70;
-82.80 -81.95 -81.30 -80.20 -81.80;
-85.20 -84.02 -83.18 -84.17 -84.86;
-94.79 -93.37 -93.02 -93.95 -94.28
];

d_1st_24ghz_los=[5,10,15,20,25,30,35,40,45,50,55,60,65,70];
Pr_dbm_1st_24ghz_los=-[
70.90 65.20 62.00 67.40 63.18;
67.20 70.90 66.30 68.20 65.90;
72.90 66.20 65.80 69.90 72.10;
74.60 72.80 75.90 78.40 73.10;
71.20 74.40 73.20 79.90 72.40;
75.60 79.30 74.50 82.10 74.00;
81.20 74.30 73.20 79.00 82.10;
70.70 68.90 66.20 65.40 72.30;
70.10 69.20 69.70 70.20 65.60;
74.30 72.30 71.40 75.60 79.00;
75.20 70.10 69.20 74.90 79.20;
77.30 72.10 76.90 78.70 80.60;
76.90 77.90 76.40 75.70 73.20;
74.90 73.20 75.40 77.60 78.10

```

];

d_2nd_24ghz_lo=[5,10,15,20,25,30,35,40,45,50,55,60,65,70,75];

Pr_dbm_2nd_24ghz_lo=[

-71.6 -70.33 -73.04 -70.8 -72.9;
 -79.88 -78.06 -76.7 -82.39 -79.85;
 -81.49 -77.96 -81.72 -83.38 -85.14;
 -70.02 -83.95 -80.56 -77.09 -84.56;
 -86.48 -86.44 -86.46 -85.56 -85.14;
 -85.55 -85.56 -85.58 -85.54 -85.16;
 -86.54 -87.21 -87.5 -77.6 -82.15;
 -87.94 -82.89 -88.04 -87.06 -87.91;
 -90.95 -87.62 -89.44 -89.44 -87.79;
 -87.71 -91.01 -87.92 -89 -90.11;
 -87.01 -87.09 -87.04 -87.01 -86.97;
 -87.05 -87.07 -87.08 -87.06 -87.08;
 -93.63 -93.47 -96.14 -93.61 -94.45;
 -94.61 -94.51 -94.31 -94.45 -94.67;
 -94.1 -94.22 -91.88 -94.11 -93.89

];

d_3rd_24ghz_lo=[5,10,15,20,25,30,35,40,45,50,55,60,65,70,75];

Pr_dbm_3rd_24ghz_lo=[

-70.40 -70.70 -70.30 -74.06 -69.20;
 -70.40 -71.20 -71.70 -76.20 -76.20;
 -77.20 -75.30 -74.30 -78.60 -78.00;
 -78.40 -75.90 -74.20 -70.50 -70.20;
 -81.80 -82.60 -85.40 -86.40 -84.40;
 -77.80 -75.30 -74.10 -76.70 -80.20;
 -68.70 -68.40 -69.30 -69.10 -70.20;
 -79.50 -77.20 -75.10 -74.30 -73.80;
 -77.60 -76.20 -75.10 -72.90 -72.10;
 -81.30 -85.40 -86.20 -84.40 -82.70;
 -79.20 -79.30 -78.80 -77.50 -76.30;
 -83.40 -82.40 -82.30 -81.60 -81.90;
 -88.40 -89.90 -92.90 -87.60 -87.10;
 -86.90 -84.30 -82.40 -81.30 -81.80;
 -91.10 -90.90 -90.40 -89.90 -88.30

];

d_4th_24ghz_lo=[5,10,15,20,25,30,35,40,45];;

Pr_dbm_4th_24ghz_lo=[

-77.55 -71.24 -68.44 -73.35 -79.06;
 -85.85 -84.99 -83.88 -82.12 -85.08;
 -87.88 -86.32 -87.31 -91.84 -79.73;

```
-87.65 -86.83 -87.3 -87.02 -87.73;
-84.51 -86.03 -86.87 -87.78 -86.81;
-86.38 -87.3 -85.72 -84.57 -87.17;
-86.41 -86.92 -86.61 -86.91 -85.34;
-85.93 -86.35 -85.97 -85.67 -85.37;
-86.31 -84.32 -86.07 -85.98 -85.44
]';
```

```
%-----
% NLOS / 2.4GHz / Stocker
%-----
```

```
d_grd_24ghz_nlos=[
21.02379604;
21.84032967;
23.70653918;
26.40075756;
29.69848481;
17.88854382;
21.58703314;
23.2594067;
25.8069758;
26.01922366;
31.01612484;
36.01388621;
41.01219331;
46.01086828
]';
```

```
Pr_dbm_grd_24ghz_nlos=[
79.50 83.20 88.50 89.20 89.50;
92.90 88.90 90.40 91.30 89.92;
89.30 90.70 90.72 91.05 92.42;
91.30 89.30 90.09 88.61 90.50;
81.80 79.20 81.20 81.40 82.00;
90.20 90.40 88.90 90.90 90.70;
90.70 90.58 91.20 90.28 90.15;
89.80 90.01 90.13 89.78 89.00;
89.88 89.72 89.60 89.00 89.13;
81.70 79.20 81.30 79.40 79.60;
80.30 78.90 79.50 79.30 79.00;
79.10 81.30 79.97 80.23 80.14;
81.20 79.60 78.00 81.90 79.20;
80.40 80.30 79.20 81.20 80.30
]';
```



```
d_2nd_24ghz_nlos=[
33.96998675;
34.53925303;
37.21505072;
41.96093421;
52.96413881;
59.28709809;
61.60324667;
76.85336687
]';
```

```
Pr_dbm_2nd_24ghz_nlos=[
-89.92 -89.98 -89.95 -89.9 -89.96;
-90.4 -90.48 -90.1 -90.02 -89.58;
-89.31 -89.5 -89.42 -89.34 -89.26;
-90.01 -90.13 -89.85 -89.88 -89.82;
-90.04 -90.11 -90.05 -90.08 -90.19;
-89.43 -89.56 -89.6 -89.57 -89.51;
-89.47 -89.38 -89.57 -89.61 -89.54;
-89.77 -89.7 -89.67 -89.76 -89.72
]';
```

```
d_3rd_24ghz_nlos=[
39.597284;
45.50535023;
51.54206923;
60.24832695;
66.56912873;
72.95763771;
78.7292633;
79.04869955;
79.55769542;
80.65194914;
]';
```

```
Pr_dbm_3rd_24ghz_nlos=-[
89.2 89.12 89.3 89.1 88.7;
88.7 88.9 88.93 88.01 88.7;
89.1 89.3 89.9 90.07 90.3;
92.9 92.78 93.2 93.26 92.8;
93.3 92.9 93 93.09 92.7;
95.8 96.4 96.3 96.5 95.72;
```

```

96.5  96.2  95.7  95.5  94.8;
84.2  84.5  84.1  85.6  84.3;
93.7  94    94.4  94.3  94.8;
92.6  92.06 91.8  91.69 91.2;
]';

```

```

%*****
% Modeling
%*****

```

```

%=====
% 900MHZ
%=====

```

```

%-----
% LOS / 900Mhz / Ground Floor
%-----

```

```

[n_grd_900mhz_los,rou_grd_900mhz_los,PL_grd_900mhz_los, ...
yhat_grd_900mhz_los,D_grd_900mhz_los, ...
MaxSprd_grd_900mhz_los,MinSprd_grd_900mhz_los]= ...
PathLossModel(Pr_dbm_grd_900mhz_los,d_grd_900mhz_los,Pr0_dbm_grd_900mhz,d0
);

```

```

PathLossGraph(n_grd_900mhz_los,rou_grd_900mhz_los, ...
              MaxSprd_grd_900mhz_los,MinSprd_grd_900mhz_los, ...
              PL_grd_900mhz_los,yhat_grd_900mhz_los,d_grd_900mhz_los, ...
              'k',2,1,1);
title(['Propagation in Ground Floor of Stocker,LOS,900MHz']);

```

```

%-----
% LOS / 900Mhz / First Floor
%-----

```

```

[n_1st_900mhz_los,rou_1st_900mhz_los,PL_1st_900mhz_los, ...
yhat_1st_900mhz_los,D_1st_900mhz_los, ...
MaxSprd_1st_900mhz_los,MinSprd_1st_900mhz_los]= ...
PathLossModel(Pr_dbm_1st_900mhz_los,d_1st_900mhz_los,Pr0_dbm_1st_900mhz,d0);

```

```

PathLossGraph(n_1st_900mhz_los,rou_1st_900mhz_los, ...
              MaxSprd_1st_900mhz_los,MinSprd_1st_900mhz_los, ...
              PL_1st_900mhz_los,yhat_1st_900mhz_los,d_1st_900mhz_los, ...
              'k',2,1,1);
title(['Propagation in First Floor of Stocker,LOS,900MHz']);

```

```

%-----
%  LOS / 900Mhz / Second Floor
%-----

[n_2nd_900mhz_los,rou_2nd_900mhz_los,PL_2nd_900mhz_los, ...
yhat_2nd_900mhz_los,D_2nd_900mhz_los, ...
MaxSprd_2nd_900mhz_los,MinSprd_2nd_900mhz_los]= ...
PathLossModel(Pr_dbm_2nd_900mhz_los,d_2nd_900mhz_los,Pr0_dbm_2nd_900mhz,d
0);

PathLossGraph(n_2nd_900mhz_los,rou_2nd_900mhz_los, ...
              MaxSprd_2nd_900mhz_los,MinSprd_2nd_900mhz_los, ...
              PL_2nd_900mhz_los,yhat_2nd_900mhz_los,d_2nd_900mhz_los, ...
              'k',2,1,1);
title(['Propagation in Second Floor of Stocker,LOS,900MHz']);

%-----
%  LOS / 900Mhz / Third Floor
%-----

[n_3rd_900mhz_los,rou_3rd_900mhz_los,PL_3rd_900mhz_los, ...
yhat_3rd_900mhz_los,D_3rd_900mhz_los, ...
MaxSprd_3rd_900mhz_los,MinSprd_3rd_900mhz_los]= ...
PathLossModel(Pr_dbm_3rd_900mhz_los,d_3rd_900mhz_los,Pr0_dbm_3rd_900mhz,d0
);

PathLossGraph(n_3rd_900mhz_los,rou_3rd_900mhz_los, ...
              MaxSprd_3rd_900mhz_los,MinSprd_3rd_900mhz_los, ...
              PL_3rd_900mhz_los,yhat_3rd_900mhz_los,d_3rd_900mhz_los, ...
              'k',2,1,1);
title(['Propagation in Third Floor of Stocker,LOS,900MHz']);

%-----
%  LOS / 900Mhz / Fourth Floor
%-----

[n_4th_900mhz_los,rou_4th_900mhz_los,PL_4th_900mhz_los, ...
yhat_4th_900mhz_los,D_4th_900mhz_los, ...
MaxSprd_4th_900mhz_los,MinSprd_4th_900mhz_los]= ...
PathLossModel(Pr_dbm_4th_900mhz_los,d_4th_900mhz_los,Pr0_dbm_4th_900mhz,d0)
;

PathLossGraph(n_4th_900mhz_los,rou_4th_900mhz_los, ...
              MaxSprd_4th_900mhz_los,MinSprd_4th_900mhz_los, ...

```

```

        PL_4th_900mhz_los,yhat_4th_900mhz_los,d_4th_900mhz_los, ...
        'k',2,1,1);
title(['Propagation in Fourth Floor of Stocker,LOS,900MHz']);

%-----
%  LOS / 900Mhz / Entire Building
%-----

Pr_dbm_900mhz_los=[Pr_dbm_grd_900mhz_los,Pr_dbm_1st_900mhz_los, ...
Pr_dbm_2nd_900mhz_los, Pr_dbm_3rd_900mhz_los,Pr_dbm_4th_900mhz_los];

d_900mhz_los=[d_grd_900mhz_los,d_1st_900mhz_los,d_2nd_900mhz_los, ...
d_3rd_900mhz_los,d_4th_900mhz_los];

[n_900mhz_los,rou_900mhz_los,PL_900mhz_los, ...
yhat_900mhz_los,D_900mhz_los, ...
MaxSprd_900mhz_los,MinSprd_900mhz_los]= ...
PathLossModel(Pr_dbm_900mhz_los,d_900mhz_los,Pr0_dbm_900mhz,d0);

PathLossGraph(n_grd_900mhz_los,rou_grd_900mhz_los, ...
MaxSprd_grd_900mhz_los,MinSprd_grd_900mhz_los, ...
PL_grd_900mhz_los,yhat_grd_900mhz_los,d_grd_900mhz_los, ...
'c',1,1,1);

PathLossGraph(n_1st_900mhz_los,rou_1st_900mhz_los, ...
MaxSprd_1st_900mhz_los,MinSprd_1st_900mhz_los, ...
PL_1st_900mhz_los,yhat_1st_900mhz_los,d_1st_900mhz_los, ...
'g',1,0,1);

PathLossGraph(n_2nd_900mhz_los,rou_2nd_900mhz_los, ...
MaxSprd_2nd_900mhz_los,MinSprd_2nd_900mhz_los, ...
PL_2nd_900mhz_los,yhat_2nd_900mhz_los,d_2nd_900mhz_los, ...
'm',1,0,1);

PathLossGraph(n_3rd_900mhz_los,rou_3rd_900mhz_los, ...
MaxSprd_3rd_900mhz_los,MinSprd_3rd_900mhz_los, ...
PL_3rd_900mhz_los,yhat_3rd_900mhz_los,d_3rd_900mhz_los, ...
'b',1,0,1);

PathLossGraph(n_4th_900mhz_los,rou_4th_900mhz_los, ...
MaxSprd_4th_900mhz_los,MinSprd_4th_900mhz_los, ...
PL_4th_900mhz_los,yhat_4th_900mhz_los,d_4th_900mhz_los, ...
'r',1,0,1);

PathLossGraph(n_900mhz_los,rou_900mhz_los, ...

```

```

        MaxSprd_900mhz_los,MinSprd_900mhz_los, ...
        PL_900mhz_los,yhat_900mhz_los,d_900mhz_los, ...
        'k',2,0,0);

title(['Propagation in Stocker,LOS,900MHz']);

%-----
%  NLOS / 900Mhz / Ground Floor
%-----

[n_grd_900mhz_nlos,rou_grd_900mhz_nlos,PL_grd_900mhz_nlos, ...
yhat_grd_900mhz_nlos,D_grd_900mhz_nlos, ...
MaxSprd_grd_900mhz_nlos,MinSprd_grd_900mhz_nlos]= ...
PathLossModel(Pr_dbm_grd_900mhz_nlos,d_grd_900mhz_nlos,Pr0_dbm_grd_900mhz,
d0);

PathLossGraph(n_grd_900mhz_nlos,rou_grd_900mhz_nlos, ...
        MaxSprd_grd_900mhz_nlos,MinSprd_grd_900mhz_nlos, ...
        PL_grd_900mhz_nlos,yhat_grd_900mhz_nlos,d_grd_900mhz_nlos, ...
        'k',2,1,1);
title(['Propagation in Ground Floor of Stocker,NLOS,900MHz']);

%-----
%  NLOS / 900Mhz / Second Floor
%-----

[n_2nd_900mhz_nlos,rou_2nd_900mhz_nlos,PL_2nd_900mhz_nlos, ...
yhat_2nd_900mhz_nlos,D_2nd_900mhz_nlos, ...
MaxSprd_2nd_900mhz_nlos,MinSprd_2nd_900mhz_nlos]= ...
PathLossModel(Pr_dbm_2nd_900mhz_nlos,d_2nd_900mhz_nlos,Pr0_dbm_2nd_900mhz
,d0);

PathLossGraph(n_2nd_900mhz_nlos,rou_2nd_900mhz_nlos, ...
        MaxSprd_2nd_900mhz_nlos,MinSprd_2nd_900mhz_nlos, ...
        PL_2nd_900mhz_nlos,yhat_2nd_900mhz_nlos,d_2nd_900mhz_nlos, ...
        'k',2,1,1);
title(['Propagation in Second Floor of Stocker,NLOS,900MHz']);

%-----

```

```
% NLOS / 900Mhz / Third Floor
%-----
```

```
[n_3rd_900mhz_nlos,rou_3rd_900mhz_nlos,PL_3rd_900mhz_nlos, ...
yhat_3rd_900mhz_nlos,D_3rd_900mhz_nlos, ...
MaxSprd_3rd_900mhz_nlos,MinSprd_3rd_900mhz_nlos]= ...
PathLossModel(Pr_dbm_3rd_900mhz_nlos,d_3rd_900mhz_nlos,Pr0_dbm_3rd_900mhz,
d0);
```

```
PathLossGraph(n_3rd_900mhz_nlos,rou_3rd_900mhz_nlos, ...
    MaxSprd_3rd_900mhz_nlos,MinSprd_3rd_900mhz_nlos, ...
    PL_3rd_900mhz_nlos,yhat_3rd_900mhz_nlos,d_3rd_900mhz_nlos, ...
    'k',2,1,1);
title(['Propagation in Third Floor of Stocker,NLOS,900MHz']);
```

```
%-----
% NLOS / 900Mhz / Entire Building
%-----
```

```
Pr_dbm_900mhz_nlos=[Pr_dbm_grd_900mhz_nlos,Pr_dbm_2nd_900mhz_nlos, ...
Pr_dbm_3rd_900mhz_nlos];
d_900mhz_nlos=[d_grd_900mhz_nlos,d_2nd_900mhz_nlos,d_3rd_900mhz_nlos];
```

```
[n_900mhz_nlos,rou_900mhz_nlos,PL_900mhz_nlos, ...
yhat_900mhz_nlos,D_900mhz_nlos, ...
MaxSprd_900mhz_nlos,MinSprd_900mhz_nlos]= ...
PathLossModel(Pr_dbm_900mhz_nlos,d_900mhz_nlos,Pr0_dbm_900mhz,d0);
```

```
PathLossGraph(n_grd_900mhz_nlos,rou_grd_900mhz_nlos, ...
    MaxSprd_grd_900mhz_nlos,MinSprd_grd_900mhz_nlos, ...
    PL_grd_900mhz_nlos,yhat_grd_900mhz_nlos,d_grd_900mhz_nlos, ...
    'c',1,1,1);
```

```
PathLossGraph(n_2nd_900mhz_nlos,rou_2nd_900mhz_nlos, ...
    MaxSprd_2nd_900mhz_nlos,MinSprd_2nd_900mhz_nlos, ...
    PL_2nd_900mhz_nlos,yhat_2nd_900mhz_nlos,d_2nd_900mhz_nlos, ...
    'm',1,0,1);
```

```
PathLossGraph(n_3rd_900mhz_nlos,rou_3rd_900mhz_nlos, ...
    MaxSprd_3rd_900mhz_nlos,MinSprd_3rd_900mhz_nlos, ...
    PL_3rd_900mhz_nlos,yhat_3rd_900mhz_nlos,d_3rd_900mhz_nlos, ...
    'b',1,0,1);
```

```
PathLossGraph(n_900mhz_nlos,rou_900mhz_nlos, ...
```

```

        MaxSprd_900mhz_nlos,MinSprd_900mhz_nlos, ...
        PL_900mhz_nlos,yhat_900mhz_nlos,d_900mhz_nlos, ...
        'k',2,0,0);

title(['Propagation in Stocker,NLOS,900MHz']);

%-----
% (LOS + NLOS) / 900Mhz / Ground Floor
%-----

Pr_dbm_grd_900mhz=[Pr_dbm_grd_900mhz_los,Pr_dbm_grd_900mhz_nlos];
d_grd_900mhz=[d_grd_900mhz_los,d_grd_900mhz_nlos];

[n_grd_900mhz,rou_grd_900mhz,PL_grd_900mhz,yhat_grd_900mhz,D_grd_900mhz, ...
MaxSprd_grd_900mhz,MinSprd_grd_900mhz]= ...
PathLossModel(Pr_dbm_grd_900mhz,d_grd_900mhz,Pr0_dbm_grd_900mhz,d0);

PathLossGraph(n_grd_900mhz,rou_grd_900mhz, ...
        MaxSprd_grd_900mhz,MinSprd_grd_900mhz, ...
        PL_grd_900mhz,yhat_grd_900mhz,d_grd_900mhz, ...
        'k',2,1,1);
title(['Propagation in Ground Floor of Stocker,LOS+NLOS,900MHz']);

%-----
% (LOS + NLOS) / 900Mhz / Second Floor
%-----

Pr_dbm_2nd_900mhz=[Pr_dbm_2nd_900mhz_los,Pr_dbm_2nd_900mhz_nlos];
d_2nd_900mhz=[d_2nd_900mhz_los,d_2nd_900mhz_nlos];

[n_2nd_900mhz,rou_2nd_900mhz,PL_2nd_900mhz,yhat_2nd_900mhz,D_2nd_900mhz,
...
MaxSprd_2nd_900mhz,MinSprd_2nd_900mhz]= ...
PathLossModel(Pr_dbm_2nd_900mhz,d_2nd_900mhz,Pr0_dbm_2nd_900mhz,d0);

PathLossGraph(n_2nd_900mhz,rou_2nd_900mhz, ...
        MaxSprd_2nd_900mhz,MinSprd_2nd_900mhz, ...
        PL_2nd_900mhz,yhat_2nd_900mhz,d_2nd_900mhz, ...
        'k',2,1,1);
title(['Propagation in Second Floor of Stocker,LOS+NLOS,900MHz']);

%-----
% (LOS + NLOS) / 900Mhz / Third Floor
%-----

```

```

Pr_dbm_3rd_900mhz=[Pr_dbm_3rd_900mhz_los,Pr_dbm_3rd_900mhz_nlos];
d_3rd_900mhz=[d_3rd_900mhz_los,d_3rd_900mhz_nlos];

[n_3rd_900mhz,rou_3rd_900mhz,PL_3rd_900mhz,yhat_3rd_900mhz,D_3rd_900mhz, ...
MaxSprd_3rd_900mhz,MinSprd_3rd_900mhz]= ...
PathLossModel(Pr_dbm_3rd_900mhz,d_3rd_900mhz,Pr0_dbm_3rd_900mhz,d0);

PathLossGraph(n_3rd_900mhz,rou_3rd_900mhz, ...
    MaxSprd_3rd_900mhz,MinSprd_3rd_900mhz, ...
    PL_3rd_900mhz,yhat_3rd_900mhz,d_3rd_900mhz, ...
    'k',2,1,1);
title(['Propagation in Third Floor of Stocker,LOS+NLOS,900MHz']);

%-----
% (LOS + NLOS) / 900Mhz / Entire Building
%-----

Pr_dbm_900mhz=[Pr_dbm_grd_900mhz_los,Pr_dbm_1st_900mhz_los,Pr_dbm_2nd_900mhz_los, ...
    Pr_dbm_3rd_900mhz_los,Pr_dbm_4th_900mhz_los, ...

Pr_dbm_grd_900mhz_nlos,Pr_dbm_2nd_900mhz_nlos,Pr_dbm_3rd_900mhz_nlos];

d_900mhz=[d_grd_900mhz_los,d_1st_900mhz_los,d_2nd_900mhz_los, ...
    d_3rd_900mhz_los,d_4th_900mhz_los, ...
    d_grd_900mhz_nlos,d_2nd_900mhz_nlos,d_3rd_900mhz_nlos];

[n_900mhz,rou_900mhz,PL_900mhz,yhat_900mhz,D_900mhz, ...
MaxSprd_900mhz,MinSprd_900mhz]= ...

PathLossModel(Pr_dbm_900mhz,d_900mhz,Pr0_dbm_900mhz,d0);

PathLossGraph(n_grd_900mhz,rou_grd_900mhz, ...
    MaxSprd_grd_900mhz,MinSprd_grd_900mhz, ...
    PL_grd_900mhz,yhat_grd_900mhz,d_grd_900mhz, ...
    'c',1,1,1);

PathLossGraph(n_2nd_900mhz,rou_2nd_900mhz, ...
    MaxSprd_2nd_900mhz,MinSprd_2nd_900mhz, ...
    PL_2nd_900mhz,yhat_2nd_900mhz,d_2nd_900mhz, ...
    'm',1,0,1);

PathLossGraph(n_3rd_900mhz,rou_3rd_900mhz, ...
    MaxSprd_3rd_900mhz,MinSprd_3rd_900mhz, ...

```



```

        PL_3rd_900mhz,yhat_3rd_900mhz,d_3rd_900mhz, ...
        'b',1,0,1);

PathLossGraph(n_900mhz,rou_900mhz, ...
        MaxSprd_900mhz,MinSprd_900mhz, ...
        PL_900mhz,yhat_900mhz,d_900mhz, ...
        'k',2,0,0);

title(['Propagation in Stocker,LOS+NLOS,900MHz']);

%=====
% 2.4GHZ
%=====

%-----
% LOS / 2.4GHz / Ground Floor
%-----

[n_grd_24ghz_los,rou_grd_24ghz_los,PL_grd_24ghz_los, ...
yhat_grd_24ghz_los,D_grd_24ghz_los,...
MaxSprd_grd_24ghz_los,MinSprd_grd_24ghz_los]= ...
PathLossModel(Pr_dbm_grd_24ghz_los,d_grd_24ghz_los,Pr0_dbm_grd_24ghz,d0);

PathLossGraph(n_grd_24ghz_los,rou_grd_24ghz_los, ...
        MaxSprd_grd_24ghz_los,MinSprd_grd_24ghz_los, ...
        PL_grd_24ghz_los,yhat_grd_24ghz_los,d_grd_24ghz_los, ...
        'k',2,1,1);
title(['Propagation in Ground Floor of Stocker,LOS,2.4GHz']);

%-----
% LOS / 2.4GHz / First Floor
%-----

[n_1st_24ghz_los,rou_1st_24ghz_los,PL_1st_24ghz_los, ...
yhat_1st_24ghz_los,D_1st_24ghz_los,...
MaxSprd_1st_24ghz_los,MinSprd_1st_24ghz_los]= ...
PathLossModel(Pr_dbm_1st_24ghz_los,d_1st_24ghz_los,Pr0_dbm_1st_24ghz,d0);

PathLossGraph(n_1st_24ghz_los,rou_1st_24ghz_los, ...
        MaxSprd_1st_24ghz_los,MinSprd_1st_24ghz_los, ...
        PL_1st_24ghz_los,yhat_1st_24ghz_los,d_1st_24ghz_los, ...
        'k',2,1,1);
title(['Propagation in First Floor of Stocker,LOS,2.4GHz']);

```

```

%-----
%  LOS / 2.4GHz / Second Floor
%-----

[n_2nd_24ghz_los,rou_2nd_24ghz_los,PL_2nd_24ghz_los, ...
yhat_2nd_24ghz_los,D_2nd_24ghz_los,...
MaxSprd_2nd_24ghz_los,MinSprd_2nd_24ghz_los]= ...
PathLossModel(Pr_dbm_2nd_24ghz_los,d_2nd_24ghz_los,Pr0_dbm_2nd_24ghz,d0);

PathLossGraph(n_2nd_24ghz_los,rou_2nd_24ghz_los, ...
              MaxSprd_2nd_24ghz_los,MinSprd_2nd_24ghz_los, ...
              PL_2nd_24ghz_los,yhat_2nd_24ghz_los,d_2nd_24ghz_los, ...
              'k',2,1,1);
title(['Propagation in Second Floor of Stocker,LOS,2.4GHz']);

%-----
%  LOS / 2.4GHz / Third Floor
%-----

[n_3rd_24ghz_los,rou_3rd_24ghz_los,PL_3rd_24ghz_los, ...
yhat_3rd_24ghz_los,D_3rd_24ghz_los,...
MaxSprd_3rd_24ghz_los,MinSprd_3rd_24ghz_los]= ...
PathLossModel(Pr_dbm_3rd_24ghz_los,d_3rd_24ghz_los,Pr0_dbm_3rd_24ghz,d0);

PathLossGraph(n_3rd_24ghz_los,rou_3rd_24ghz_los, ...
              MaxSprd_3rd_24ghz_los,MinSprd_3rd_24ghz_los, ...
              PL_3rd_24ghz_los,yhat_3rd_24ghz_los,d_3rd_24ghz_los, ...
              'k',2,1,1);
title(['Propagation in Third Floor of Stocker,LOS,2.4GHz']);

%-----
%  LOS / 2.4GHz / Fourth Floor
%-----

[n_4th_24ghz_los,rou_4th_24ghz_los,PL_4th_24ghz_los, ...
yhat_4th_24ghz_los,D_4th_24ghz_los,...
MaxSprd_4th_24ghz_los,MinSprd_4th_24ghz_los]= ...
PathLossModel(Pr_dbm_4th_24ghz_los,d_4th_24ghz_los,Pr0_dbm_4th_24ghz,d0);

PathLossGraph(n_4th_24ghz_los,rou_4th_24ghz_los, ...
              MaxSprd_4th_24ghz_los,MinSprd_4th_24ghz_los, ...
              PL_4th_24ghz_los,yhat_4th_24ghz_los,d_4th_24ghz_los, ...

```

```

    'k',2,1,1);
title(['Propagation in Fourth Floor of Stocker,LOS,2.4GHz']);

%-----
%  LOS / 2.4GHz / Entire Building
%-----
Pr_dbm_24ghz_los=[Pr_dbm_grd_24ghz_los,Pr_dbm_1st_24ghz_los,Pr_dbm_2nd_24gh
z_los, ...
                Pr_dbm_3rd_24ghz_los,Pr_dbm_4th_24ghz_los];

d_24ghz_los=[d_grd_24ghz_los,d_1st_24ghz_los,d_2nd_24ghz_los, ...
            d_3rd_24ghz_los,d_4th_24ghz_los];

[n_24ghz_los,rou_24ghz_los,PL_24ghz_los, ...
 yhat_24ghz_los,D_24ghz_los,...
 MaxSprd_24ghz_los,MinSprd_24ghz_los]= ...
PathLossModel(Pr_dbm_24ghz_los,d_24ghz_los,Pr0_dbm_24ghz,d0);

PathLossGraph(n_grd_24ghz_los,rou_grd_24ghz_los, ...
              MaxSprd_grd_24ghz_los,MinSprd_grd_24ghz_los, ...
              PL_grd_24ghz_los,yhat_grd_24ghz_los,d_grd_24ghz_los, ...
              'c',1,1,1);

PathLossGraph(n_1st_24ghz_los,rou_1st_24ghz_los, ...
              MaxSprd_1st_24ghz_los,MinSprd_1st_24ghz_los, ...
              PL_1st_24ghz_los,yhat_1st_24ghz_los,d_1st_24ghz_los, ...
              'g',1,0,1);

PathLossGraph(n_2nd_24ghz_los,rou_2nd_24ghz_los, ...
              MaxSprd_2nd_24ghz_los,MinSprd_2nd_24ghz_los, ...
              PL_2nd_24ghz_los,yhat_2nd_24ghz_los,d_2nd_24ghz_los, ...
              'm',1,0,1);

PathLossGraph(n_3rd_24ghz_los,rou_3rd_24ghz_los, ...
              MaxSprd_3rd_24ghz_los,MinSprd_3rd_24ghz_los, ...
              PL_3rd_24ghz_los,yhat_3rd_24ghz_los,d_3rd_24ghz_los, ...
              'b',1,0,1);

PathLossGraph(n_4th_24ghz_los,rou_4th_24ghz_los, ...
              MaxSprd_4th_24ghz_los,MinSprd_4th_24ghz_los, ...
              PL_4th_24ghz_los,yhat_4th_24ghz_los,d_4th_24ghz_los, ...
              'r',1,0,1);

PathLossGraph(n_24ghz_los,rou_24ghz_los, ...

```

```

        MaxSprd_24ghz_los,MinSprd_24ghz_los, ...
        PL_24ghz_los,yhat_24ghz_los,d_24ghz_los, ...
        'k',2,0,0);

title(['Propagation in Stocker,LOS,2.4GHz']);

%-----
%  NLOS / 2.4GHz / Ground Floor
%-----

[n_grd_24ghz_nlos,rou_grd_24ghz_nlos,PL_grd_24ghz_nlos, ...
yhat_grd_24ghz_nlos,D_grd_24ghz_nlos,...
MaxSprd_grd_24ghz_nlos,MinSprd_grd_24ghz_nlos]= ...
PathLossModel(Pr_dbm_grd_24ghz_nlos,d_grd_24ghz_nlos,Pr0_dbm_grd_24ghz,d0);

PathLossGraph(n_grd_24ghz_nlos,rou_grd_24ghz_nlos, ...
        MaxSprd_grd_24ghz_nlos,MinSprd_grd_24ghz_nlos, ...
        PL_grd_24ghz_nlos,yhat_grd_24ghz_nlos,d_grd_24ghz_nlos, ...
        'k',2,1,1);
title(['Propagation in Ground Floor of Stocker,NLOS,2.4GHz']);

%-----
%  NLOS / 2.4GHz / Second Floor
%-----

[n_2nd_24ghz_nlos,rou_2nd_24ghz_nlos,PL_2nd_24ghz_nlos, ...
yhat_2nd_24ghz_nlos,D_2nd_24ghz_nlos,...
MaxSprd_2nd_24ghz_nlos,MinSprd_2nd_24ghz_nlos]= ...
PathLossModel(Pr_dbm_2nd_24ghz_nlos,d_2nd_24ghz_nlos,Pr0_dbm_2nd_24ghz,d0);

PathLossGraph(n_2nd_24ghz_nlos,rou_2nd_24ghz_nlos, ...
        MaxSprd_2nd_24ghz_nlos,MinSprd_2nd_24ghz_nlos, ...
        PL_2nd_24ghz_nlos,yhat_2nd_24ghz_nlos,d_2nd_24ghz_nlos, ...
        'k',2,1,1);
title(['Propagation in Second Floor of Stocker,NLOS,2.4GHz']);

%-----
%  NLOS / 2.4GHz / Third Floor
%-----

[n_3rd_24ghz_nlos,rou_3rd_24ghz_nlos,PL_3rd_24ghz_nlos, ...
yhat_3rd_24ghz_nlos,D_3rd_24ghz_nlos,...
MaxSprd_3rd_24ghz_nlos,MinSprd_3rd_24ghz_nlos]= ...

```

```

PathLossModel(Pr_dbm_3rd_24ghz_nlos,d_3rd_24ghz_nlos,Pr0_dbm_3rd_24ghz,d0);

PathLossGraph(n_3rd_24ghz_nlos,rou_3rd_24ghz_nlos, ...
    MaxSprd_3rd_24ghz_nlos,MinSprd_3rd_24ghz_nlos, ...
    PL_3rd_24ghz_nlos,yhat_3rd_24ghz_nlos,d_3rd_24ghz_nlos, ...
    'k',2,1,1);
title(['Propagation in Third Floor of Stocker,NLOS,2.4GHz']);

%-----
%  NLOS / 2.4GHz / Entire Building
%-----

Pr_dbm_24ghz_nlos=[Pr_dbm_grd_24ghz_nlos,Pr_dbm_2nd_24ghz_nlos,Pr_dbm_3rd_
24ghz_nlos];
d_24ghz_nlos=[d_grd_24ghz_nlos,d_2nd_24ghz_nlos,d_3rd_24ghz_nlos];

[n_24ghz_nlos,rou_24ghz_nlos,PL_24ghz_nlos, ...
yhat_24ghz_nlos,D_24ghz_nlos,...
MaxSprd_24ghz_nlos,MinSprd_24ghz_nlos]= ...
PathLossModel(Pr_dbm_24ghz_nlos,d_24ghz_nlos,Pr0_dbm_24ghz,d0);

PathLossGraph(n_grd_24ghz_nlos,rou_grd_24ghz_nlos, ...
    MaxSprd_grd_24ghz_nlos,MinSprd_grd_24ghz_nlos, ...
    PL_grd_24ghz_nlos,yhat_grd_24ghz_nlos,d_grd_24ghz_nlos, ...
    'c',1,1,1);

PathLossGraph(n_2nd_24ghz_nlos,rou_2nd_24ghz_nlos, ...
    MaxSprd_2nd_24ghz_nlos,MinSprd_2nd_24ghz_nlos, ...
    PL_2nd_24ghz_nlos,yhat_2nd_24ghz_nlos,d_2nd_24ghz_nlos, ...
    'm',1,0,1);

PathLossGraph(n_3rd_24ghz_nlos,rou_3rd_24ghz_nlos, ...
    MaxSprd_3rd_24ghz_nlos,MinSprd_3rd_24ghz_nlos, ...
    PL_3rd_24ghz_nlos,yhat_3rd_24ghz_nlos,d_3rd_24ghz_nlos, ...
    'b',1,0,1);

PathLossGraph(n_24ghz_nlos,rou_24ghz_nlos, ...
    MaxSprd_24ghz_nlos,MinSprd_24ghz_nlos, ...
    PL_24ghz_nlos,yhat_24ghz_nlos,d_24ghz_nlos, ...
    'k',2,0,0);

title(['Propagation in Stocker,NLOS,2.4GHz']);
% leg0=strcat('0: n=',num2str(n_grd_24ghz_nlos),',
',rou=',num2str(rou_grd_24ghz_nlos),'[dB]');

```

```

% leg2=strcat('2: n=',num2str(n_2nd_24ghz_nlos),'
','rou=',num2str(rou_2nd_24ghz_nlos),'[dB]');
% leg3=strcat('3: n=',num2str(n_3rd_24ghz_nlos),'
','rou=',num2str(rou_3rd_24ghz_nlos),'[dB]');

%-----
% (LOS + NLOS) / 2.4GHz / Ground Floor
%-----

Pr_dbm_grd_24ghz=[Pr_dbm_grd_24ghz_los,Pr_dbm_grd_24ghz_nlos];
d_grd_24ghz=[d_grd_24ghz_los,d_grd_24ghz_nlos];

[n_grd_24ghz,rou_grd_24ghz,PL_grd_24ghz,yhat_grd_24ghz,D_grd_24ghz,...
MaxSprd_grd_24ghz,MinSprd_grd_24ghz]= ...
PathLossModel(Pr_dbm_grd_24ghz,d_grd_24ghz,Pr0_dbm_grd_24ghz,d0);

PathLossGraph(n_grd_24ghz,rou_grd_24ghz, ...
              MaxSprd_grd_24ghz,MinSprd_grd_24ghz, ...
              PL_grd_24ghz,yhat_grd_24ghz,d_grd_24ghz, ...
              'k',2,1,1);
title(['Propagation in Ground Floor of Stocker,LOS+NLOS,2.4GHz']);

%-----
% (LOS + NLOS) / 2.4GHz / Second Floor
%-----

Pr_dbm_2nd_24ghz=[Pr_dbm_2nd_24ghz_los,Pr_dbm_2nd_24ghz_nlos];
d_2nd_24ghz=[d_2nd_24ghz_los,d_2nd_24ghz_nlos];

[n_2nd_24ghz,rou_2nd_24ghz,PL_2nd_24ghz,yhat_2nd_24ghz,D_2nd_24ghz,...
MaxSprd_2nd_24ghz,MinSprd_2nd_24ghz]= ...
PathLossModel(Pr_dbm_2nd_24ghz,d_2nd_24ghz,Pr0_dbm_2nd_24ghz,d0);

PathLossGraph(n_2nd_24ghz,rou_2nd_24ghz, ...
              MaxSprd_2nd_24ghz,MinSprd_2nd_24ghz, ...
              PL_2nd_24ghz,yhat_2nd_24ghz,d_2nd_24ghz, ...
              'k',2,1,1);
title(['Propagation in Second Floor of Stocker,LOS+NLOS,2.4GHz']);

%-----
% (LOS + NLOS) / 2.4GHz / Third Floor
%-----

```

```

Pr_dbm_3rd_24ghz=[Pr_dbm_3rd_24ghz_los,Pr_dbm_3rd_24ghz_nlos];
d_3rd_24ghz=[d_3rd_24ghz_los,d_3rd_24ghz_nlos];

[n_3rd_24ghz,rou_3rd_24ghz,PL_3rd_24ghz,yhat_3rd_24ghz,D_3rd_24ghz,...
MaxSprd_3rd_24ghz,MinSprd_3rd_24ghz]= ...
PathLossModel(Pr_dbm_3rd_24ghz,d_3rd_24ghz,Pr0_dbm_3rd_24ghz,d0);

PathLossGraph(n_3rd_24ghz,rou_3rd_24ghz, ...
    MaxSprd_3rd_24ghz,MinSprd_3rd_24ghz, ...
    PL_3rd_24ghz,yhat_3rd_24ghz,d_3rd_24ghz, ...
    'k',2,1,1);
title(['Propagation in Third Floor of Stocker,LOS+NLOS,2.4GHz']);

%-----
% (LOS + NLOS) / 2.4GHz / Entire Building
%-----

Pr_dbm_24ghz=[Pr_dbm_grd_24ghz_los,Pr_dbm_1st_24ghz_los,Pr_dbm_2nd_24ghz_lo
s, ...
    Pr_dbm_3rd_24ghz_los,Pr_dbm_4th_24ghz_los, ...
    Pr_dbm_grd_24ghz_nlos,Pr_dbm_2nd_24ghz_nlos,Pr_dbm_3rd_24ghz_nlos];

d_24ghz=[d_grd_24ghz_los,d_1st_24ghz_los,d_2nd_24ghz_los, ...
    d_3rd_24ghz_los,d_4th_24ghz_los, ...
    d_grd_24ghz_nlos,d_2nd_24ghz_nlos,d_3rd_24ghz_nlos];

[n_24ghz,rou_24ghz,PL_24ghz,yhat_24ghz,D_24ghz,...
MaxSprd_24ghz,MinSprd_24ghz]= ...
PathLossModel(Pr_dbm_24ghz,d_24ghz,Pr0_dbm_24ghz,d0);

PathLossGraph(n_grd_24ghz,rou_grd_24ghz, ...
    MaxSprd_grd_24ghz,MinSprd_grd_24ghz, ...
    PL_grd_24ghz,yhat_grd_24ghz,d_grd_24ghz, ...
    'c',1,1,1);

PathLossGraph(n_2nd_24ghz,rou_2nd_24ghz, ...
    MaxSprd_2nd_24ghz,MinSprd_2nd_24ghz, ...
    PL_2nd_24ghz,yhat_2nd_24ghz,d_2nd_24ghz, ...
    'm',1,0,1);

PathLossGraph(n_3rd_24ghz,rou_3rd_24ghz, ...
    MaxSprd_3rd_24ghz,MinSprd_3rd_24ghz, ...
    PL_3rd_24ghz,yhat_3rd_24ghz,d_3rd_24ghz, ...
    'b',1,0,1);

```

```

PathLossGraph(n_24ghz,rou_24ghz, ...
              MaxSprd_24ghz,MinSprd_24ghz, ...
              PL_24ghz,yhat_24ghz,d_24ghz, ...
              'k',2,0,0);

title(['Propagation in Stocker,LOS+NLOS,2.4GHz']);

```

F.2. Matlab program for Amplitude Transfer Functions and Amplitude Autocorrelation Functions

Function correlation.m takes the received power at each frequency as the input and calculates the autocorrelation.

ChannelEstimation.m is the main program. It takes in the measured data and calls the correlation function. It calculates the range of power for each floor at every distance and generates the power vs. frequency and spaced frequency correlation plots.

Correlation.m

```

%To calculate the autocorrelation
function k=correlation(b)
%For reading 1
a=10.^(b/10);
k=xcorr(a,'coeff');
% Taking the correlated values from n+1 to 2*n-1 i.e
%for deltaf 1 to n-1
k=k(length(b)+1:length(k));

```

ChannelEstimation.m

```

clear all
%The readings
%Range of frequencies
freq=[902:1:928];

%Ground Floor
pr_grnd=[-54.95    -54.56 -61.65 -61.35 -53.47 -58.95 -61.16 -64.72
          -54.29    -54.59 -61.24 -60.42 -54.62 -58.99 -60.65 -63.95

```



```

-55.2   -54.01 -62.68 -60.61 -62.41 -58.18 -60.77 -64.86
-54.84  -55.03 -63.74 -62.55 -61.99 -57.87 -61.31 -65.46
-54.91  -55.78 -63.77 -62.23 -62.21 -57.95 -60.84 -64.5
-54.81  -55.03 -62.47 -60.65 -62.19 -58.02 -60.38 -63.4
-54.87  -55.51 -61.97 -59      -62.13      -57.43 -61.22 -63.94
-55.82  -56.38 -61.64 -59.26 -63.94 -58.09 -61.35 -63.49
-55.9    -55.75 -61.4  -59.11 -65.32 -58.93 -60.89 -63.1
-55.68  -55.46 -60.81 -58.81 -66.3  -58.76 -61      -63.26
-54.99  -56.1  -61.09 -59.49 -65.02 -58.27 -61.86 -63.56
-55.74  -56.17 -62.38 -59.91 -67.5  -59.89 -61.38 -63.31
-55.68  -56.24 -61.19 -59.32 -67.07 -60.95 -61.23 -62.85
-55.94  -56.63 -59.06 -58.1  -65.54 -59.03 -61.6  -62.28
-56.24  -56.47 -58.26 -57.73 -65.46 -58.74 -61.65 -62.69
-55.68  -57.33 -58.07 -57.54 -66.94 -59.44 -60.39 -62.09
-56.16  -57.68 -58.17 -57.1  -64.98 -59.56 -60.15 -61.93
-56.99  -57.79 -59.17 -57.47 -64.41 -59.03 -60.59 -62.12
-57.92  -58.01 -59.97 -58.03 -63.53 -59.23 -60.47 -61.91
-57.9    -58.63 -59.37 -58.82 -63.71 -58.74 -60.53 -62.36
-57.68  -58.66 -58.23 -58.02 -63.56 -59.08 -60.62 -62.28
-57.92  -57.02 -57.73 -57.51 -63.56 -59.23 -60.29 -62.08
-57.21  -57.13 -58.39 -57.49 -63.65 -59.74 -60.6  -61.82
-57.39  -57.2  -58.92 -57.01 -64.38 -60.12 -60.95 -61.41
-57.23  -57.33 -59.07 -56.86 -64.14 -59.93 -61.08 -61.7
-57.13  -55.85 -59.58 -57.67 -64.2  -59.79 -61.78 -62.35
-58.12  -59.51 -59.3  -58.87 -64.52 -60.83 -61.92 -62.5

```

```
];
```

```

s1=size(pr_grnd);
for i=1:2:s1(2)
hmaxgrnd((i+1)/2)=max(pr_grnd(:,i))-min(pr_grnd(:,i));
end

```

```

figure
plot(freq,pr_grnd(:,1)-max(pr_grnd(:,1)));
title('Normalized Power measured on Ground floor at 10m');
xlabel('Frequency(Mhz)');
ylabel('Normalized Power(dBm)');

```

```

figure
plot(freq,pr_grnd(:,3)-max(pr_grnd(:,3)));
title('Normalized Power measured on Ground floor at 20m');
xlabel('Frequency(Mhz)');
ylabel('Normalized Power(dBm)');

```

```
figure
```

```

plot(freq,pr_grnd(:,5)-max(pr_grnd(:,5)));
title('Normalized Power measured on Ground floor at 30m');
xlabel('Frequency(Mhz)');
ylabel('Normalized Power(dBm)');

```

```

figure
plot(freq,pr_grnd(:,7)-max(pr_grnd(:,7)));
title('Normalized Power measured on Ground floor at 40m');
xlabel('Frequency(Mhz)');
ylabel('Normalized Power(dBm)');

```

% First Floor

```

pr_fst=[
-66.41 -65.86 -66.7  -66.33 -69.96 -71.53 -72.55 -71.1  -75.37 -73.83 -76.05 -74.46
      -74.52 -74.18
-65.29 -66.13 -67.44 -66.06 -70.7  -70.91 -70.87 -69.74 -73.23 -72.86 -74.92 -75.02
      -74.49 -75.26
-66.12 -66.67 -67.43 -66.58 -70.53 -69.45 -71.43 -68.89 -73.46 -73.5  -75.08 -75.43
      -74.28 -74.33
-66.6  -67.28 -67.15 -66.61 -70.91 -69.74 -71.7  -69.28 -74.99 -72.48 -74.85 -75.86
      -74.31 -74.29
-67.42 -67.67 -66.58 -66.1  -69.88 -68.98 -69.49 -68.69 -72.88 -73.2  -73.96 -75.51
      -72.83 -73.55
-67.93 -67.05 -67.46 -65.97 -69.86 -67.74 -69.65 -68.2  -72.07 -72.24 -72.04 -74.46
      -73.75 -73.27
-68.95 -66.69 -66.71 -66.42 -70.75 -68.8  -70.32 -67.48 -73.22 -71.01 -72.95 -74.25
      -73.81 -73.78
-68.62 -65.57 -66.47 -65.6  -69.63 -68.71 -68.21 -67.2  -71.48 -70.34 -73.26 -74.96
      -73.29 -73.12
-68.08 -64.82 -65.69 -66.71 -69.24 -66.97 -68.74 -66.46 -71.81 -69.51 -72.57 -74.05
      -72.25 -72.98
-67.22 -63.86 -64.83 -65.34 -68.58 -67.09 -68.21 -66.3  -71.39 -67.73 -71.86 -73.6
      -72.24 -71.51
-67.1  -63.41 -64.71 -64.32 -68.08 -66.49 -67.42 -65.94 -70.84 -68.76 -71.64 -73.25
      -70.35 -71.03
-66.62 -62.99 -64.64 -64.37 -68.23 -66.27 -67.53 -65.35 -70.28 -68.31 -71.89 -73.37
      -72      -70.83
-65.67 -62.4  -64.59 -64.68 -67.95 -65.93 -67.1  -65.29 -71.17 -68.28 -70.68 -73.55
      -70.7  -71.22
-63.76 -61.47 -64.82 -64.07 -67.58 -65.73 -66.71 -64.4  -70.58 -68.57 -69.63 -71.8
      -70.2  -70.29
-63.57 -60.51 -65.5  -64.48 -67.48 -66.04 -65.86 -64.66 -70.13 -68.47 -69.69 -72.89
      -70.22 -70.12

```

```

-63.04 -59.77 -65.95 -64.82 -67.11 -66      -66.5      -64.62 -70.5  -68.11 -69.89
      -72.99 -70.07 -69.81
-60.12 -59.33 -65.86 -64.43 -66.15 -65.49 -66.06 -64.43 -70.41 -68.06 -69.78 -71.73
      -70.14 -68.28
-62.96 -58.74 -65.43 -64.87 -66.05 -66.06 -65.95 -63.97 -70.39 -68.07 -69.11 -73.1
      -69.83 -69.46
-62.13 -58.52 -64.85 -64.19 -65.4  -65.95 -65.44 -63.53 -68.76 -67.82 -69.21 -72.21
      -69.66 -69.31
-61.83 -58.76 -64.76 -63.38 -65.73 -65.69 -65.61 -63.42 -69.06 -67.71 -68.95 -71.62
      -68.64 -69.03
-61.3  -57.3  -63.96 -63      -65.48      -65.3  -65.61 -63.2  -68.39 -67.18 -68.05
      -72.38 -69.67 -69.05
-61.06 -57.43 -63.38 -63.15 -65.41 -65.64 -64.94 -62.62 -68.72 -68.61 -68.04 -71.66
      -68.83 -67.76
-60.33 -56.94 -63.28 -62.75 -65.29 -64.85 -64.65 -61.84 -68      -66.53      -67.98
      -70.82 -68.74 -67.11
-61.06 -56.72 -62.97 -62.4  -65.52 -64.6  -64.47 -62.42 -67.81 -66      -67.42
      -70.84 -68.45 -67.76
-61.04 -56.82 -62.37 -62.96 -65.28 -64.92 -65.17 -61.96 -68.47 -65.92 -67.51 -71.35
      -68.51 -67.12
-61.33 -56.49 -62.5  -62.38 -65.34 -65.19 -65.94 -62.32 -68.32 -65.76 -67.85 -72.57
      -68.47 -67.54
-61.03 -56.72 -62.28 -62.81 -65.86 -64.81 -64.79 -62.8  -67.49 -65.16 -67.49 -72.66
      -68      -67.1

```

```
];
```

```

s2=size(pr_fst);
for i=1:2:s2(2)
hmaxfst((i+1)/2)=max(pr_fst(:,i))-min(pr_fst(:,i));
end

```

```

figure
plot(freq,pr_fst(:,1)-max(pr_fst(:,1)));
title('Normalized Power measured on First floor at 10m');
xlabel('Frequency(Mhz)');
ylabel('Normalized Power(dBm)');

```

```

figure
plot(freq,pr_fst(:,3)-max(pr_fst(:,3)));
title('Normalized Power measured on First floor at 20m');
xlabel('Frequency(Mhz)');
ylabel('Normalized Power(dBm)');

```

```
figure
```

```

plot(freq,pr_fst(:,5)-max(pr_fst(:,5)));
title('Normalized Power measured on First floor at 30m');
xlabel('Frequency(Mhz)');
ylabel('Normalized Power(dBm)');

```

```

figure
plot(freq,pr_fst(:,7)-max(pr_fst(:,7)));
title('Normalized Power measured on First floor at 40m');
xlabel('Frequency(Mhz)');
ylabel('Normalized Power(dBm)');

```

```

figure
plot(freq,pr_fst(:,9)-max(pr_fst(:,9)));
title('Normalized Power measured on First floor at 50m');
xlabel('Frequency(Mhz)');
ylabel('Normalized Power(dBm)');

```

```

figure
plot(freq,pr_fst(:,11)-max(pr_fst(:,11)));
title('Normalized Power measured on First floor at 60m');
xlabel('Frequency(Mhz)');
ylabel('Normalized Power(dBm)');

```

```

figure
plot(freq,pr_fst(:,13)-max(pr_fst(:,13)));
title('Normalized Power measured on First floor at 70m');
xlabel('Frequency(Mhz)');
ylabel('Normalized Power(dBm)');

```

% Second Floor

```

pr_snd=[-58.21      -61.24 -63.68 -60.1  -65.61 -66.14 -69.72 -68.91 -75.29 -72.5
        -71.71 -72.85
        -58.45  -62.58 -64.17 -60.68 -65.84 -66.96 -70.64 -68.94 -75.4  -73.9  -73.67
        -72.39
        -58.57  -62.29 -64.82 -60.95 -66.17 -67.09 -70.92 -69.27 -74.85 -71.8  -72.36
        -72.84
        -58.11  -61.87 -64.92 -61.2  -68.68 -67.06 -70.03 -69.73 -74.79 -73.94 -73.21
        -72.59
        -57.48  -61.95 -65.44 -61.23 -66.4  -67.03 -71.23 -69.61 -74.1  -73.64 -72.32
        -72.4
        -56.93  -60.91 -66.67 -61.79 -66.31 -66.41 -71.98 -69.86 -74.43 -74.09 -73.31
        -73.15
        -56.92  -59.54 -66.06 -61.54 -66.2  -66.26 -70.25 -69.66 -74.77 -72.35 -73.06
        -71.01

```

```

-56.64 -59.48 -67.11 -61.72 -65.54 -66.17 -70.75 -69.42 -74.38 -74.28 -74.77
-72.75
-57.1 -58.58 -66.68 -61.71 -66.38 -66.13 -70.06 -68.36 -74.54 -72.62 -73.04
-73.59
-56.9 -58.13 -68.43 -61.69 -64.71 -65.7 -70.44 -67.85 -74.87 -71.96 -73.9
-72.18
-56.73 -57.74 -67.98 -61.92 -65.78 -65.88 -70.34 -67.88 -73.14 -72.72 -72.58
-71.07
-56.78 -57.61 -67.82 -61.93 -65.18 -66.31 -69.98 -67.81 -74.64 -73.95 -71.9
-73.23
-56.99 -57.69 -68.4 -61.86 -65.34 -65.13 -69.82 -67.99 -76.09 -73.92 -71.6
-72.15
-56.87 -57.98 -68.67 -61.61 -65.48 -65.91 -69.43 -67.4 -74.33 -71.79 -73.39
-72.86
-56.93 -57.05 -68.52 -61.38 -64.92 -65.69 -69.68 -67.83 -73.88 -72.87 -70.97
-72.49
-56.72 -57.01 -68.07 -61.08 -64.68 -65.88 -69.5 -66.53 -74.19 -73.41 -71.31
-70.77
-57.08 -57.19 -68.28 -60.84 -64.41 -65.54 -68.81 -67.02 -74.53 -72.14 -72.09
-71.61
-57.05 -57.71 -68.47 -60.69 -64.46 -66 -69.29 -67.06 -74.55 -72.03
-73.37 -70.82
-57.38 -57.65 -68.38 -60.67 -65.2 -65.74 -69.53 -67.27 -74.46 -71.84 -71.8
-71.26
-57.64 -57.64 -66.37 -60.98 -65.06 -66.09 -68.84 -67.43 -75.1 -71.43 -72.76
-72.12
-57.57 -58.05 -65.93 -60.98 -66.23 -66.03 -69.69 -66.69 -73.43 -72.17 -71.26
-72.2
-58.19 -58.21 -65.65 -61.31 -65.49 -67.36 -69.79 -66.62 -72.95 -71.81 -71.93
-71.62
-57.99 -58.03 -66.08 -61.29 -66.42 -66.89 -68.6 -67.09 -73.16 -73.7 -73.11
-71.62
-57.99 -58.29 -65.41 -60.64 -64.48 -67.6 -69.77 -66.52 -74.04 -73.45 -72.86
-72.61
-57.8 -58.13 -65.31 -60.38 -65.48 -67.76 -69.87 -67.24 -73.85 -74 -
73.09 -71.18
-57.73 -57.08 -64.24 -60.12 -63.99 -67.28 -68.62 -66.45 -74.82 -72.89 -72.42
-70.79
-57.6 -57.14 -63 -60.01 -64.18 -66.4 -67.96 -66.31 -74.82 -71.47
-72.2 -70.51

```

```
];
```

```
s3=size(pr_scd);
```

```
for i=1:2:s3(2)
```

```
hmaxscd((i+1)/2)=max(pr_scd(:,i))-min(pr_scd(:,i));
```

```
end
```

```
figure
plot(freq,pr_scd(:,1)-max(pr_scd(:,1)));
title('Normalized Power measured on Second floor at 10m');
xlabel('Frequency(Mhz)');
ylabel('Normalized Power(dBm)');
```

```
figure
plot(freq,pr_scd(:,3)-max(pr_scd(:,3)));
title('Normalized Power measured on Second floor at 20m');
xlabel('Frequency(Mhz)');
ylabel('Normalized Power(dBm)');
```

```
figure
plot(freq,pr_scd(:,5)-max(pr_scd(:,5)));
title('Normalized Power measured on Second floor at 30m');
xlabel('Frequency(Mhz)');
ylabel('Normalized Power(dBm)');
```

```
figure
plot(freq,pr_scd(:,7)-max(pr_scd(:,7)));
title('Normalized Power measured on Second floor at 40m');
xlabel('Frequency(Mhz)');
ylabel('Normalized Power(dBm)');
```

```
figure
plot(freq,pr_scd(:,9)-max(pr_scd(:,9)));
title('Normalized Power measured on Second floor at 50m');
xlabel('Frequency(Mhz)');
ylabel('Normalized Power(dBm)');
```

```
figure
plot(freq,pr_scd(:,11)-max(pr_scd(:,11)));
title('Normalized Power measured on Second floor at 60m');
xlabel('Frequency(Mhz)');
ylabel('Normalized Power(dBm)');
```

```
%Third Floor
```

```
pr_trd=[
-53.99 -53.79 -56.87 -55.77 -63.66 -62.19 -63.43 -62.16 -66.9 -68.08 -69.92 -72.01
        -67.86 -67.89
-53.9 -53.69 -56.39 -55.37 -63.8 -62.25 -62.99 -61.4 -66.57 -68.79 -70.2 -71.81
        -67.24 -67.27
```

-53.92 -53.51 -55.57 -54.78 -63.87 -61.35 -62.85 -61.39 -66.2 -68.04 -69.25 -71.32
 -67.16 -67.24
 -53.96 -53.67 -55.59 -54.14 -63.29 -60.77 -62.57 -61.26 -66.69 -67.7 -68.64 -71.29
 -66.96 -67.73
 -53.38 -54.13 -55.42 -53.98 -63.43 -61.52 -62.86 -61.38 -65.9 -67.06 -68.97 -72.17
 -66.7 -67.51
 -54.2 -55.35 -55.91 -53.46 -63.3 -61.26 -62.67 -61.06 -66.38 -68.22 -67.93 -71.48
 -67.4 -67.69
 -54.06 -55.53 -56.21 -53.37 -63.04 -61.27 -63.1 -60.99 -66.4 -67.58 -67.67 -71.5
 -67.56 -67.71
 -53.94 -55.21 -56.5 -53.16 -63.19 -61.5 -63.08 -60.65 -66.19 -68.71 -67.89 -71.77
 -67.27 -67.72
 -53.63 -55.37 -55.81 -53.13 -63.29 -60.85 -62.62 -60.63 -66.33 -68.13 -67.71 -71.28
 -67.74 -67.76
 -53.5 -54.97 -55.7 -52.9 -63.02 -61.28 -62.21 -60.73 -66.74 -69.04 -67.92 -70.68
 -67.68 -67.32
 -53.61 -55.06 -55.69 -52.85 -63.1 -61.59 -62.08 -60.12 -66.63 -68.53 -67.63 -72.69
 -68.25 -67.53
 -53.6 -55.22 -55.75 -52.73 -63.13 -61.24 -61.65 -60.32 -66.35 -68.39 -67.66 -71.65
 -67.76 -67.26
 -53.51 -55.4 -56.03 -52.11 -63.31 -60.84 -61.5 -60.73 -67.38 -68.26 -67.48 -71.43
 -67.89 -67.48
 -53.35 -55.37 -56.01 -52.02 -62.97 -61.12 -60.99 -60.26 -66.86 -68.22 -67.02 -71.41
 -67.97 -67.38
 -53.38 -55.14 -55.9 -51.74 -63.06 -60.26 -61.3 -60.03 -66.32 -67.77 -66.08 -70.42
 -67.81 -67.04
 -53.47 -54.6 -55.91 -51.66 -63.22 -59.49 -60.97 -60.04 -66.79 -68.18 -67.01 -68.88
 -67.64 -67.14
 -53.33 -54.46 -56.09 -51.74 -62.58 -62.26 -59.98 -60.03 -67.28 -68.42 -67.06 -68.78
 -67.65 -67.38
 -53.51 -53.82 -56.28 -51.68 -62.42 -60.81 -60.32 -60.29 -66.35 -69.21 -66.77 -68.78
 -67.41 -67.01
 -53.95 -53.62 -56.41 -51.78 -62.6 -60.74 -59.86 -59.99 -67.2 -69.57 -66.69 -68.43
 -67.47 -67.25
 -54.51 -53.17 -56.37 -51.94 -62.68 -59.92 -60.31 -60.1 -66.53 -69.91 -66.65 -69.13
 -67.52 -67.55
 -54.86 -53.41 -56.29 -52.03 -62.81 -60.12 -59.72 -60.33 -66.77 -69.9 -66.47 -68.47
 -67.58 -67.37
 -55.32 -53.51 -56.34 -52.18 -62.67 -59.77 -59.7 -60.53 -65.31 -70.19 -65.96 -68.56
 -67.16 -67.26
 -55.81 -53.54 -56.41 -52.2 -62.89 -59.39 -59.46 -60.1 -66.8 -70.88 -65.87 -68.14
 -68.18 -66.92
 -55.96 -53.53 -56.4 -52.12 -63 -60.33 -60.07 -60 -67.11 -69.91
 -66.88 -68.2 -68.3 -66.8

```

-56.06 -53.49 -56.4 -52.03 -63.1 -60.07 -60.38 -60.15 -66.56 -70.89 -66.71 -67.81
        -68.46 -67.2
-56.01 -53.57 -56.06 -51.94 -63.16 -60.71 -60.32 -60.26 -67.89 -70.65 -67.47 -68.16
        -68.36 -66.54
-56.05 -53.65 -56.02 -52.04 -63.37 -61.29 -60.65 -60.15 -68        -71.81        -67.93
        -67.99 -68.28 -67.43
];

```

```

s4=size(pr_trd);
for i=1:2:s4(2)
hmaxtrd((i+1)/2)=max(pr_trd(:,i))-min(pr_trd(:,i));
end

```

```

figure
plot(freq,pr_trd(:,1)-max(pr_trd(:,1)));
title('Normalized Power measured on Third floor at 10m');
xlabel('Frequency(Mhz)');
ylabel('Normalized Power(dBm)');

```

```

figure
plot(freq,pr_trd(:,3)-max(pr_trd(:,3)));
title('Normalized Power measured on Third floor at 20m');
xlabel('Frequency(Mhz)');
ylabel('Normalized Power(dBm)');

```

```

figure
plot(freq,pr_trd(:,5)-max(pr_trd(:,5)));
title('Normalized Power measured on Third floor at 30m');
xlabel('Frequency(Mhz)');
ylabel('Normalized Power(dBm)');

```

```

figure
plot(freq,pr_trd(:,7)-max(pr_trd(:,7)));
title('Normalized Power measured on Third floor at 40m');
xlabel('Frequency(Mhz)');
ylabel('Normalized Power(dBm)');

```

```

figure
plot(freq,pr_trd(:,9)-max(pr_trd(:,9)));
title('Normalized Power measured on Third floor at 50m');
xlabel('Frequency(Mhz)');
ylabel('Normalized Power(dBm)');

```

```

figure
plot(freq,pr_trd(:,11)-max(pr_trd(:,11)));

```



```

title('Normalized Power measured on Third floor at 60m');
xlabel('Frequency(Mhz)');
ylabel('Normalized Power(dBm)');

```

```

figure
plot(freq,pr_trd(:,13)-max(pr_trd(:,13)));
title('Normalized Power measured on Third floor at 70m');
xlabel('Frequency(Mhz)');
ylabel('Normalized Power(dBm)');

```

```

% Fourth Floor

```

```

pr_frth=[-64.21      -60.2  -68.01 -66.16 -64.03 -62.93 -69.32 -67.27
-64.61  -60.26 -67.77 -65.33 -63.95 -62.16 -67.79 -67.54
-65.46  -59.89 -68.26 -64.67 -63.93 -62.39 -68.58 -67.38
-67.11  -60.01 -68      -65.6      -63.3  -62.65 -68.07 -67.03
-66.35  -60.09 -67.57 -64.73 -63.12 -61.99 -67.47 -67.3
-65.4    -59.39 -67.31 -63.89 -62.77 -61.8   -67.09 -66.89
-65.16  -59.34 -67.21 -63.45 -62.78 -61.81 -67.5   -66.24
-64.42  -58.94 -67.25 -62.71 -62.97 -61.73 -67.08 -66.18
-62.39  -59.11 -67.64 -62.76 -63.04 -62.15 -67.22 -65.89
-62.8    -59.06 -67.5   -62.97 -63.06 -62.08 -66.39 -65.55
-62.65  -59.63 -67.77 -63.19 -62.52 -62.92 -67.4   -65.64
-62.58  -60.06 -67.09 -62.9   -62.8   -62.99 -67.91 -64.96
-62.89  -61.08 -68.28 -62.76 -62.46 -63.1   -67.06 -65.74
-62.99  -62.01 -68.94 -63.01 -62.11 -62.81 -67.75 -65.41
-63.45  -63.42 -70.5   -62.55 -61.99 -62.03 -68.27 -65.22
-63.87  -65.38 -69.7   -63.16 -61.88 -62.67 -68.13 -65.09
-64.1    -67.81 -70.15 -64.36 -62.39 -62.18 -67.85 -65.94
-64.29  -70.74 -66.98 -63.96 -61.93 -62.14 -68.36 -66.61
-64.69  -72.96 -69.47 -64.8   -62.24 -62.3   -70.07 -66.68
-64.85  -71.81 -71.66 -65.36 -62.52 -62.7   -69.67 -67.05
-64.84  -70.78 -70.52 -65.48 -62.2   -62.45 -70.43 -66.71
-64.57  -68.97 -69.94 -65.24 -61.64 -62.34 -69.87 -66.62
-64.35  -68.29 -68.46 -66.07 -61.5   -61.63 -68.79 -66.47
-64.11  -68.14 -72.24 -65.07 -61.05 -60.94 -68.48 -66.84
-63.52  -72.5   -72.87 -64.94 -61.19 -60.67 -70.13 -67
-62.72  -70.17 -71.21 -64.27 -60.91 -61.09 -70      -66.87
-62.07  -68.12 -69.44 -64.28 -61.18 -60.8   -68      -66.53
];

```

```

s5=size(pr_frth);
for i=1:2:s5(2)
hmaxfrth((i+1)/2)=max(pr_frth(:,i))-min(pr_frth(:,i));
end

```

```
figure
plot(freq,pr_frth(:,1)-max(pr_frth(:,1)));
title('Normalized Power measured on Fourth floor at 10m');
xlabel('Frequency(Mhz)');
ylabel('Normalized Power(dBm)');
```

```
figure
plot(freq,pr_frth(:,3)-max(pr_frth(:,3)));
title('Normalized Power measured on Fourth floor at 20m');
xlabel('Frequency(Mhz)');
ylabel('Normalized Power(dBm)');
```

```
figure
plot(freq,pr_frth(:,5)-max(pr_frth(:,5)));
title('Normalized Power measured on Fourth floor at 30m');
xlabel('Frequency');
ylabel('Normalized Power(dBm)');
```

```
figure
plot(freq,pr_frth(:,7)-max(pr_frth(:,7)));
title('Normalized Power measured on Fourth floor at 40m');
xlabel('Frequency(Mhz)');
ylabel('Normalized Power(dBm)');
```

```
%To calculate correlations
deltaf=[1:26];
```

```
%Ground Floor
corr_grnd_10_r1=correlation(pr_grnd(:,1));
corr_grnd_10_r2=correlation(pr_grnd(:,2));
corr_grnd_20_r1=correlation(pr_grnd(:,3));
corr_grnd_20_r2=correlation(pr_grnd(:,4));
corr_grnd_30_r1=correlation(pr_grnd(:,5));
corr_grnd_30_r2=correlation(pr_grnd(:,6));
corr_grnd_40_r1=correlation(pr_grnd(:,7));
corr_grnd_40_r2=correlation(pr_grnd(:,8));
```

```
% First Floor
corr_fst_10_r1=correlation(pr_fst(:,1));
corr_fst_10_r2=correlation(pr_fst(:,2));
```

```

corr_fst_20_r1=correlation(pr_fst(:,3));
corr_fst_20_r2=correlation(pr_fst(:,4));
corr_fst_30_r1=correlation(pr_fst(:,5));
corr_fst_30_r2=correlation(pr_fst(:,6));
corr_fst_40_r1=correlation(pr_fst(:,7));
corr_fst_40_r2=correlation(pr_fst(:,8));
corr_fst_50_r1=correlation(pr_fst(:,9));
corr_fst_50_r2=correlation(pr_fst(:,10));
corr_fst_60_r1=correlation(pr_fst(:,11));
corr_fst_60_r2=correlation(pr_fst(:,12));
corr_fst_70_r1=correlation(pr_fst(:,13));
corr_fst_70_r2=correlation(pr_fst(:,14));

```

% Second Floor

```

corr_scnd_10_r1=correlation(pr_scnd(:,1));
corr_scnd_10_r2=correlation(pr_scnd(:,2));
corr_scnd_20_r1=correlation(pr_scnd(:,3));
corr_scnd_20_r2=correlation(pr_scnd(:,4));
corr_scnd_30_r1=correlation(pr_scnd(:,5));
corr_scnd_30_r2=correlation(pr_scnd(:,6));
corr_scnd_40_r1=correlation(pr_scnd(:,7));
corr_scnd_40_r2=correlation(pr_scnd(:,8));
corr_scnd_50_r1=correlation(pr_scnd(:,9));
corr_scnd_50_r2=correlation(pr_scnd(:,10));
corr_scnd_60_r1=correlation(pr_scnd(:,11));
corr_scnd_60_r2=correlation(pr_scnd(:,12));

```

%Third Floor

```

corr_trd_10_r1=correlation(pr_trd(:,1));
corr_trd_10_r2=correlation(pr_trd(:,2));
corr_trd_20_r1=correlation(pr_trd(:,3));
corr_trd_20_r2=correlation(pr_trd(:,4));
corr_trd_30_r1=correlation(pr_trd(:,5));
corr_trd_30_r2=correlation(pr_trd(:,6));
corr_trd_40_r1=correlation(pr_trd(:,7));
corr_trd_40_r2=correlation(pr_trd(:,8));
corr_trd_50_r1=correlation(pr_trd(:,9));
corr_trd_50_r2=correlation(pr_trd(:,10));
corr_trd_60_r1=correlation(pr_trd(:,11));
corr_trd_60_r2=correlation(pr_trd(:,12));
corr_trd_70_r1=correlation(pr_trd(:,13));

```

```
corr_trd_70_r2=correlation(pr_trd(:,14));
```

```
%Fourth Floor
```

```
corr_frth_10_r1=correlation(pr_frth(:,1));
corr_frth_10_r2=correlation(pr_frth(:,2));
corr_frth_20_r1=correlation(pr_frth(:,3));
corr_frth_20_r2=correlation(pr_frth(:,4));
corr_frth_30_r1=correlation(pr_frth(:,5));
corr_frth_30_r2=correlation(pr_frth(:,6));
corr_frth_40_r1=correlation(pr_frth(:,7));
corr_frth_40_r2=correlation(pr_frth(:,8));
```

```
%Averaging the autocorrelations
```

```
%For Method 1
```

```
%Ground Floor
```

```
%For reading 1
```

```
corr_grnd_r1=[corr_grnd_10_r1+corr_grnd_20_r1+corr_grnd_30_r1+corr_grnd_
40_r1]/4;
```

```
%For reading 2
```

```
corr_grnd_r2=[corr_grnd_10_r2+corr_grnd_20_r2+corr_grnd_30_r2+corr_grnd_
40_r2]/4;
```

```
% %First Floor
```

```
%For reading 1
```

```
corr_fst_r1=[corr_fst_10_r1+corr_fst_20_r1+corr_fst_30_r1+corr_fst_40_r1+corr_fst_50
_r1+corr_fst_60_r1+corr_fst_70_r1]/7;
```

```
%For reading 2
```

```
corr_fst_r2=[corr_fst_10_r2+corr_fst_20_r2+corr_fst_30_r2+corr_fst_40_r2+corr_fst_50
_r2+corr_fst_60_r2+corr_fst_70_r2]/7;
```

```
% %Second Floor
```

```
%For reading 1
```

```
corr_snd_r1=[corr_snd_10_r1+corr_snd_20_r1+corr_snd_30_r1+corr_snd_40_r1+c
orr_snd_50_r1+corr_snd_60_r1]/6;
```

```
%For reading 2
```

```
corr_snd_r2=[corr_snd_10_r2+corr_snd_20_r2+corr_snd_30_r2+corr_snd_40_r2+c
orr_snd_50_r2+corr_snd_60_r2]/6;
```

```
% %Third Floor
```

```
% %For reading 1
```

```

corr_trd_r1=[corr_trd_10_r1+corr_trd_20_r1+corr_trd_30_r1+corr_trd_40_r1+corr_trd_
50_r1+corr_trd_60_r1+corr_trd_70_r1]/7;
% %For reading 2
corr_trd_r2=[corr_trd_10_r2+corr_trd_20_r2+corr_trd_30_r2+corr_trd_40_r2+corr_trd_
50_r2+corr_trd_60_r2+corr_trd_70_r2]/7;
%
%Fourth Floor
%For reading 1
corr_frth_r1=[corr_frth_10_r1+corr_frth_20_r1+corr_frth_30_r1+corr_frth_40_r1]/4;
%For reading 2
corr_frth_r2=[corr_frth_10_r2+corr_frth_20_r2+corr_frth_30_r2+corr_frth_40_r2]/4;

%Ground Floor
%Reading 1
figure
plot(deltaf,corr_grnd_r1);
xlabel('Frequency shift');
ylabel('Normalized autocorrelation');
Title('Normalized frequency autocorrelation function for Ground floor: Reading 1');

%Reading 2
figure
plot(deltaf,corr_grnd_r2);
xlabel('Frequency shift');
ylabel('Normalized autocorrelation');
Title('Normalized frequency autocorrelation function for Ground floor: Reading 2');

%First Floor
%Reading 1
figure;
plot(deltaf,corr_fst_r1);
xlabel('Frequency shift(Mhz)');
ylabel('Normalized autocorrelation');
Title('Normalized frequency autocorrelation function for First floor: Reading 1');

%Reading 2
figure;
plot(deltaf,corr_fst_r2);
xlabel('Frequency shift(Mhz)');
ylabel('Normalized autocorrelation');
Title('Normalized frequency autocorrelation function for First floor: Reading 2');

%Second Floor
%Reading 1
figure;

```

```
plot(deltaf,corr_scnd_r1);  
xlabel('Frequency shift(Mhz)');  
ylabel('Normalized autocorrelation');  
Title('Normalized frequency autocorrelation function for Second floor: Reading 1');
```

```
%Reading 2  
figure;  
plot(deltaf,corr_scnd_r2);  
xlabel('Frequency shift(Mhz)');  
ylabel('Normalized autocorrelation');  
Title('Normalized frequency autocorrelation function for Second floor: Reading 2');
```